Applications of Heegaard Floer Homology to Knot and Link Concordance

Adam Simon Levine

Submitted in partial fulfillment of the

requirements for the degree

of Doctor of Philosophy

in the Graduate School of Arts and Sciences

COLUMBIA UNIVERSITY

2010

Abstract

Applications of Heegaard Floer Homology to Knot and Link Concordance

Adam Simon Levine

We consider several applications of Heegaard Floer homology to the study of knot and link concordance.

Using the techniques of bordered Heegaard Floer homology developed recently by Lipshitz, Ozsváth, and Thurston, we compute the concordance invariant τ for a family of satellite knots that generalizes Whitehead doubles. We use this computation to show that the all-positive Whitehead doubles of certain links obtained by iterated Bing doubling are not smoothly slice.

We also present an algorithm for computing the knot Floer homology of the inverse image of a knot in its m-fold cyclic branched cover. Using this algorithm, as well as earlier work of Ozsváth and Szabó on the Floer homology of double branched covers, we determine the smooth concordance orders of numerous knots through eleven crossings.

Table of Contents

List of Figures

List of Tables

I am deeply grateful to my advisor, Peter Ozsváth, for all of his guidance during the past five years. He proposed fascinating questions to investigate, provided helpful advice in my research, and never hesitated to challenge me to dig deeper. I look forward to continuing to learn from him in years to come.

Thanks to Denis Auroux, Robert Lipshitz, Paul Melvin, and Dylan Thurston for serving on my dissertation defense committee. Their questions and suggestions were very helpful in preparing the final version of this thesis.

It has been an incredible privilege to be part of the low-dimensional topology community at Columbia and beyond. I am extremely grateful to my colleagues and teachers for countless helpful discussions during the past five years. Special thanks go to John Baldwin, Joan Birman, Jonathan Bloom, Allison Gilmore, Josh Greene, Eli Grigsby, Matthew Hedden, Jen Hom, Peter Horn, Adam Knapp, Joan Licata, Chuck Livingston, John Morgan, Walter Neumann, Tom Peters, Ina Petkova, Jacob Rasmussen, Danny Ruberman, Sucharit Sarkar, Rob Schneiderman, Peter Teichner, and Rumen Zarev.

I thank my classmates at Columbia — Mark Branson, Joelle Brichard, Chen-Yun Lin, Qing Lu, Natalia Mosina, Mingmin Shen, Dmitry Zakharov, and Christian Zickert — for being wonderful friends and for sharing their insights about other areas of mathematics, and I wish them the best of luck in their future pursuits.

I was fortunate to spend three months at the Mathematics Science Research Institute as part of the Homology Theories of Knots and Links program in Spring 2010. I am also grateful to the National Science Foundation for its support (grant DMS-0739392).

I owe my inspiration to pursue a career in mathematics to my high school calculus teacher, Robert Arrigo, who opened my eyes to the beauty of the subject.

I thank my parents, Eric Levine and Terri Simon, my brother, Ben Levine, and my maternal grandparents, John and Laura Lee Simon, for their valiant efforts to understand my explanations of topology and for their unceasing love and support.

Finally, I dedicate this thesis to my paternal grandparents, Morton and Diana Levine, whose memory is a blessing.

Chapter 1

Introduction

A knot in the 3-sphere is called *topologically slice* if it bounds a locally flatly embedded disk in the 4-ball, and *smoothly slice* if the disk can be taken to be smoothly embedded. Two knots are called (topologically or smoothly) *concordant* if they are the ends of an embedded annulus in $S^3 \times I$; thus, a knot is slice if and only if it is concordant to the unknot. More generally, a link is (topologically or smoothly) *slice* if it bounds a disjoint union of appropriately embedded disks. The study of concordance — especially regarding the relationship between the notions of topological and smooth sliceness — is one of the major areas of active research in knot theory, and it is closely tied to the perplexing differences between topological and smooth 4-manifold theory.

The study of concordance began in the 1950s with the work of Fox and Milnor [10], who showed that many classical knot invariants, such as the Alexander polynomial and the signature, can be used to obstruct a knot from being slice. In the 1960s and 1970s, the work of Levine [33, 32], Casson–Gordon [4], and many others revealed many more sophisticated invariants that obstruct knots from being slice. These authors were primarily interested in smooth concordance, since the only known constructions of slice disks were smooth; nevertheless, their tools are essentially descriptions of the algebraic topology of the knot complement, so they only obstruct a knot from being

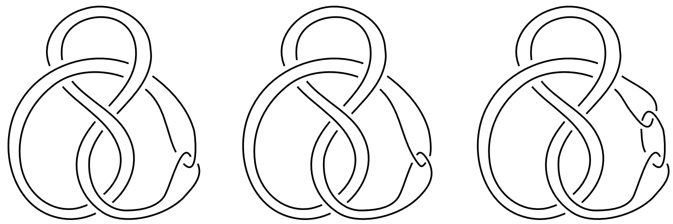

Figure 1: The positive and negative Whitehead doubles and the Bing double of the figure-eight knot.

topologically slice.

Two major revolutions in four-dimensional topology in the 1980s began to illustrate the vast differences between topological and smooth concordance. As part of his major work on topological 4-manifolds and surgery, Freedman [11] showed that any knot whose Alexander polynomial is 1 is topologically slice, even though it is difficult to describe the slice disks explicitly. In particular, the *untwisted, positive and negative Whitehead doubles* of any knot K, denoted $Wh_\pm(K)$ (Figure 1), are topologically slice. Moreover, some of the major outstanding conjectures regarding topological 4-manifolds — notably, whether the surgery techniques Freedman used to classify simply-connected 4-manifolds can be extended to 4-manifolds with arbitrary fundamental group — are equivalent to conjectures about the sliceness of particular families of links in S^3.

Around the same time, the advent of Donaldson's gauge theory made it possible to show that some of Freedman's examples of topologically slice knots are not smoothly slice. Akbulut [unpublished] first proved in 1983 that the positive, untwisted Whitehead double of the right-handed trefoil is not smoothly slice. Later, using results of Kronheimer and Mrowka on Seiberg–Witten theory, Rudolph [60] showed that any nontrivial knot that is *strongly quasipositive* cannot be smoothly slice. In particular, the positive, untwisted Whitehead double of a strongly quasipositive knot is strongly quasipositive; thus, by induction, any iterated positive Whitehead double of a strongly quasipositive knot is topologically but not smoothly slice. Bižaca [2] used this result to give explicit constructions of exotic smooth structures on $\mathbb{R}^4$.

In the 2000s, Ozsváth and Szabó [50, 53] introduced *Heegaard Floer homology*, a package of invariants for 3- and 4-dimensional manifolds that are conjecturally equivalent to earlier gauge-theoretic invariants but whose construction is much more topological in flavor. In its simplest form, given a *Heegaard diagram* $\mathcal{H}$ for a 3-manifold Y (a certain combinatorial description of the manifold), the theory assigns a chain complex $\widehat{\mathrm{CF}}(\mathcal{H})$ whose chain homotopy type is independent of the choice of diagram; thus, the homology $\widehat{\mathrm{HF}}(Y) = H_*(\widehat{\mathrm{CF}}(\mathcal{H}))$ is an invariant of the 3-manifold. A 4-dimensional cobordism between two 3-manifolds induces a well-defined map between their Heegaard Floer homology groups. Ozsváth and Szabó [49] and Rasmussen [56] also showed that a nulhomologous knot $K \subset Y$ induces a filtration on the chain complex of a suitably defined Heegaard diagram, yielding an knot invariant $\widehat{\mathrm{HFK}}(Y, K)$ that is the E^1 page of a spectral sequence converging to $\widehat{\mathrm{HF}}(Y)$. For knots in S^3, the invariant $\widehat{\mathrm{HFK}}(S^3, K)$ categorifies the Alexander polynomial Δ_K, and it is powerful enough to detect the unknot [48] and whether or not K is fibered [12, 44].

Furthermore, the spectral sequence from $\widehat{\mathrm{HFK}}(S^3, K)$ to $\widehat{\mathrm{HF}}(S^3) \cong \mathbb{Z}$ provides an integer-valued concordance invariant $\tau(K)$, which yields a lower bound on genus of smooth surfaces in the four-ball bounded by K: $|\tau(K)| \leq g_4(K)$ [46]. In particular, any smoothly slice knot must have $\tau(K) = 0$. The τ invariant obstructs many topologically slice knots from being smoothly slice. For example, Hedden [20] computed the value of τ for all *twisted Whitehead doubles* in terms of τ of the original knot:

$$\tau(Wh_+(K,t)) = \begin{cases} 1 & t < 2\tau(K) \\ 0 & t \geq 2\tau(K). \end{cases} \tag{1.1}$$

(An analogous formula for negative Whitehead doubles follows from the fact that $\tau(\bar{K}) = -\tau(K)$.) In particular, if $\tau(K) > 0$, then $\tau(Wh_+(K,0)) = 1$, so $Wh_+(K,0)$ (the untwisted Whitehead double of K) is not smoothly slice. Since the τ invariant of a strongly quasipositive knot is equal to its genus [36], Rudolph's result follows from

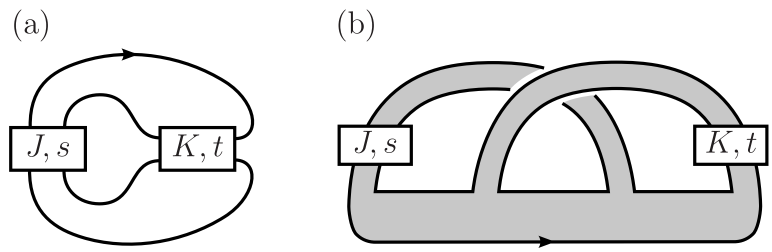

Figure 2: (a) The knot $D_{J,s}(K,t)$. (b) A genus-1 Seifert surface for $D_{J,s}(K,t)$.

Hedden's.

We consider the following generalization of Whitehead doubling. For knots J, K and integers s, t, let $D_{J,s}(K,t)$ denote the knot shown in Figure 2(a); the box marked K, t (resp. J, s) indicates that the strands are tied along t-framed (resp. s-framed) parallel copies of the tangle $K \smallsetminus \{\text{pt}\}$ (resp. $J \smallsetminus \{\text{pt}\}$. (We give a more formal definition in Chapter 2.) If J is the unknot and $s = \pm 1$, then $D_{J,s}(K,t)$ is the t-twisted $\mp$ Whitehead double of K.

A genus-1 Seifert surface for $D_{J,s}(K,t)$ is shown in Figure 2(b). From the Seifert form of this surface, we can compute that the Alexander polynomial of $D_{J,s}(K,t)$ is

$$\Delta_{D_{J,s}(K,t)}(T) = stT + (1 - 2st) + stT^{-1}.$$

In particular, this equals 1 whenever $s = 0$ or $t = 0$. By Freedman's theorem, $D_{J,s}(K,0)$ is therefore topologically slice. Moreover, if K is smoothly slice, then $D_{J,s}(K,0)$ is smoothly slice for any (J,s). To see this, perform a ribbon move to eliminate the band that is tied into J; the resulting two-component link, consisting of two parallel copies of K with linking number 0, is then the boundary of two parallel copies of a slice disk for K. There is a famous conjecture (Problem 1.38 on Kirby's problem list [26]) that the untwisted Whitehead double of K is smoothly slice if and only if K is smoothly slice; this conjecture has many potential generalizations in terms of $D_{J,s}(K,0)$ satellites.

As a partial result in this direction, we prove the following theorem:

Theorem 1.1. *Let J and K be knots, and let $s, t \in \mathbb{Z}$. Then*

$$\tau(D_{J,s}(K,t)) = \begin{cases} 1 & s < 2\tau(J) \text{ and } t < 2\tau(K) \\ -1 & s > 2\tau(J) \text{ and } t > 2\tau(K) \\ 0 & \text{otherwise.} \end{cases}$$

In particular, if $\tau(K) > 0$ and $s < 2\tau(J)$, or if $\tau(K) < 0$ and $s > 2\tau(J)$, then $D_{J,s}(K,0)$ is topologically but not smoothly slice.

Although the definition of the Heegaard Floer invariants is more topological than that of the earlier gauge-theoretic invariants, it still depends on studying moduli spaces of holomorphic curves, which is in general a difficult analytic problem. Many recent advances [41, 42, 62, 1, 43] make it possible to compute any particular Heegaard Floer invariant algorithmically, but they require large amounts of computing power and generally cannot be used to prove statements about infinite families of manifolds or knots, such as Theorem 1.1. The theory of *bordered Heegaard Floer homology*, developed recently by Lipshitz, Ozsváth, and Thurston [35, 34], is well-suited to this problem. Briefly, it associates to a 3-manifold with boundary a module over an algebra associated to the boundary, so that if $Y = Y_1 \cup Y_2$, the chain complex $\widehat{\mathrm{CF}}(Y)$ may be computed as the derived tensor product of the invariants associated to Y_1 and Y_2. If a knot K is contained in, say, Y_1, then we may obtain the filtration on $\widehat{\mathrm{CF}}(Y)$ corresponding to K via a filtration on the algebraic invariant of Y_1. (We give a longer description of this theory in Section 3.1.) Satellite knots such as $D_{J,s}(K,t)$ are easily described in terms of such gluings, so the bordered package is useful for computing the Heegaard Floer invariants of such knots.

Theorem 1.1 has a useful application to the study of Whitehead doubles of links (which was the author's original motivation for considering it). Specifically, we consider the Whitehead doubles of links obtained by *iterated Bing doubling.* Given a knot K, the *(untwisted) Bing double* of K is the two-component link $BD(K)$ shown in Figure 1. More generally, given a link L, we may replace a component by its

Bing double (contained in a tubular neighborhood of that component), and iterate this procedure. Bing doubling one component of the Hopf link yields the Borromean rings; accordingly, we define the family of *generalized Borromean links* as the set of all links obtained as iterated Bing doubles of the Hopf link. We prove:

Theorem 1.2. *Let L be any link obtained by iterated Bing doubling from either:*

1. *Any knot K with $\tau(K) > 0$, or*

2. *The Hopf link.*

Then the all-positive Whitehead double of L, $Wh_+(L)$, is not smoothly slice.

The links considered in Theorem 1.2 play an important role in the work of Freedman on topological 4-manifolds. First, notice that any iterated Bing double of a knot is a *boundary link*, i.e., its components bound disjoint Seifert surfaces. (See, e.g., [8] for a proof.) Freedman proved that the Whitehead doubles (with any choice of signs of the clasps) of any boundary link are topologically slice. Theorem 1.2 thus provides a large family of links that are topologically but not smoothly slice. On the other hand, the generalized Borromean links are not boundary links, and whether or not their Whitehead doubles (again, with any signs) are topologically slice is a major open question in 4-manifold theory, equivalent to the surgery conjecture for 4-manifolds with arbitrary fundamental group. Most experts nowadays conjecture that Whitehead doubles of generalized Borromean links are *not* topologically slice, but the problem remains unsolved after nearly twenty-five years.

The requirement that we consider all-positive Whitehead doubles is necessary for our proof of Theorem 1.2. By taking mirrors, we also see that the all-negative Whitehead doubles of iterated Bing doubles of knots with $\tau(K) < 0$ or of generalized Borromean links are not smoothly slice, but our method always fails when both positive and negative Whitehead doubling are used. Indeed, all of the gauge-theoretic invariants known to date suffer from the same asymmetry; it is still not known whether, for instance, the positive untwisted Whitehead double of the left-handed trefoil is smoothly slice.

Because the proof of Theorem 1.1 is quite technical, we begin by proving its corollary, Theorem 1.2, in Chapter 2. (That proof first appeared in [30].) We then provide an introduction to bordered Heegaard Floer homology and prove Theorem 1.1 in Chapter 3.

In another direction, the Heegaard Floer homology of branched covers of knots can be used to study the *smooth knot concordance group.* Because the connect sum of a knot and its reversed-orientation mirror is always smoothly slice, the set of smooth concordance classes of oriented knots forms an abelian group $\mathcal{C}_1$ under the connect sum operation. The *smooth concordance order* of a knot is the order of K in $\mathcal{C}_1$. The structure of the torsion in $\mathcal{C}_1$ is of considerable interest, especially by comparison to the higher-dimensional concordance groups $\mathcal{C}_n$ (consisting of concordance classes of knotted n-dimensional spheres in S^{n+2} for n odd). J. Levine [33, 32] showed in the 1960s that for $n > 1$, certain algebraic invariants coming from Seifert forms completely determine the concordance class of an n-knot. Specifically, his invariants determine a map

$$\Phi_n : \mathcal{C}_n \to \mathbb{Z}^\infty \oplus \mathbb{Z}_2^\infty \oplus \mathbb{Z}_4^\infty,$$

which is an isomorphism for $n > 1$. In contrast, for $n = 1$, this classification theorem fails. While Φ_1 is surjective, Casson and Gordon [4] found knots that are *algebraically slice* but not smoothly (or even topologically) slice and hence represent nontrivial elements of $\ker \Phi_1$. Moreover, the only known torsion in $\mathcal{C}_1$ is 2-torsion coming from amphichiral knots; no knots of finite concordance order greater than 2 are known. At the same time, obstructing knots from representing torsion elements of $\mathcal{C}_1$ is difficult. In particular, integer-valued concordance invariants that are additive under connected sum — such as the classical signature, τ, the Manolescu–Owens δ invariant [40], and Rasmussen's s invariant coming from Khovanov homology [55] — necessarily vanish for any knot that is torsion.

Around 2000, Livingston and Naik [37, 38] used Casson–Gordon invariants to find the first known examples of knots that have algebraic concordance order 4 but infinite smooth concordance order. Shortly thereafter, Jabuka and Naik [24] and Grigsby, Ruberman, and Strle [16] used the *correction terms* coming from Heegaard Floer homology to find other such examples. Both of these arguments rely on obstructing the intersection forms of 4-manifolds that are bounded by cyclic branched covers of a knot K; thus, computing the Heegaard Floer homology of these covers acquires great importance. Grigsby, Ruberman, and Strle also found invariants coming from the knot Floer homology of the preimage of a knot in its cyclic branched covers, providing further obstructions to finite concordance order.

Using techniques of Ozsváth and Szabó for computing correction terms, we show that many of the knots through eleven crossings whose smooth concordance orders were previously unknown have infinite order [29]. Additionally, we describe an algorithm for computing the knot Floer homology of the preimage of a knot in any cyclic branched cover [31] and use it to compute the Grigsby–Ruberman–Strle invariants of some of the remaining knots on the list. This work is presented in Chapter 4.

Chapter 2

Whitehead doubles of iterated Bing doubles

In this chapter, we prove Theorem 1.2, making use of Theorem 1.1. An earlier version of this work appeared in [30].

2.1 Infection and doubling operators

We begin by giving more precise definitions of some of the terms used in the Introduction.

We always work with *oriented* knots and links. For any knot $K \subset S^3$, let K^r denote K with reversed orientation, let $\bar{K}$ denote the mirror of K (the image of K under a reflection of S^3), and let $-K = \bar{K}^r$. As $K\#-K$ is always smoothly slice, the concordance classes of K and $-K$ are inverses in $\mathcal{C}_1$, which justifies this choice of notation. Note that the invariants coming from Heegaard Floer homology ($\widehat{\mathrm{HFK}}(S^3, K)$, $\tau(K)$, etc.) are sensitive to mirroring but not to reversing the orientation of a knot.

Suppose L is a link in S^3, and γ is an oriented curve in $S^3 \smallsetminus L$ that is unknotted in S^3. For any knot $K \subset S^3$ and $t \in \mathbb{Z}$, we may form a new link $I_{\gamma,K,t}(L)$, the *t-twisted infection of L by K along* γ, by deleting a neighborhood of γ and gluing in a copy of the exterior of K by a map that takes a Seifert-framed longitude of K to a meridian of γ and a meridian of K to a t-framed longitude of γ. Since $S^3 \smallsetminus \gamma = S^1 \times D^2$, the resulting 3-manifold is simply ∞ surgery on K, i.e. S^3; the new link $I_{\gamma,K,t}(L)$ is defined as the image of L. Alternately, let $\hat{K} \subset D^2 \times I$ be the $(1,1)$-tangle obtained by cutting K at a point, oriented from $\hat{K} \cap D^2 \times \{0\}$ to $\hat{K} \cap D^2 \times \{1\}$. If D is an oriented disk in S^3 with boundary γ, meeting L transversely in n points, we may obtain $I_{\gamma,K,t}(L)$ by cutting open L along D and inserting the tangle consisting of n parallel copies of $\hat{K}$, following the t framing. In a link diagram, a box labeled K, t in a group of parallel strands indicates t-twisted infection by K along the boundary of a disk perpendicular to those strands. To be precise, we adopt the following orientation convention: If the label K, t is written horizontally and right-side-up, then $\hat{K}$ is oriented either from bottom to top or from left to right, depending on whether the strands meeting the box are positioned vertically or horizontally.[1] Using this convention, we may easily verify that the two oriented knots in Figure 2 are isotopic.

Given unlinked infection curves γ_1, γ_2, the image of γ_2 in $I_{\gamma_1,K_1,t_1}(L \cup \gamma_2)$ is again an unknot, so we may then infect by another pair K_2, t_2. We obtain the same result if we infect along γ_2 first and then γ_1. In general, given an unlink $\gamma_1, \dots, \gamma_n$, we may infect simultaneously along all the γ_i; the result may be denoted $I_{\gamma_1,K_1,t_1;\cdots;\gamma_n,K_n,t_n}(L)$, and the order of the tuples (γ_i, K_i, t_i) does not matter.

If P is a knot (or link) in the standardly embedded solid torus in S^3 and K is any knot, the *t-twisted satellite of K with pattern P*, $P(K, t)$, is defined as $I_{\gamma,K,t}(P)$, where γ is the core of the complementary solid torus. The knot K is called the *companion*. More generally, if we have a link L, we may replace a component of L by its satellite with pattern P, working in a tubular neighborhood disjoint from the other components.

Let $B = B_1 \cup B_2 \cup B_3$ denote the Borromean rings in S^3, oriented as shown in Figure 3. Then $D_{J,s}(K, t)$ is the knot obtained from B_3 by performing s-twisted

[1]We allow both types of notation to avoid writing labels vertically.

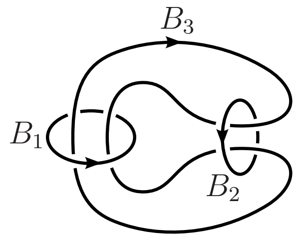

Figure 3: The Borromean rings.

infection by J along B_1 and t-twisted infection by K along B_2:

$$D_{J,s}(K,t) = I_{B_1,J,s;\,B_2,K,t}(B_3).$$

In particular, $D_{O,\pm1}(K,t) = I_{B_1,O,\pm1;B_2,K,t}(B_3)$ is the t-twisted $\mp$ Whitehead double of K (where O denotes the unknot). Under our orientation conventions, this definition agrees with the definition of $D_{J,s}(K,t)$ given in the Introduction. The symmetries of the Borromean rings imply:

$$D_{J,s}(K,t)^r = D_{J^r,s}(K,t) = D_{J,s}(K^r,t) = D_{K,t}(J,s)$$
$$\overline{D_{J,s}(K,t)} = D_{\bar{J},-s}(\bar{K},-t)$$

We also introduce the convention that when the t argument is omitted, it is taken to be zero: $D_{J,s}(K) = D_{J,s}(K,0)$.

The Bing double of K may be defined as $BD(K) = I_{B_1,K,0}(B_2 \cup B_3)$; we may also see this as a satellite operation where the pattern is a two-component link. We may consider *iterated Bing doubles* of any link: at each stage in the iteration, we replace some component by its Bing double. Specifically, given a knot K, a binary tree T specifies such a link $B_T(K)$, as illustrated in Figure 4, with one component for each leaf of T. For a link $L = K_1 \cup \cdots \cup K_n$ and binary trees $T_1, \ldots, T_n$, we may similarly obtain a link $B_{T_1,\ldots,T_n}(L) = B_{T_1}(K_1) \cup \cdots \cup B_{T_n}(K_n)$. As stated in the Introduction, the *generalized Borromean links* are those obtained as $B_{T_1,T_2}(H)$, where H is the Hopf link.

The *all-positive Whitehead double* of a link L, $Wh_+(L)$, is obtained by replacing every component of L by its untwisted, positive Whitehead double.

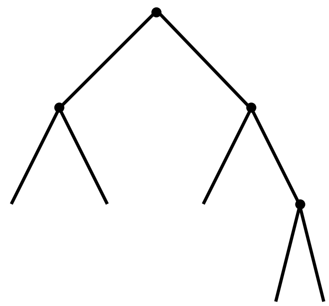

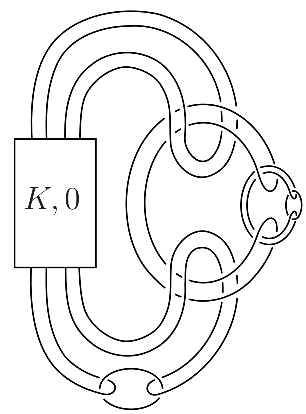

Figure 4: A binary tree T and the corresponding iterated Bing double $B_T(K)$.

Using this terminology, a more precise statement of Theorem 1.2 is as follows:

Theorem 2.1.

1. *Let K be a knot with $\tau(K) > 0$, and let T be any binary tree. Then the all-positive Whitehead double of $B_T(K)$, $Wh_+(B_T(K))$, is not smoothly slice.*

2. *Let $H = K_1 \cup K_2$ denote the Hopf link, and let T_1, T_2 be binary trees. Then $Wh_+(B_{T_1,T_2}(H))$ is not smoothly slice.*

The basic strategy in the proof of the first part of Theorem 2.1 is to use the *covering link calculus* developed by Cha and Kim [5] to obtain from $Wh_+(B_T(K))$ a new knot K', such that if $Wh_+(B_T(K))$ is smoothly slice, then K' is *rationally smoothly slice* — i.e., it bounds a smoothly embedded disk in a smooth rational homology 4-ball with boundary S^3. The knot K' is a satellite of the form $D_{J_1,s_1} \circ \cdots \circ D_{J_n,s_n}(K)$, where $s_i < 2\tau(J_i)$ for each i. If $\tau(K) > 0$, induction using Theorem 1.1 (which we prove in Chapter 3) shows that $\tau(K') = 1$, so K' cannot be rationally smoothly slice, so $Wh_+(D_T(K))$ cannot be smoothly slice.[2] A similar argument works for the second part of the theorem. These proofs are found in the next section.

[2]Cha and Kim used this technique to study when iterated Bing doubles of a knot are slice, which

2.2 Covering link calculus

Let R denote any of the rings $\mathbb{Z}$, $\mathbb{Q}$, or $\mathbb{Z}_{(p)}$ (for p prime). A link L in an R-homology 3-sphere Y is called *topologically (resp. smoothly) R-slice* if there exists a topological (resp. smooth) 4-manifold X such that $\partial X = Y$, $H_*(X;R) = H_*(B^4;R)$, and L bounds a locally flat (resp. smoothly embedded), disjoint union of disks in X. A link that is $\mathbb{Z}$-slice (in either category) is $\mathbb{Z}_{(p)}$-slice for all p, and a link that is $\mathbb{Z}_{(p)}$-slice for some p is $\mathbb{Q}$-slice. Also, a link in S^3 that is slice (in B^4) is clearly $\mathbb{Z}$-slice. The key result of Ozsváth and Szabó [46] is that the τ invariant of any knot that is smoothly $\mathbb{Q}$-slice is 0.

Cha and Kim [5] define two moves on links in $\mathbb{Z}_{(p)}$-homology spheres, called *covering moves*:

1. Given a link $L \subset Y$, consider a sublink $L' \subset L$.

2. Given a link $L \subset Y$, choose a component K with trivial self-linking. For any $a \in \mathbb{N}$, the p^a-fold cyclic branched cover of Y branched over K, denoted $\tilde{Y}$, is a $\mathbb{Z}_{(p)}$-homology sphere, and we consider the preimage L' of L in $\tilde{Y}$.

We say that $L' \subset Y'$ is a *p-covering link* of $L \subset Y$ if L' can be obtained from Y' using these moves. If L is $\mathbb{Z}_{(p)}$-slice, then any p-covering link of L is also $\mathbb{Z}_{(p)}$ slice (in either category). For the second move, the p^a-fold cyclic branched cover of X over a slice disk for K becomes the new 4-manifold bounded by $\tilde{Y}$; it is a $\mathbb{Z}_{(p)}$-homology sphere by a well-known argument [25, page 346]. Henceforth, we restrict to the case where $p = 2$ and omit further reference to p.

Note that if L is a link in S^3 whose components are unknotted, then the branched cover branched over one component is again S^3. The putative 4-manifold containing a slice disk, however, may change.

---

is challenging since the classical sliceness obstructions all vanish [8, 7]. They showed that if any iterated Bing double of K is topologically slice, then K is algebraically slice; if it is smoothly slice, then $\tau(K) = 0$. Our techniques are based on their work and a reformulation by Van Cott [63].

To prove Theorem 2.1, we need the following lemmas:

Lemma 2.2. *Let L be a link in S^3, and suppose there is an unknotted solid torus $U \subset S^3$ such that $L \cap U$ consists of two components K_1, K_2 embedded as follows: if A_1, A_2 are the components of the untwisted Bing double of the core C of U, then $K_1 = D_{P_k,s_k} \circ \cdots \circ D_{P_1,s_1}(A_1)$ and $K_2 = D_{Q_l,t_l} \circ \cdots \circ D_{Q_1,t_1}(A_2)$, for some knots $P_1, \dots, P_k, Q_1, \dots, Q_l$ and integers $s_1, \dots, s_k, t_1, \dots, t_l$. Let L' be the link obtained from L by replacing K_1 and K_2 by the satellite knot*

$$C' = D_{P_k,s_k} \circ \cdots \circ D_{P_1,s_1} \circ D_{R,u}(C) \tag{2.1}$$

of C, where

$$(R,u) = \begin{cases} (Q_1 \# Q_1^r,\ 2t_1) & l = 1 \\ (D_{Q_1,t_1} \circ \cdots \circ D_{Q_{l-2},t_{l-2}}(D_{Q_{l-1},t_{l-1}}(Q_l \# Q_l^r, 2t_l)),\ 0) & l > 1. \end{cases} \tag{2.2}$$

Then L' is a covering link of L.

Proof. Let $T = S^3 \smallsetminus U$; then $L \smallsetminus (K_1 \cup K_2)$ is contained in T. Note that K_1 and K_2 are each unknotted, since $D_{J,s}(O,0) = O$ for any J, s. We may untangle K_2 as in Figures 5–6. Specifically, L is shown in Figures 5(a) and (b). To obtain Figure 5(c), we pull the two strands of the companion curve for K_1 through the infection region marked Q_1, t_1, and then untangle the companion curve for K_2. We then repeat this procedure to obtain Figure 5(d), and $l-2$ more times to obtain Figure 6.

The branched double cover of S^3 branched along K_2 is again S^3; consider the preimage of $K_1 \cup (L \cap T)$, shown in Figure 7. (The knot orientation conventions for infections are important here, since the knots Q_i need not be reversible.) Since T is contained in a ball disjoint from K_1, the sublink $L \cap T$ lifts to two identical copies, each contained in a solid torus. The preimage of K_2 also consists of two components, and each is the $D_{P_k,s_k} \circ \cdots \circ D_{P_1,s_1}$ satellite of the companion curve shown. A sublink consisting of one lift of each component (either the blue or the black part of Figure

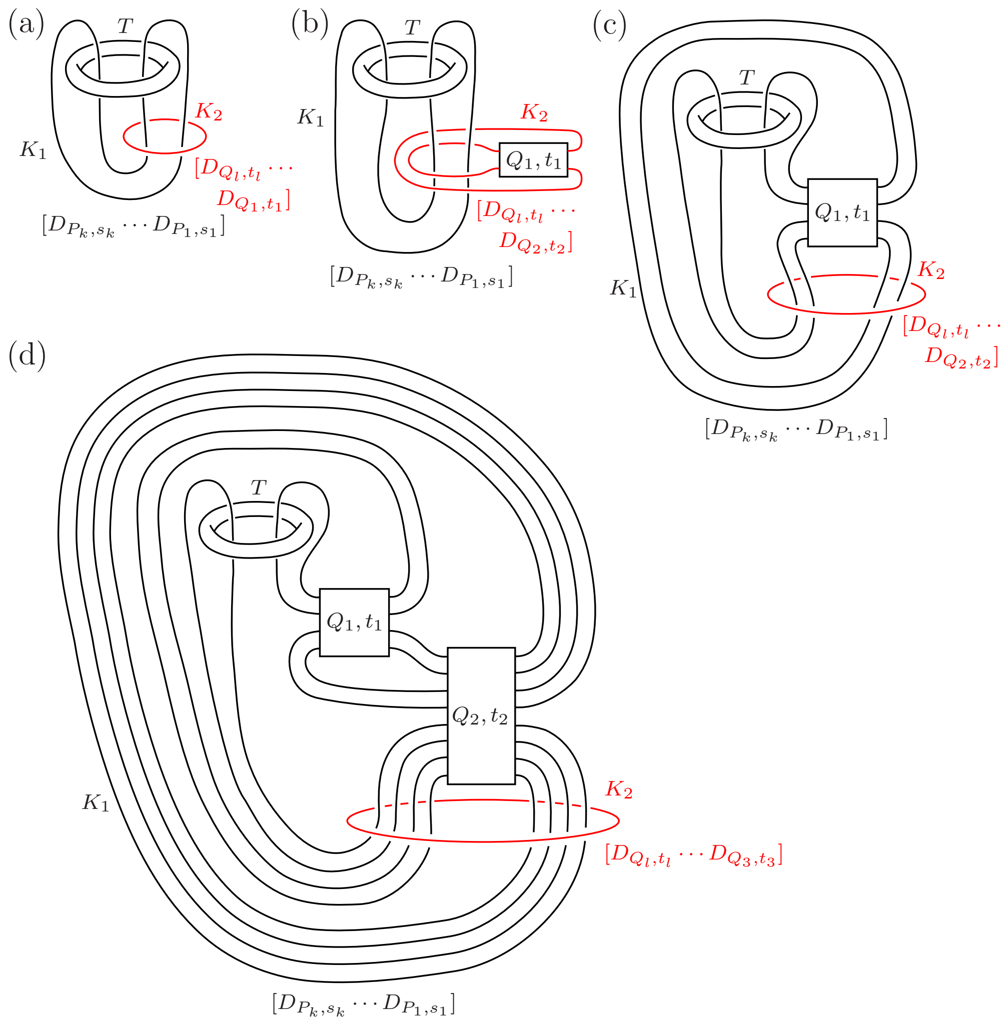

Figure 5: The link described in Lemma 2.2. All but the two components shown are contained in the interior of the solid torus T. We denote a satellite knot by writing the pattern in brackets near the companion curve; thus, for instance, $K_1 = D_{P_k,s_k} \circ \cdots \circ D_{P_1,s_1}(A_1)$, where A_1 is the curve shown.

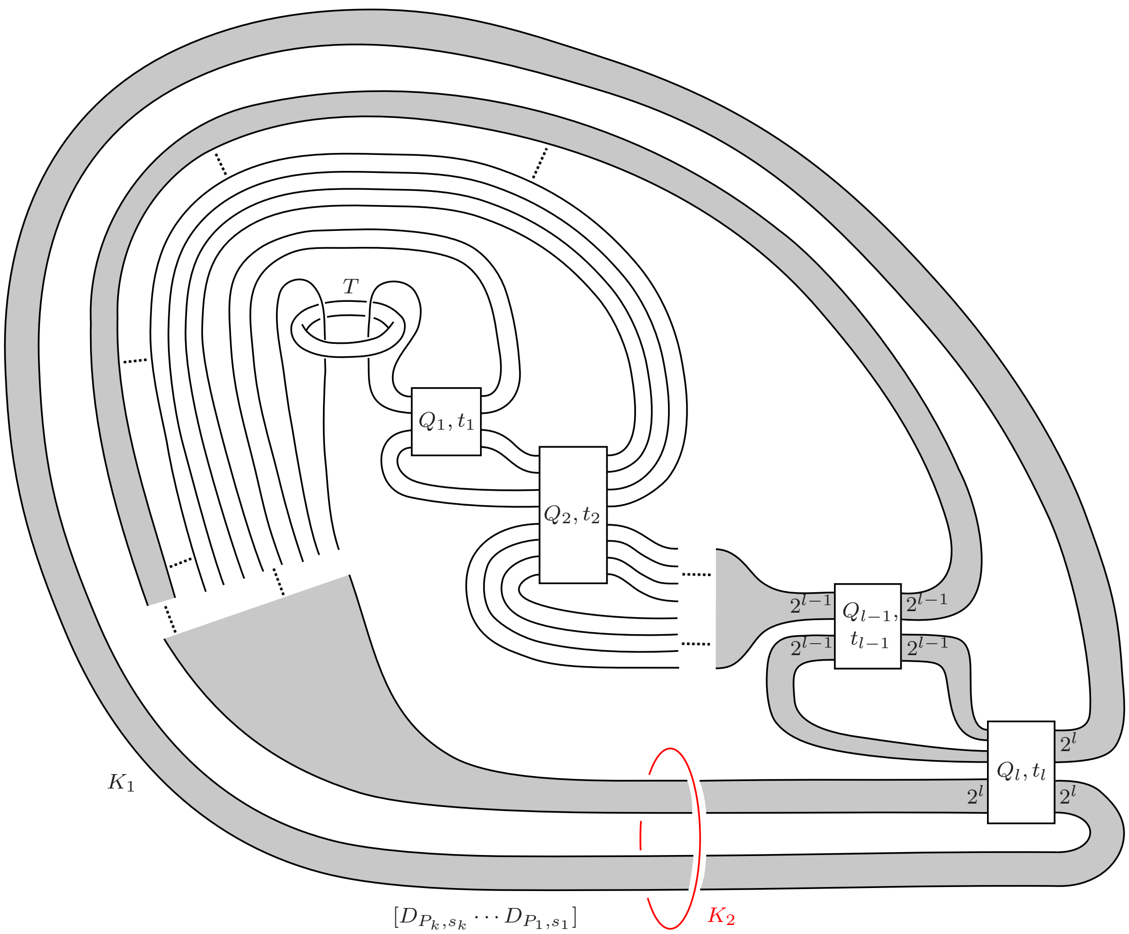

Figure 6: The link described in Lemma 2.2, after isotopies. A shaded region with a number represents that many parallel strands.

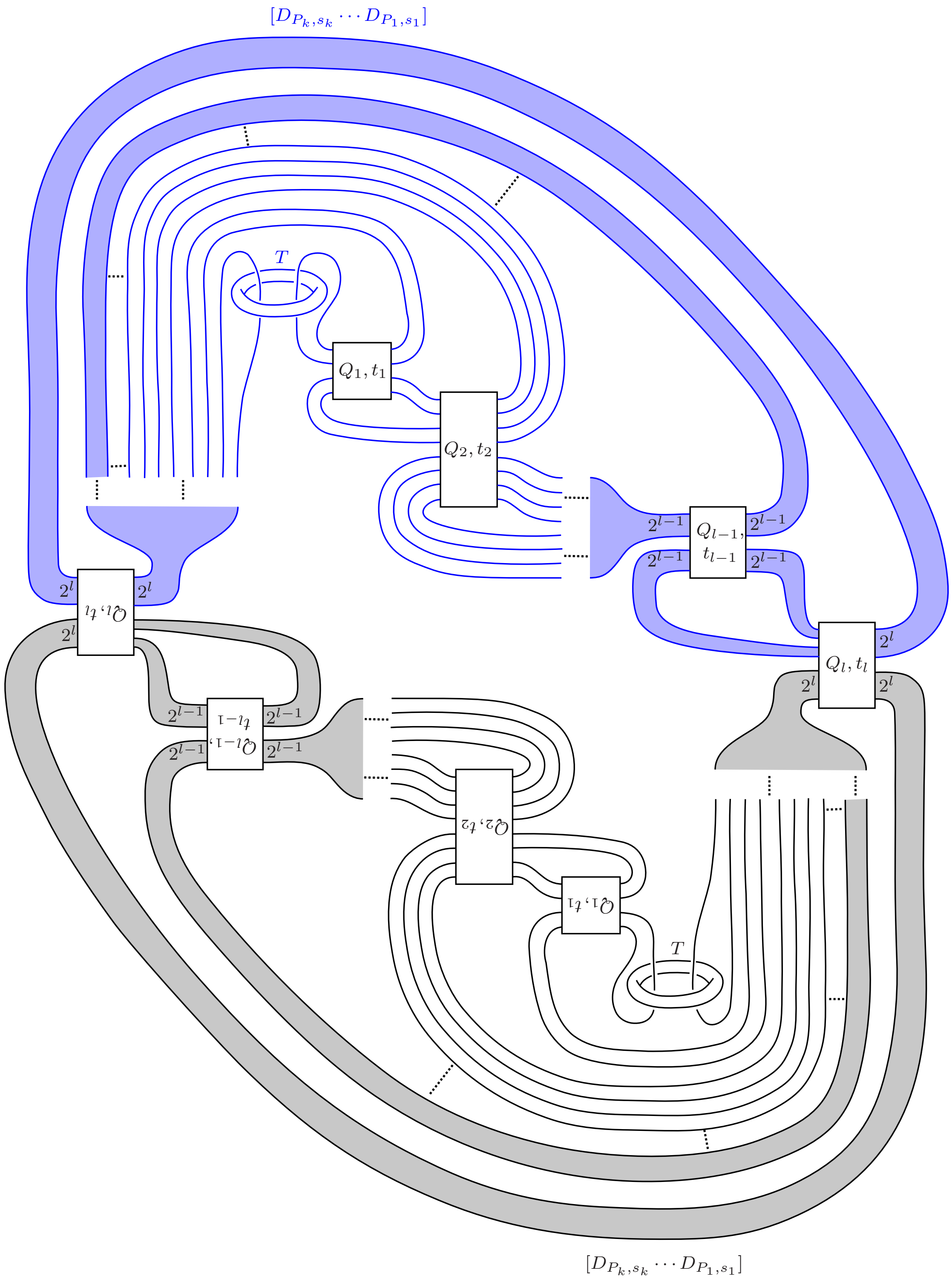

Figure 7: The preimage of the link in Figure 6 in the double-branched cover of S^3 over K_2 (shown without the upstairs branch set).

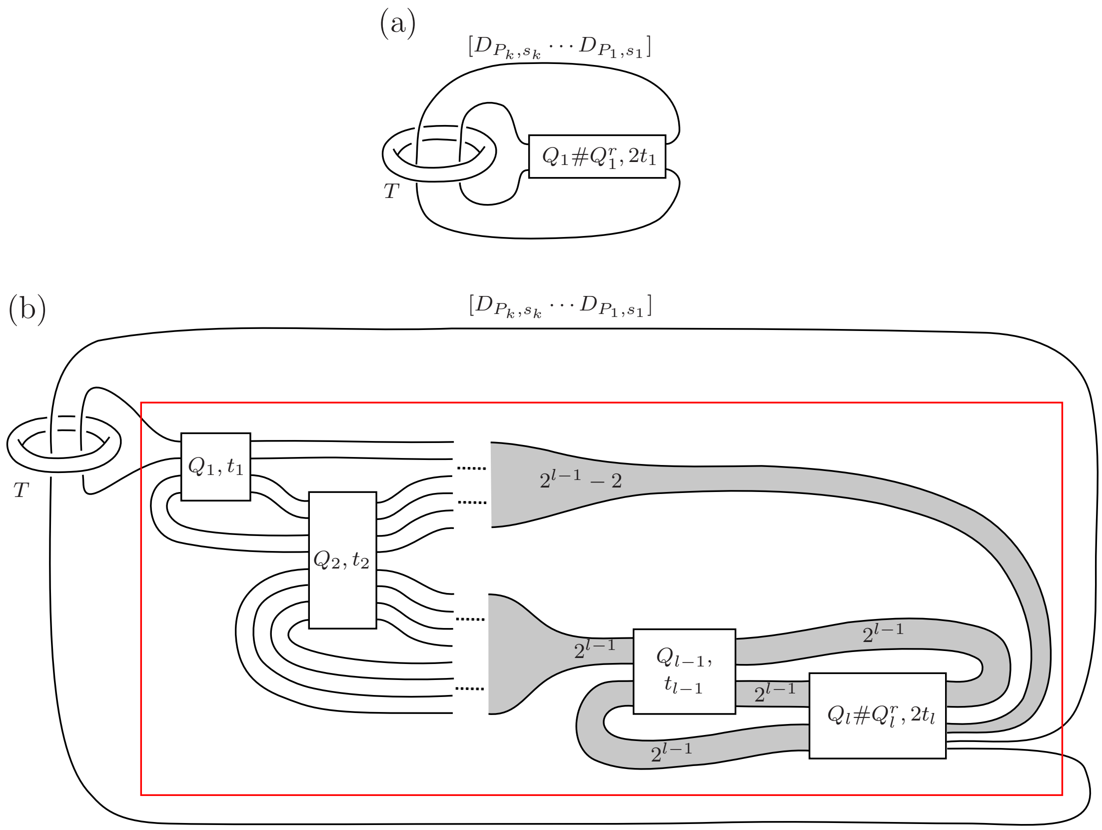

Figure 8: The sublink shown in blue in Figure 7 is the $D_{P_k,s_k} \circ \cdots \circ D_{P_1,s_1}$ satellite of: (a) when $l = 1$, $D_{Q_1 \# Q_1^r, 2t_1}(C)$; (b) when $l > 1$, $D_{R,0}(C)$, where R is the knot in Figure 9.

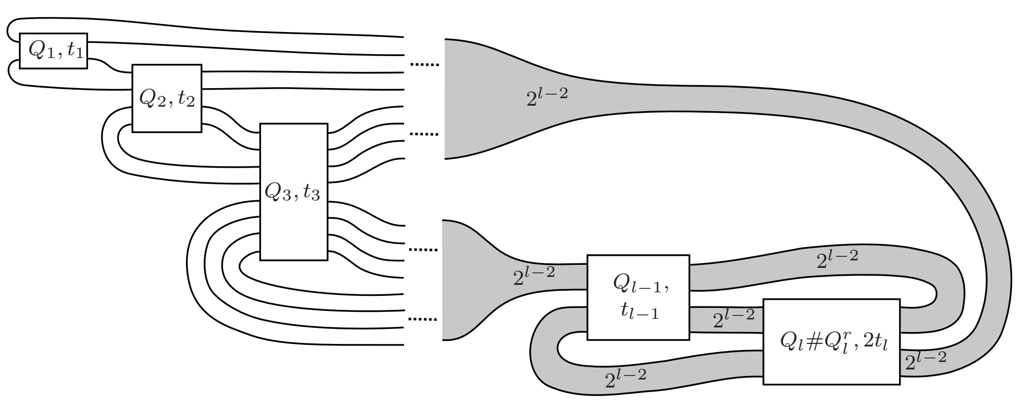

Figure 9: The knot R in the proof of Lemma 2.2.

7) is redrawn in Figure 8(a) in the case where $l = 1$ and in Figure 8(b) in the case where $l > 1$. In the former case, the companion curve shown is $D_{Q_l \# Q_l^r, 2t_l}(C)$, where C is the core circle of the complement of T. In the latter case, it is $D_{R,0}(C)$, where we obtain R by connecting the ends of one of the two parallel strands that pass through the red box in Figure 8(b). (A local computation shows that the linking number of these two strands is zero, so $D_{R,0}$ is the correct operator.) The knot R, shown in Figure 9, is then identified as

$$D_{Q_1,t_1} \circ \cdots \circ D_{Q_{l-2},t_{l-2}}(D_{Q_{l-1},t_{l-1}}(Q_l \# Q_l^r, 2t_l)). \qquad \square$$

Lemma 2.3. *Let C be a knot, let U be a regular neighborhood of C, and let $A_1, A_2 \subset U$ be the components of $BD(C)$. Let $K_1 = D_{P_k,s_k} \circ \cdots \circ D_{P_1,s_1}(A_1)$ and $K_2 = D_{Q_l,t_l} \circ \cdots \circ D_{Q_1,t_1}(A_2)$, for some knots $P_1, \ldots, P_k, Q_1, \ldots, Q_l$ and integers $s_1, \ldots, s_k, t_1, \ldots, t_l$. Let C' be the knot defined by* (2.1) *and* (2.2)*. Then C' is a covering link of $K_1 \cup K_2$.*

Proof. The proof is almost identical to that of Lemma 2.2. The only difference is that $S^3 \smallsetminus U$ is now a knot complement rather than a solid torus containing some additional link components. The double branched cover over K_2 contains consists of the complement of the two solid tori shown in Figure 7, glued to two copies of $S^3 \smallsetminus U$, gluing Seifert-framed longitude to meridian and vice versa. The resulting manifold is again S^3, however. The rest of the proof proceeds *mutatis mutandis.* (Alternately, we may simply replace each of the solid tori in Figures 5–9 by a box marked $C, 0$, and proceed as before.) $\square$

A *labeled binary tree* is a binary tree with each leaf labeled with a satellite operation. Given a knot K and binary tree $\mathcal{T}$ with underlying tree T, let $S_{\mathcal{T}}(K)$ be the link obtained from $B_T(K)$ by replacing each component with the satellite specified by the label of the corresponding leaf. If $\mathcal{T}$ has two adjacent leaves labeled $D_{P_k,s_k} \circ \cdots \circ D_{P_1,s_1}$ and $D_{Q_l,t_l} \circ \cdots \circ D_{Q_1,t_1}$, form a new labeled tree $\mathcal{T}'$ by deleting these two leaves and labeling the new leaf either $D_{P_k,s_k} \circ \cdots \circ D_{P_1,s_1} \circ D_{Q_1 \# Q_1^r, 2t_1}(C)$ or $D_{P_k,s_k} \circ \cdots \circ D_{P_1,s_1} \circ D_{R,0}$, according to whether $l = 1$ or $l > 1$, respectively, where,

$R = D_{Q_1,t_1} \circ \cdots \circ D_{Q_{l-2},t_{l-2}}(D_{Q_{l-1},t_{l-1}}(Q_l \# Q_l^r, 2t_1))$ in the latter case. We call this move a *collapse*. Lemmas 2.2 and 2.3 then say that $S_{\mathcal{T}'}(K)$ is a covering link of $S_{\mathcal{T}}(K)$.

Theorem 1.1 and equations (2.1) and (2.2), along with the additivity of τ under connect sum, imply:

Proposition 2.4. *Suppose $\mathcal{T}'$ is obtained from $\mathcal{T}$ by collapsing leaves labeled $D_{P_k,s_k} \circ \cdots \circ D_{P_1,s_1}$ and $D_{Q_l,t_l} \circ \cdots \circ D_{Q_1,t_1}$, where $s_i < 2\tau(P_i)$ and $t_i < 2\tau(Q_i)$ for all i. Then the label of the new leaf of $\mathcal{T}'$ has the form $D_{R_{k+1},u_{k+1}} \circ \cdots \circ D_{R_1,u_1}$, where $u_i < 2\tau(R_i)$.* □

Proof of Theorem 2.1. For the first part of the theorem, note that in the new notation, $Wh_+(B_T(K)) = S_{\mathcal{T}}(K)$, where every leaf of $\mathcal{T}$ is labeled $D_{O,-1}$. Every label in $\mathcal{T}$ satisfies the hypotheses of Proposition 2.4. Using this proposition, we inductively collapse every pair of leaves of $\mathcal{T}$ until we have a single vertex labeled $D_{P_k,s_k} \circ \cdots \circ D_{P_1,s_1}$, for knots $P_1, \ldots, P_k$ and integers $s_1, \ldots, s_k$ with $s_i < 2\tau(P_i)$. Thus, the knot $D_{P_k,s_k} \circ \cdots \circ D_{P_1,s_1}(K)$ is a covering link of $Wh_+(B_T(K))$. By Theorem 1.1, $\tau(D_{P_k,s_k} \circ \cdots \circ D_{P_1,s_1}(K)) = 1$. Thus, $D_{P_k,s_k} \circ \cdots \circ D_{P_1,s_1}(K)$ cannot be smoothly slice in a rational homology 4-ball, so $Wh_+(B_T(K))$ cannot be smoothly slice.

For the second part, the same argument as above shows that by using covering moves, we may replace $Wh_+(B_{T_1}(K_1) \cup B_{T_2}(K_2))$ with a two-component link of the form

$$D_{P_k,s_k} \circ \cdots \circ D_{P_1,s_1}(K_1) \cup D_{Q_l,t_l} \circ \cdots \circ D_{Q_0,t_0}(K_2),$$

shown in Figure 10(a), where $s_i < 2\tau(P_i)$ and $t_i < 2\tau(Q_i)$ for all i. (We start with Q_0 and t_0 for notational reasons.) After the isotopies in Figure 10(a–c), note the similarity to Figure 5. We may thus proceed just as in the proof of Lemma 2.2, with suitable modifications to Figures 6–8, to obtain the knot shown in Figure 10(d) as a covering link of $Wh_+(B_{T_1}(K_1) \cup B_{T_2}(K_2))$. This knot is

$$D_{P_k,s_k} \circ \cdots \circ D_{P_1,s_1}(D_{R,u}(Q_0, t_0)),$$

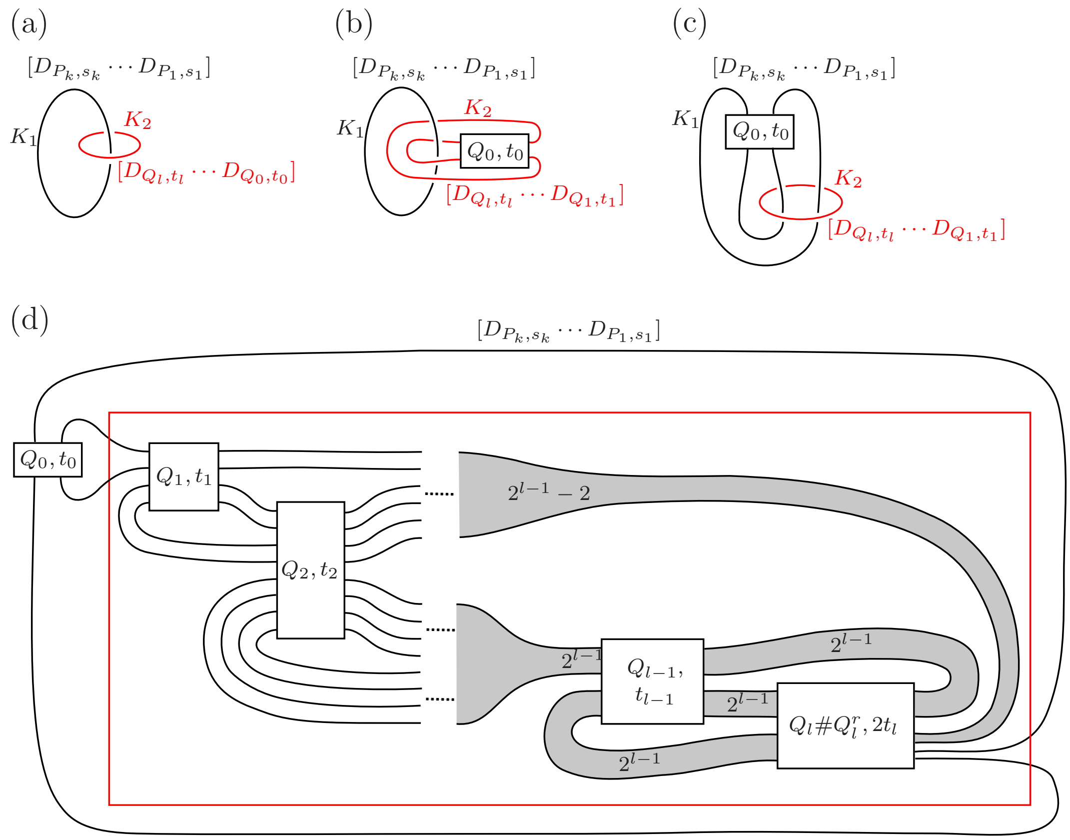

Figure 10: The proof of the second part of Theorem 2.1.

where (R, u) is as in (2.2). This knot has $\tau = 1$ by Theorem 1.1, completing the proof. □

2.3 Strongly quasipositive knots and sliceness

We conclude this section with a brief discussion of strongly quasipositive knots, which played a role in an earlier version of Theorem 2.1.

A knot or link L is called *quasipositive* if it is the closure of a braid that is the product of conjugates of the standard positive braid generators σ_i (but not their inverses). It is called *strongly quasipositive* if it is the closure of a braid that is the product of words of the form $\sigma_i \dots \sigma_{j-1}\sigma_j\sigma_{j-1}^{-1} \dots \sigma_i^{-1}$ for $i < j$. A strongly quasipositive link naturally admits a particular type of Seifert surface determined by this braid form, and an embedded surface in S^3 is called *quasipositive* if it is isotopic to such a surface. In other words, a link is strongly quasipositive if and only if it bounds a quasipositive Seifert surface.

A link L is quasipositive if and only if it is a *transverse* $\mathbb{C}$*-link*: the transverse intersection of $S^3 \subset \mathbb{C}^2$ with a complex curve V. If L is strongly quasipositive, then the Seifert surface determined by the braid form is isotopic to $V \cap B^4$.

For a knot K and $t \in \mathbb{Z}$, let $A(K, t)$ be an annulus in S^3 whose core circle is K and whose two boundary components are t-framed longitudes of the core. Given two unlinked annuli A and A', let $A * A'$ denote the surface obtained by plumbing A and A' together. (To be precise, we must orient the core circles of A and A' and specify the sign of their intersection in $A * A'$.)

The following is a summary of some of Rudolph's results [59, 60, 61] on strongly quasipositive knots:

Theorem 2.5.

1. *If K is a strongly quasipositive knot other than the unknot, then K is not smoothly slice.*

2. *A knot K is strongly quasipositive if and only if $A(K,0)$ is a quasipositive surface.*

3. *If K and K' are strongly quasipositive, then $K\#K'$ is strongly quasipositive.*

4. *The annulus $A(K,t)$ is quasipositive if and only if $t \leq TB(K)$, where $TB(K)$ denotes the maximal Thurston–Bennequin number of K.*

5. *If A and A' are annuli, then the surface $A * A'$ is quasipositive if and only if A and A' are both quasipositive.*

Rudolph's original proof of (1) relies on the fact that complex curves are genus-minimizing, a major theorem proven by Kronheimer and Mrowka [27] using gauge theory. Since a strongly quasipositive knot K has a Seifert surface that is isomorphic to a complex curve, we thus see that $g_4(K) = g(K)$; in particular, if K is nontrivial, then $g_4(K) > 0$. Subsequently, Livingston [36] proved that both of these genera are equal to $\tau(K)$ when K is strongly quasipositive. (For more on the relationship between τ and quasipositivity, see Hedden [19].)

The untwisted $\pm$ Whitehead double of K, $Wh_\pm(K)$, is the boundary of $A(K,0) * A(O,\mp 1)$, where O denotes the unknot. Thus, Theorem 2.5 implies that if K is strongly quasipositive and nontrivial, then $Wh_+(K)$ is strongly quasipositive and nontrivial, hence not smoothly slice. More generally, the Seifert surface for $D_{J,s}(K,t)$ shown in Figure 2(b) is $A(J,s) * A(K,t)$, so if J and K are strongly quasipositive and $s,t \leq 0$, then $D_{J,s}(K,t)$ is strongly quasipositive. Moreover, if neither of the pairs (J,s) and (K,t) equals $(O,0)$, then $D_{J,s}(K,t)$ is nontrivial, hence not smoothly slice. Furthermore, in this case $\tau(D_{J,s}(K,t)) = 1$ since the τ invariant of a strongly quasipositive knot is equal to its genus by a result of Livingston [36]. Using this observation, we may prove a weakened version of Theorem 2.1 in which the knot K is assumed to be strongly quasipositive without ever making reference to Theorem 1.1. (See [30] for this argument.)

Chapter 3

Bordered Heegaard Floer homology and knot doubling operators

In this chapter, we shall prove Theorem 1.1, which we restate here:

Theorem 3.1. *Let J and K be knots, and let $s, t \in \mathbb{Z}$. Then*

$$\tau(D_{J,s}(K,t)) = \begin{cases} 1 & s < 2\tau(J) \text{ and } t < 2\tau(K) \\ -1 & s > 2\tau(J) \text{ and } t > 2\tau(K) \\ 0 & \text{otherwise.} \end{cases}$$

Notice that it suffices to consider only the cases where $s \leq 2\tau(J)$, since if $s >$

$2\tau(J)$, the behavior of τ under mirroring implies:

$$\begin{aligned}\tau(D_{J,s}(K,t)) &= -\tau\left(\overline{D_{J,s}(K,t)}\right) \\ &= -\tau(D_{\bar{J},-s}(\bar{K},-t)) \\ &= \begin{cases} -1 & -t < 2\tau(\bar{K}) \\ 0 & -t \geq 2\tau(\bar{K}) \end{cases} \\ &= \begin{cases} -1 & t > -2\tau(K) \\ 0 & t \leq -2\tau(K) \end{cases}\end{aligned}$$

We shall introduce the assumption that $s \leq 2\tau(J)$ at an appropriate point in the discussion that follows.

Recall the construction of $D_{J,s}(K,t)$ given in the previous chapter as the knot obtained from one component of the Borromean rings ($B = B_1 \cup B_2 \cup B_3$) after twisted infection on the other two components. Specifically, let X_J and X_K denote the exteriors of J and K, respectively, and let Y denote the exterior of $B_1 \cup B_2$, with boundary components denoted $\partial_L Y$ and $\partial_R Y$. Then B_3 is a nulhomologous knot in Y with a genus-1 Seifert surface. There is an identification of S^3 with $(Y \cup_{\partial_L Y} X_J) \cup_{\partial_R Y} X_K$, with suitable gluing maps, taking $B_3 \subset Y$ to $D_{J,s}(K,t)$. We shall define *bordered structures* $\mathcal{Y}$, $\mathcal{X}_J^s$, and $\mathcal{X}_K^t$ on Y, X_J, and X_K, respectively, so as to induce the correct gluing maps on the boundaries. The theory of bordered Heegaard Floer homology [35, 34] associates an algebraic object to each of these bordered structures, denoted $\widehat{\mathrm{CFD}}(\mathcal{X}_J^s)$, $\widehat{\mathrm{CFD}}(\mathcal{X}_K^t)$, and $\widehat{\mathrm{CFAA}}(\mathcal{Y}, B_3, 0)$. By the gluing theorem of Lipshitz, Ozsváth, and Thurston, we may compute the filtered chain complex $\widehat{\mathrm{CFK}}(S^3, D_{J,s}(K,t))$ as a derived tensor product of these objects:

$$\widehat{\mathrm{CFK}}(S^3, D_{J,s}(K,t)) \cong (\widehat{\mathrm{CFAA}}(\mathcal{Y}, B_3, 0) \boxtimes \widehat{\mathrm{CFD}}(\mathcal{X}_J^s)) \boxtimes \widehat{\mathrm{CFD}}(\mathcal{X}_K^t). \tag{3.1}$$

The invariant $\tau(D_{J,s}(K,t))$ may then be extracted from this filtered chain complex.

In Section 3.1, we recall some of the terminology and background for bordered Heegaard Floer homology, including the complete description of $\widehat{\mathrm{CFD}}(\mathcal{X}_J^s)$ and $\widehat{\mathrm{CFD}}(\mathcal{X}_K^t)$.

Next, in Section 3.2, we compute $\widehat{\mathrm{CFAA}}(\mathcal{Y}, B_3, 0)$ using an explicit count of holomorphic disks in a bordered Heegaard diagram. In Section 3.3, we then evaluate the two tensor products in (3.1) to obtain the filtered chain complex $\widehat{\mathrm{CFK}}(S^3, D_{J,s}(K,t))$. By taking the homology of this complex while keeping track of the filtration, we compute the value of $\tau(D_{J,s}(K,t))$. While the proof is fairly technical, it illustrates the power of the new bordered techniques: using a single computation involving holomorphic disks (which can in principle be performed entirely combinatorially) and some lengthy but straightforward algebra, we are able to obtain a statement about the Floer homology an infinite family of knots. With only slightly more bookkeeping, we could also write down a formula for the knot Floer homology groups $\widehat{\mathrm{HFK}}(D_{J,s}(K,t))$, but since we are primarily interested in the value of τ and its applications to knot and link concordance, we do not bother to do that here.[1]

Finally, in Section 3.4, we present a few other results regarding knots of the form $D_{J,s}(K,t)$. Specifically, we prove a partial version of Theorem 1.1 that holds for any invariant ν that shares some of the formal properties of τ, and we exhibit instances where $D_{J,s}(K,t)$ is actually smoothly slice.

3.1 Background on bordered Heegaard Floer homology

In this section, we give a brief description of the bordered Heegaard Floer invariants, with the aim of defining the terms used later in the paper and illustrating the procedures for computation. We discuss only bordered manifolds with toroidal boundary components, which has the advantage of greatly simplifying some of the definitions. All of this material can be found in the two *magna opera* of Lipshitz, Ozsváth, and Thurston [35, 34].

[1] The reader is also advised to consult the author's paper [30, Section 4], which presents a simpler version of the argument in which the knot J is assumed to be the unknot.

3.1.1 Algebraic objects

We recall the main algebraic constructions used in [35, 34], with the aim of describing how to work with them computationally. Let $(\mathcal{A}, d)$ be a unital differential algebra over $\mathbb{F} = \mathbb{F}_2$. (All of the definitions that follow can be stated in terms of differential graded algebras, but we suppress all grading information for brevity.) Let $\mathcal{I} \subset \mathcal{A}$ denote the subring of idempotents in $\mathcal{A}$, and assume that $\{\iota_i\}$ is an orthogonal basis for $\mathcal{I}$ over $\mathbb{F}$ with the property that $\sum_i \iota_i = \mathbf{1}$, the identity element of $\mathcal{A}$.

- A *(right)* $\mathcal{A}_\infty$ *algebra* or *type A structure* over $\mathcal{A}$ is an $\mathbb{F}$-vector space M, equipped with a right action of $\mathcal{I}$ such that $M = \bigoplus_i M\iota_i$ as a vector space, and multiplication maps

  $$m_{k+1}\colon M \otimes_{\mathcal{I}} \underbrace{\mathcal{A} \otimes_{\mathcal{I}} \cdots \otimes_{\mathcal{I}} \mathcal{A}}_{k \text{ times}} \to M$$

  satisfying the $\mathcal{A}_\infty$ relations: for any $x \in M$ and $a_1, \dots, a_n \in \mathcal{A}$,

  $$\begin{aligned} 0 = &\sum_{i=0}^{n} m_{n-i+1}(m_{i+1}(x, a_1, \dots, a_i), a_{i+1}, \dots, a_n) \\ &+ \sum_{i=1}^{n} m_{n+1}(x, a_1, \dots, a_{i-1}, d(a_i), a_{i+1}, \dots, a_n) \\ &+ \sum_{i=1}^{n-1} m_n(x, a_1, \dots, a_{i-1}, a_i a_{i+1}, a_{i+2}, \dots, a_n). \end{aligned} \tag{3.2}$$

  We also require that $m_2(x, \mathbf{1}) = x$ and $m_k(x, \dots, \mathbf{1}, \dots) = 0$ for $k > 2$.

  The module M is called *bounded* if $m_k = 0$ for all k sufficiently large. If M is a bounded type A structure with basis $\{x_1, \dots, x_n\}$, we encode the multiplications using a matrix whose entries are formal sums of finite sequences of elements of $\mathcal{A}$, where having an $(a_1, \dots, a_k)$ term in the i, j^{th} entry means that the coefficient of x_j in $m_{k+1}(x_i, a_1, \dots, a_k)$ is nonzero. We write 1 rather than an empty sequence to signify the m_1 multiplication. For brevity, we frequently write $a_1 \cdots a_k$ rather than $(a_1, \dots, a_k)$; in this context, concatenation is *not* interpreted as multiplication in the algebra $\mathcal{A}$.

- A *(left) type D structure* over $\mathcal{A}$ is an $\mathbb{F}$-vector space N, equipped with a left action of $\mathcal{I}$ such that $N = \bigoplus_i \iota_i N$, and a map

  $$\delta_1 \colon N \to A \otimes_{\mathcal{I}} N$$

  satisfying the relation

  $$(\mu \otimes \mathrm{id}_N) \circ (\mathrm{id}_{\mathcal{A}} \otimes \delta_1) \circ \delta_1 + (d \otimes \mathrm{id}_N) \circ \delta_1 = 0, \tag{3.3}$$

  where $\mu \colon \mathcal{A} \otimes \mathcal{A} \to \mathcal{A}$ denotes the multiplication on $\mathcal{A}$.

  If N is a type D structure, the tensor product $\mathcal{A} \otimes_{\mathcal{I}} N$ is naturally a left differential module over $\mathcal{A}$, with module structure given by $a \cdot (b \otimes x) = ab \otimes x$, and differential $\partial(a \otimes x) = a \cdot \delta_1(x) + d(a) \otimes x$. Condition (3.3) translates to $\partial^2 = 0$.

  Given a type-D module N, define maps

  $$\delta_k \colon N \to \underbrace{\mathcal{A} \otimes_{\mathcal{I}} \cdots \otimes_{\mathcal{I}} \mathcal{A}}_{k \text{ times}} \otimes_{\mathcal{I}} N$$

  by $\delta_0 = \mathrm{id}_N$ and $\delta_k = (\mathrm{id}_{\mathcal{A}^{\otimes k-1}} \otimes \delta_1) \circ \delta_{k-1}$. We say N is *bounded* if $\delta_k = 0$ for all k sufficiently large.

  Given a basis $\{y_1, \dots, y_n\}$ for N, we may encode δ_1 as an $n \times n$ matrix (b_{ij}) with entries in $\mathcal{A}$, such that $\delta_1 x_i = \sum_{j=1}^n b_{ij} \otimes x_j$. To encode δ_k in matrix form, we take the k^{th} power of the matrix for δ_1, except that instead of evaluating multiplication in $\mathcal{A}$, we simply concatenate tensor products of elements.

  If $d = 0$, (3.3) is equivalent to the statement that the square of the matrix for δ_1 (where now we do evaluate multiplication in $\mathcal{A}$) is zero.

- If M is a right type A structure, N is a left type D structure, and at least one of them is bounded, we may form the *box tensor product* $M \boxtimes N$. As a vector space, this is $M \otimes_{\mathcal{I}} N$, with differential

  $$\partial^{\boxtimes}(x \otimes y) = \sum_{k=0}^{\infty} (m_{k+1} \otimes \mathrm{id}_N)(x \otimes \delta_k(y)).$$

Given matrix representations of the multiplications on M and the δ_k maps on N, it is easy to write down the differential on $M \boxtimes N$ in terms of the basis $\{x_i \otimes y_j\}$.

- Now let $(\mathcal{A}, d_{\mathcal{A}})$ and $(\mathcal{B}, d_{\mathcal{B}})$ be differential algebras. Lipshitz, Ozsváth, and Thurston [34] define various types of $(\mathcal{A}, \mathcal{B})$-bimodules. We do not define these in full detail, but we mention some of the basic notions.

  A *type DD structure* is simply a type D structure over the ring $\mathcal{A} \otimes_{\mathbb{F}} \mathcal{B}$. That is, the map δ_1 outputs terms of the form $a \otimes b \otimes x$, where $a \in \mathcal{A}$ and $b \in \mathcal{B}$.

  A *type AA structure* consists of a vector space M with multiplications

  $$m_{1,i,j} \colon M \otimes \mathcal{A}^{\otimes i} \otimes \mathcal{B}^{\otimes j} \to M,$$

  satisfying a version of the $\mathcal{A}_\infty$ relation (3.2). As above, all tensor products are taken over the rings of idempotents, $\mathcal{I}_\rho \subset \mathcal{A}$ and $\mathcal{I}_\sigma \subset \mathcal{B}$. Our notation differs a bit from that of [34] in that we think of both algebras as acting on the right.

  A *type DA structure* is a vector space N with maps

  $$\delta_1^{1+j} \colon N \otimes \mathcal{B}^{\otimes j} \to \mathcal{A} \otimes N$$

  satisfying an appropriate relation that combines (3.2) and (3.3). A *type AD structure* is defined similarly, except that the roles of $\mathcal{A}$ and $\mathcal{B}$ are interchanged.

  The box tensor product of two bimodules, or of a module and a bimodule, can be defined assuming at least one of the factors is bounded (in an appropriate sense). See [34, Subsection 2.3.2] for details.

- A filtration on a type A structure M is a filtration $\dots \subseteq \mathcal{F}_p \subseteq \mathcal{F}_{p+1} \subseteq \dots$ of M as a vector space, such that $m_{k+1}(\mathcal{F}_p \otimes \mathcal{A}^{\otimes k}) \subseteq \mathcal{F}_p$ for any $a_1, \dots, a_k$. Similarly, a filtration on a type D structure N is a filtration of N such that $\delta_1(\mathcal{F}_p) \subseteq \mathcal{A} \otimes \mathcal{F}_p$. It is easy to extend these definitions to the various types of bimodules. A filtration on M or N naturally induces a filtration on $M \boxtimes N$.

3.1.2 The torus algebra

The *pointed matched circle for the torus*, $\mathcal{Z}$, consists of an oriented circle Z, equipped with a basepoint $z \in Z$, a tuple $\mathbf{a} = (a_1, a_2, a_3, a_4)$ of points in $Z \smallsetminus \{z\}$ (ordered according to the orientation on $Z \smallsetminus \{z\}$), and the equivalence relation $a_1 \sim a_3$, $a_2 \sim a_4$. The genus-1, one-boundary-component surface $F^\circ(\mathcal{Z})$ is obtained by identifying Z with the boundary of a disk D and attaching 1-handles h_1 and h_2 that connect a_1 to a_3 and a_2 to a_4, respectively. By attaching a 2-handle along $\partial F^\circ(\mathcal{Z})$, we obtain the closed surface $F(\mathcal{Z})$. There is an orientation-reversing involution $r \colon Z \to Z$ that fixes z, interchanges a_1 and a_4, and interchanges a_2 and a_3, which extends to a diffeomorphism $r \colon F(\mathcal{Z}) \to -F(\mathcal{Z})$ that interchanges h_1 and h_2.

The algebra $\mathcal{A} = \mathcal{A}(\mathcal{Z}, 0)$ is generated as a vector space over $\mathbb{F}$ by two *idempotents* ι_0, ι_1 and six *Reeb elements* $\rho_1, \rho_2, \rho_3, \rho_{12}, \rho_{23}, \rho_{123}$. For each sequence of consecutive integers $I = (i_1, \dots, i_k) \subset \{1, 2, 3\}$, we have $\iota_{[i_1-1]}\rho_I = \rho_I \iota_{[i_k]} = \rho_I$, where $[j]$ denotes the residue of j modulo 2. The nonzero multiplications among the Reeb elements are: $\rho_1\rho_2 = \rho_{12}$, $\rho_2\rho_3 = \rho_{23}$, $\rho_1\rho_{23} = \rho_{12}\rho_3 = \rho_{123}$. All other products are zero. Let $\mathcal{I}$ denote the subring of idempotents of $\mathcal{A}$; it is generated as a vector space by ι_0 and ι_1. The identity element is $\mathbf{1} = \iota_0 + \iota_1$.

By abuse of notation, we identify ρ_1 with the oriented arc of Z from a_1 to a_2, ρ_2 with the arc from a_2 to a_3, ρ_3 with the arc from a_3 to a_4, and ρ_{12}, ρ_{23}, and ρ_{123} with the appropriate concatenations.

3.1.3 Bordered 3-manifolds and their invariants

A *bordered 3-manifold with boundary* $F(\mathcal{Z})$ consists of the data $\mathcal{Y} = (Y, \Delta, z', \phi)$, where Y is an oriented 3-manifold with a single boundary component, Δ is a disk in ∂Y, $z' \in \partial\Delta$, and $\phi : F(\mathcal{Z}) \to \partial(Y)$ is a diffeomorphism taking D to Δ and z to z'. The map ϕ is specified (up to isotopy fixing Δ pointwise) by the images of the core arcs of the two one-handles in $F^\circ(\mathcal{Z})$. We may analogously define a *bordered 3-manifold with boundary* $-F(\mathcal{Z})$. The diffeomorphism $r \colon F(\mathcal{Z}) \to -F(\mathcal{Z})$ provides a one-to-one correspondence between these two types of bordered manifolds.

A bordered 3-manifold $\mathcal{Y}$ may be presented by a bordered Heegaard diagram

$$\mathcal{H} = (\Sigma, \{\alpha_1^c, \ldots, \alpha_{g-1}^c, \alpha_1^a, \alpha_2^a\}, \{\beta_1, \ldots, \beta_g\}, z),$$

where Σ is a surface of genus g with one boundary components, $\{\alpha_1^c, \ldots, \alpha_{g-1}^c\}$ and $\{\beta_1, \ldots, \beta_g\}$ are tuples of homologically linearly independent, disjoint circles in Σ, and α_1^a and α_2^a are properly embedded arcs that are disjoint from the α circles and linearly independent from them in $H_1(\Sigma, \partial\Sigma)$. If we identify $(\partial\Sigma, z, \partial\Sigma \cap (\alpha_1^a \cup \alpha_2^a))$ with $\mathcal{Z}$ — where $\partial\Sigma$ is given the boundary orientation — we obtain a bordered 3-manifold with boundary parametrized by $F(\mathcal{Z})$ by attaching handles along the α and β circles. If instead we identify $\partial\Sigma$ with $-\mathcal{Z}$, we obtain a bordered 3-manifold with boundary parametrized by $-F(\mathcal{Z})$.

Let $\mathfrak{S}(\mathcal{H})$ denote the set of unordered g-tuples of points $\mathbf{x} = \{x_1, \ldots, x_g\}$ such that each α circle and each β circle contains exactly one point of $\mathbf{x}$ and each α arc contains at most one point of $\mathbf{x}$. Let $X(\mathcal{H})$ denote the $\mathbb{F}_2$-vector space spanned by $\mathfrak{S}(H)$.

For generators $\mathbf{x}, \mathbf{y} \in \mathfrak{S}(\mathcal{H})$, let $\pi_2(\mathbf{x}, \mathbf{y})$ denote the set of homology classes of maps $u\colon S \to \Sigma \times [0,1] \times [-2,2]$, where S is a surface with boundary, taking ∂S to

$$((\boldsymbol{\alpha} \times \{1\} \cup \boldsymbol{\beta} \times \{2\} \cup (\partial\Sigma \smallsetminus z) \times [0,1]) \times [-2,2]) \cup \\ (\mathbf{x} \times [0,1] \times \{-2\}) \cup (\mathbf{y} \times [0,1] \times \{2\})$$

and mapping to the relative fundamental homology class of $(\mathbf{x} \times [0,1] \times \{-2\}) \cup (\mathbf{y} \times [0,1] \times \{2\})$. Each element $B \in \pi_2(\mathbf{x}, \mathbf{y})$ is determined by its *domain*, the projection of B to $H_2(\Sigma, \boldsymbol{\alpha} \cup \boldsymbol{\beta} \cup \partial\Sigma; \mathbb{Z})$. The group $H_2(\Sigma, \boldsymbol{\alpha} \cup \boldsymbol{\beta} \cup \partial\Sigma; \mathbb{Z})$ is freely generated by the closures of the components of $\Sigma \smallsetminus (\boldsymbol{\alpha} \cup \boldsymbol{\beta})$, which we call *regions*. The domain of any $B \in \pi_2(\mathbf{x}, \mathbf{y})$ satisfies the following conditions:

- The multiplicity of the region containing the basepoint z is 0.[2]

[2] In classical Heegaard Floer homology, the definition of $\pi_2(\mathbf{x}, \mathbf{y})$ does not include this requirement.

- For each point $p \in \boldsymbol{\alpha} \cap \boldsymbol{\beta}$, if we identify an oriented neighborhood of p with $\mathbb{R}^2$, taking p to the origin and the α and β segments containing p to the x- and y-axes, respectively, and let $n_1(p)$, $n_2(p)$, $n_3(p)$, and $n_4(p)$ denote the multiplicities in D of the regions in the four quadrants, then

$$n_1(p) - n_2(p) + n_3(p) - n_4(p) = \begin{cases} 1 & p \in \mathbf{x} \smallsetminus \mathbf{y} \\ -1 & p \in \mathbf{y} \smallsetminus \mathbf{x} \\ 0 & \text{otherwise.} \end{cases} \tag{3.4}$$

Thus, finding the elements of $\pi_2(\mathbf{x}, \mathbf{y})$ is a simple matter of linear algebra. A homology class $B \in \pi_2(\mathbf{x}, \mathbf{y})$ is called *positive* if the regions in its domain all have non-negative multiplicity; only positive classes can support holomorphic representatives.

We shall describe only the invariant $\widehat{\mathrm{CFD}}$ here, since we do not compute $\widehat{\mathrm{CFA}}$ explicitly from a Heegaard diagram in this thesis.

We identify the boundary of Σ with $-\mathcal{Z}$. Assume that the α arcs are labeled so that $\alpha_1^a \cap \partial\Sigma = \{a_1, a_3\}$ and $\alpha_2^a \cap \partial\Sigma = \{a_2, a_4\}$.

Define a function $I_D \colon \mathfrak{S}(\mathcal{H}) \to \{\iota_0, \iota_1\}$ by

$$I_D(\mathbf{x}) = \begin{cases} \iota_0 & \mathbf{x} \cap \alpha_2^a \neq \varnothing \\ \iota_1 & \mathbf{x} \cap \alpha_1^a \neq \varnothing. \end{cases} \tag{3.5}$$

Define a left action of $\mathcal{I}$ on $X(\mathcal{H})$ by $\iota_i \cdot \mathbf{x} = \delta(\iota_i, I_D(\mathbf{x}))\mathbf{x}$, where δ is the Kronecker delta.

For each of the oriented arcs $\rho_I \subset \mathcal{Z}$, let $-\rho_I$ denote ρ_I with its opposite orientation. (That is, $-\rho_1$ goes from a_2 to a_1, etc.) Given $\mathbf{x} \in \mathfrak{S}(\mathcal{H})$ and a sequence $\vec{\rho} = (-\rho_{I_1}, \dots, -\rho_{I_k})$, the pair $(\mathbf{x}, \vec{\rho})$ is called *strongly boundary monotonic* if the initial point of $-\rho_{I_1}$ is on the same α circle as $\mathbf{x}$, and for each $i > 1$, the initial point of $-\rho_{I_i}$ and the final point of $-\rho_{I_{i-1}}$ are paired in $\mathbb{Z}$.

If $B \in \pi_2(\mathbf{x}, \mathbf{y})$ is a positive class, then $\partial^\partial B$ (the intersection of the domain of B with the boundary of Σ) may be expressed (non-uniquely) as a sum of arcs $-\rho_{I_i}$.

Specifically, we say that the pair $(B, \vec{\rho})$ is *compatible* if $(\mathbf{x}, \vec{\rho})$ is strongly boundary monotonic and $\partial^\partial B = \sum_{i=1}^k (-\rho_{I_i})$. If $(B, \vec{\rho})$ is compatible, the *index* of $(B, \vec{\rho})$ is defined in [35, Definition 5.46] as

$$\operatorname{ind}(B, \vec{\rho}) = e(B) + n_{\mathbf{x}}(B) + n_{\mathbf{y}}(B) + |\vec{\rho}| + \iota(\vec{\rho}), \tag{3.6}$$

where $e(B)$ is the Euler measure of B; $n_{\mathbf{x}}(B)$ (resp. $n_{\mathbf{y}}(B)$) is the sum over points $x_i \in \mathbf{x}$ (resp. $y_i \in \mathbf{y}$) of the average of the multiplicities of the regions incident to x_i (resp. y_i), $|\vec{\rho}|$ is the number of entries in $\vec{\rho}$, and $\iota(\vec{\rho})$ is a combinatorially defined quantity [35, Equation 5.44] that measures the overlapping of the arcs ρ_{I_i}. The index $\operatorname{ind}(B, \vec{\rho})$ is equal to one plus the expected dimension of a certain moduli space $\mathcal{M}^B(\mathbf{x}, \mathbf{y}, \vec{\rho})$ of J-holomorphic curves in $\Sigma \times [0,1] \times \mathbb{R}$ in the homology class B whose asymptotics near $\partial\Sigma \times [0,1] \times \mathbb{R}$ are specified by $\vec{\rho}$. In particular, if $\operatorname{ind}(B, \vec{\rho}) = 1$, then this moduli space contains finitely many points. We do not give the full definition here; see [35, Section 5] for the details.

For each $\mathbf{x}, \mathbf{y} \in \mathfrak{S}(\mathbf{x})$ and $B \in \pi_2(\mathbf{x}, \mathbf{y})$, define

$$a^B_{\mathbf{x},\mathbf{y}} = \sum_{\substack{\{\vec{\rho} = (-\rho_{I_1}, \dots, -\rho_{I_k}) \,|\\ (B, \vec{\rho}) \text{ compatible,}\\ \operatorname{ind}(B, \vec{\rho}) = 1\}}} \#(\mathcal{M}^B(\mathbf{x}, \mathbf{y}, \vec{\rho}))\, \rho_{I_1} \dots \rho_{I_k} \in \mathcal{A},$$

where the count of points in $\mathcal{M}^B(\mathbf{x}, \mathbf{y}, \vec{\rho})$ is taken modulo 2. We define $\delta_1 \colon X(\mathcal{H}) \to \mathcal{A} \otimes_{\mathcal{I}} X(\mathcal{H})$ by

$$\delta_1(\mathbf{x}) = \sum_{\mathbf{y} \in \mathfrak{S}(\mathcal{H})} \sum_{B \in \pi_2(\mathbf{x}, \mathbf{y})} a^B_{\mathbf{x},\mathbf{y}} \otimes \mathbf{y}. \tag{3.7}$$

This defines a type D structure, which we denote $\widehat{\mathrm{CFD}}(\mathcal{H})$. The verification of (3.3) is a version of the standard $\partial^2 = 0$ argument in Floer theory.

Proposition 3.2.

1. *The only sequences of chords that can contribute nonzero terms to* δ_1 *are the empty sequence,* $(-\rho_1)$, $(-\rho_2)$, $(-\rho_3)$, $(-\rho_1, -\rho_2)$, $(-\rho_2, -\rho_3)$, $(-\rho_{123})$, *and* $(-\rho_1, -\rho_2, -\rho_3)$. *Therefore, only classes whose multiplicities in the boundary regions of* Σ *are* 0 *or* 1 *can count for* δ_1.

2. *If $B \in \pi_2(\mathbf{x}, \mathbf{y})$ is a positive class whose domain has multiplicity 1 in the regions abutting ρ_1 and ρ_2 (resp. ρ_2 and ρ_3) and 0 in the region abutting ρ_3 (resp. ρ_1), then B may count for the differential only if $\mathbf{x}$ and $\mathbf{y}$ contain points of α_1^a (resp. α_2^a).*

Proof. For the first statement, the only other sequences of chords for which the product of algebra elements in the definition of $a^B_{\mathbf{x},\mathbf{y}}$ is nonzero are $(-\rho_{12})$, $(-\rho_{23})$, $(-\rho_1, -\rho_{23})$, and $(-\rho_{12}, -\rho_3)$. The two latter sequences are not strongly boundary monotonic. If $B \in \pi_2(\mathbf{x}, \mathbf{y})$ is a positive class compatible with $(-\rho_{12})$, then $\mathbf{x}$ and $\mathbf{y}$ both contain points on α_1^a, since otherwise B would have a boundary component without a β segment. Therefore, $I_D(\mathbf{y}) = \iota_1$. Since the tensor product is taken over the ring of idempotents,

$$\rho_{12} \otimes \mathbf{y} = \rho_{12} \otimes \iota_1 \mathbf{y} = \rho_{12}\iota_1 \otimes \mathbf{y} = 0,$$

so the contribution of B to $\delta_1(\mathbf{x})$ is zero. A similar argument applies for the sequence $(-\rho_{23})$. The second statement follows immediately from the same argument. □

The invariant $\widehat{\mathrm{CFA}}$ is a type A structure associated to a bordered Heegaard diagram whose boundary is identified with $\mathcal{Z}$. We do not give all the details here. The analogue of Proposition 3.2 does not hold for $\widehat{\mathrm{CFA}}$; one must consider domains with arbitrary multiplicities on the boundary and a much larger family of sequences of chords. Therefore, it is generally easier to compute $\widehat{\mathrm{CFD}}$.

We conclude this section with the *gluing theorem*:

Theorem 3.3 (Lipshitz-Ozsváth-Thurston [35])**.** *Suppose $\mathcal{Y}_1$ and $\mathcal{Y}_2$ are bordered 3-manifolds, and $Y = Y_1 \cup_\phi Y_2$ is the manifold obtained by gluing them together along their boundaries, where $\phi\colon -\partial Y_1 \to \partial Y_2$ is the map induced by the bordered structures. Then*

$$\widehat{\mathrm{CF}}(Y) \simeq \widehat{\mathrm{CFA}}(\mathcal{Y}_1) \boxtimes \widehat{\mathrm{CFD}}(\mathcal{Y}_2),$$

provided that at least one of the modules is bounded (so that the box tensor product is defined).

3.1.4 Bimodules

In [34], Lipshitz, Ozsváth, and Thurston also define invariants for a *bordered manifold with two boundary components*. Essentially, this consists of a manifold Y with two torus boundary components $\partial_L Y$ and $\partial_R Y$, with parametrizations of the two boundary components just like in the single-component case, and a framed arc connecting the two boundary components. (See [34, Chapter 5] for the full definition.)

If both boundary components are parametrized by $-F(\mathcal{Z})$, the associated invariant is a type DD structure over two copies of $\mathcal{A}$, denoted $\widehat{\mathrm{CFDD}}(\mathcal{Y})$; if both are parametrized by $F(\mathcal{Z})$, the invariant is a type AA structure, denoted $\widehat{\mathrm{CFAA}}(\mathcal{Y})$; and similarly there are invariants $\widehat{\mathrm{CFAD}}(\mathcal{Y})$ and $\widehat{\mathrm{CFDA}}(\mathcal{Y})$. We denote the two copies of $\mathcal{A}$ by $\mathcal{A}_\rho$ and $\mathcal{A}_\sigma$; in the latter, the Reeb elements are written σ_1, σ_2, etc.

In fact, we shall consider only a direct summand of each bimodule, denoted $\widehat{\mathrm{CFDD}}(\mathcal{Y}, 0)$, $\widehat{\mathrm{CFAA}}(\mathcal{Y}, 0)$, etc., which is all that is necessary to compute the Floer complex of a manifold obtained by gluing two separate one-boundary-component manifolds to the two boundary components of Y. The other summands are only necessary if one wishes to glue together the two boundary components of Y.

As in the previous discussion, we describe only the construction of $\widehat{\mathrm{CFDD}}$. A bordered manifold with two toroidal boundary components may be presented by an *arced bordered Heegaard diagram*

$$\mathcal{H} = (\Sigma, \{\alpha_1^c, \dots, \alpha_{g-2}^c, \alpha_1^L, \alpha_2^L, \alpha_1^R, \alpha_2^R\}, \{\beta_1, \dots, \beta_g\}, \mathbf{z}),$$

where now $\partial\Sigma$ has two components $\partial_L\Sigma$ and $\partial_R\Sigma$, on which the arcs α_i^L and α_i^R have their respective boundaries, and $\mathbf{z}$ is an arc in the complement of all the α and β circles and α arcs connecting the two boundary components.

We define $\mathfrak{S}(\mathcal{H})$ and $X(\mathcal{H})$ just in the single-boundary-component case. Let $\mathfrak{S}(\mathcal{H}, 0)$ be the subset of $\mathfrak{S}(\mathcal{H})$ consisting of g-tuples $\mathbf{x}$ containing one point in $\alpha_1^L \cup \alpha_2^L$ and one point in $\alpha_1^R \cup \alpha_2^R$, and let $X(\mathcal{H}, 0)$ be the $\mathbb{F}$-vector space generated by $\mathfrak{S}(\mathcal{H}, 0)$. This is the underlying vector space for the invariants $\widehat{\mathrm{CFDD}}(\mathcal{H}, 0)$, $\widehat{\mathrm{CFAA}}(\mathcal{H}, 0)$, etc.

To define $\widehat{\mathrm{CFDD}}(\mathcal{H}, 0)$, identify both boundary components of Σ with $-\mathcal{Z}$. Each generator of $\widehat{\mathrm{CFDD}}(\mathcal{H}, 0)$ has associated idempotents in $\mathcal{A}_\rho$ and $\mathcal{A}_\sigma$, as in (3.5). The differential

$$\delta_1\colon\ X(\mathcal{H}, 0) \to (\mathcal{A}_\rho \otimes \mathcal{A}_\sigma) \otimes_{\mathcal{I}_\rho \otimes \mathcal{I}_\sigma} X(\mathcal{H}, 0)$$

is then defined essentially the same way as with $\widehat{\mathrm{CFD}}$ of a single-boundary-component diagram. Specifically, for a homology class $B \in \pi_2(\mathbf{x}, \mathbf{y})$ and sequences of chords $\vec{\rho} = (-\rho_{I_1}, \ldots, -\rho_{I_k})$ and $\vec{\sigma} = (-\sigma_{J_1}, \ldots, -\sigma_{J_l})$ on the two boundary components, the definitions of compatibility and of the index $\mathrm{ind}(B, \vec{\rho}, \vec{\sigma})$ are as above. Define

$$a^B_{\mathbf{x},\mathbf{y}} = \sum_{\substack{(\vec{\rho},\vec{\sigma})\,|\\ (B,\vec{\rho},\vec{\sigma}) \text{ compatible,}\\ \mathrm{ind}(B,\vec{\rho},\vec{\sigma})=1\}}} \#(\mathcal{M}^B(\mathbf{x}, \mathbf{y}, \vec{\rho}, \vec{\sigma}))\, \rho_{I_1} \ldots \rho_{I_k} \otimes \sigma_{J_1} \ldots \sigma_{J_l} \in \mathcal{A}_\rho \otimes \mathcal{A}_\sigma.$$

The map δ_1 is then given by (3.7) just as above. An analogue of Proposition 3.2 also holds in this setting. For further details, see [34, Section 6].

The gluing theorem generalizes naturally to bimodules. For instance, if Y_1 has a single boundary component parametrized by $F(\mathcal{Z})$, Y_2 has two boundary components parametrized by $-F(\mathcal{Z})$, and $\phi\colon\ -\partial Y_1 \to \partial_L Y_2$ is the map induced by the parametrizations, then

$$\widehat{\mathrm{CFD}}(\mathcal{Y}_1 \cup_\phi \mathcal{Y}_2) \simeq \widehat{\mathrm{CFA}}(\mathcal{Y}_1) \boxtimes_{\mathcal{A}_\rho} \widehat{\mathrm{CFDD}}(\mathcal{Y}_2, 0).$$

The remaining generalizations are found in [34, Theorems 11, 12].

Finally, we mention the *identity AA bimodule* [34, Subsection 10.1]. Consider the manifold $\mathbb{I} = F(\mathcal{Z}) \times I$. Parametrize $\partial_R Y = F(\mathcal{Z}) \times \{1\}$ by inclusion and $\partial_L Y = F(\mathcal{Z}) \times \{0\}$ (whose boundary-induced orientation is opposite to the standard orientation of $F(\mathcal{Z})$) by the composition $F(\mathcal{Z}) \xrightarrow{r} -F(\mathcal{Z}) \hookrightarrow F(\mathcal{Z}) \times \{0\}$; thus, both boundary components are parametrized by $F(\mathcal{Z})$ as opposed to $-F(\mathcal{Z})$. The bijection between bordered manifolds with boundary $-F(\mathcal{Z})$ and bordered manifolds with boundary $F(\mathcal{Z})$ may be given by $Y \mapsto Y \cup \mathcal{I}$. Thus, if $\mathcal{H}$ is any bordered Heegaard diagram with one boundary component, then the type A module $\widehat{\mathrm{CFA}}(\mathcal{H})$

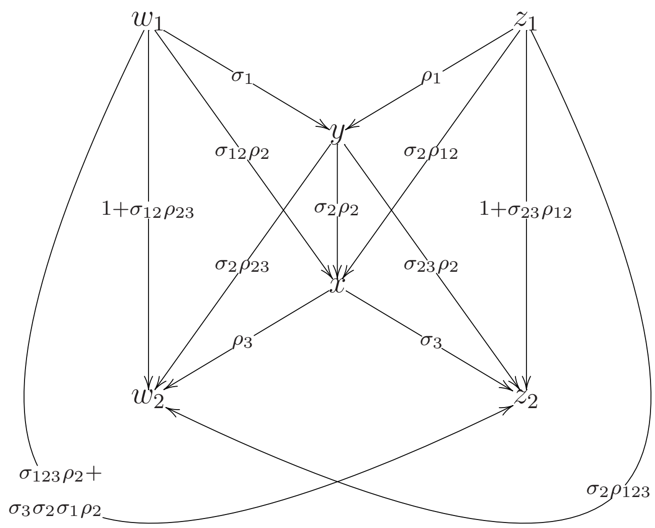

Figure 11: The identity AA bimodule, $\widehat{\mathrm{CFAA}}(\mathcal{I}, 0)$.

(where we identify $\partial\Sigma$ with $\mathcal{Z}$) is chain homotopy equivalent to $\widehat{\mathrm{CFAA}}(\mathbb{I}, 0) \boxtimes \widehat{\mathrm{CFD}}(\mathcal{H})$ (where, in the second factor, we identify $\partial\Sigma$ with $-\mathcal{Z}$). As mentioned above, it is easier to compute $\widehat{\mathrm{CFD}}$ explicitly from a Heegaard diagram than $\widehat{\mathrm{CFA}}$; by taking a tensor product with $\widehat{\mathrm{CFAA}}(\mathbb{I}, 0)$, we can always avoid the latter.

Theorem 3.4 (Lipshitz-Ozsváth-Thurston)**.** *The type AA module $\widehat{\mathrm{CFAA}}(\mathbb{I}, 0)$ has generators w_1, w_2, x, y, z_1, z_2, with $\mathcal{A}_\infty$ multiplications as illustrated in Figure 11.*

3.1.5 Knots in bordered manifolds

A *doubly-pointed bordered Heegaard diagram* consists of a bordered Heegaard diagram $\mathcal{H} = (\Sigma, \boldsymbol{\alpha}, \boldsymbol{\beta}, z)$ along with an additional basepoint $w \in \Sigma \smallsetminus (\boldsymbol{\alpha} \cup \boldsymbol{\beta})$. As explained in [35, Section 10.4], a doubly-pointed diagram determines a knot $K \subset Y$ with a single point of K meeting the basepoint on ∂Y, invariant up to isotopy fixing this point under Heegaard moves missing w. Lipshitz, Ozsváth, and Thurston define invariants $\mathrm{CFD}^-(Y, K)$ and $\mathrm{CFA}^-(Y, K)$ by working over the algebra $\mathcal{A} \otimes \mathbb{F}[U]$, where the U powers record the multiplicity of w in each domain that counts for the differential or multiplications.

If the knot K is nulhomologous in Y, we prefer the following alternate perspective. Let F be a Seifert surface for K. Just as in ordinary knot Floer homology [49, 56], each generator $\mathbf{x} \in \mathfrak{S}(\mathcal{H})$ has an associated relative spin^c structure $\mathfrak{s}_{z,w}(\mathbf{x}) \in \mathrm{Spin}^c(Y, K)$, and we may define an *Alexander grading* on $\mathfrak{S}(\mathcal{H})$ by

$$A(x) = \frac{1}{2} \langle c_1(\mathfrak{s}_{z,w}(\mathbf{x})), [F] \rangle, \tag{3.8}$$

where $c_1(\mathfrak{s}_{z,w}(\mathbf{x})) \in H^2(Y, K)$ and $[F] \in H_2(Y, K)$. The grading difference between two generators is given by

$$A(x) - A(y) = n_w(B) \tag{3.9}$$

where $B \in \pi_2(\mathbf{x}, \mathbf{y})$ is any domain from $\mathbf{x}$ to $\mathbf{y}$. To verify that the right-hand side of (3.9) is well-defined, note that for any periodic class $P \in \pi_2(\mathbf{x}, \mathbf{x})$, $n_w(P)$ equals the intersection number of K with the homology class in $H_2(Y, \partial Y)$ corresponding to P, which must be zero since K is nulhomologous. Further details are completely analogous to [49, 56].

The Alexander grading on $X(\mathcal{H})$ determines a filtration on $\widehat{\mathrm{CFA}}(\mathcal{H})$ or $\widehat{\mathrm{CFD}}(\mathcal{H})$, since any domain that counts for the differential or $\mathcal{A}_\infty$ multiplications has non-negative multiplicity at w. We denote the filtered chain homotopy type by $\widehat{\mathrm{CFA}}(\mathcal{Y}, K)$ or $\widehat{\mathrm{CFD}}(\mathcal{Y}, K)$.

When we evaluate a tensor product $\widehat{\mathrm{CFA}}(\mathcal{Y}_1) \boxtimes \widehat{\mathrm{CFD}}(\mathcal{Y}_2)$, a filtration on one factor extends naturally to a filtration on the whole complex, and the induced filtration agrees with the one that the knot induces on $\widehat{\mathrm{CF}}(Y_1 \cup Y_2)$.

A nulhomologous knot in a bordered manifold with two boundary components may be handled similarly. For invariance, one point of the knot must be constrained to lie on the arc connecting the two boundary components, and isotopies must be fixed in a neighborhood of that point.

3.1.6 The edge reduction algorithm

We now describe the well-known "edge reduction" procedure for chain complexes and its extension to $\mathcal{A}_\infty$ modules.

Suppose (C, ∂) is a free chain complex with basis $\{x_1, \dots, x_n\}$ over a ring R. For each i, j, let a_{ij} be the coefficient of x_j in ∂x_i with respect to this basis. If some a_{ij} is invertible in R, define a new basis $\{y_1, \dots, y_n\}$ by setting $y_i = x_i$, $y_j = \partial x_i$, and for each $k \neq i, j$, $y_k = x_k - a_{kj}a_{ij}^{-1}x_i$, where a_{kj} is the coefficient of x_j in ∂x_k. With respect to the new basis, the coefficient of y_j in ∂y_k is zero, so the subspace spanned by y_i and y_j is a direct summand subcomplex with trivial homology. Thus, C is chain homotopy equivalent to the subcomplex C' spanned by $\{y_k \mid k \neq i, j\}$, in which the coefficient of y_l in ∂y_k is $a_{kl} - a_{kj}a_{ij}^{-1}a_{il}$.

When $R = \mathbb{F}_2$, a convenient way to represent a chain complex (C, ∂) with basis $\{x_i\}$ is a directed graph $\Gamma_{C,\partial,\{x_i\}}$ with vertices corresponding to basis elements and an edge from x_i to x_j whenever $a_{ij} = 1$. To obtain $\Gamma_{C',\partial,\{y_k\}}$ from $\Gamma_{C,\partial,\{x_i\}}$ as above, we delete the vertices x_i and x_j and any edges going into or out of them. For each k and l with edges $x_k \to x_j$ and $x_i \to x_l$, we either add an edge from x_k to x_l (if there was not one previously) or eliminate the edge from x_k to x_l (if there was one). We call this procedure *canceling the edge from x_i to x_j*. The vertices of the resulting graph should be labeled with $\{y_k \mid k \neq i, j\}$, but by abuse of notation we frequently continue to refer to them with $\{x_k \mid k \neq i, j\}$ instead.

By iterating this procedure until no more edges remain, we compute the homology of C. If the matrix (a_{ij}) is sparse, this tends to be a very efficient algorithm for computing homology. If C is a graded complex and the basis $\{x_1, \dots, x_n\}$ consists of homogeneous elements, then y_k is clearly homogeneous with the same grading as x_k, so we can compute the homology as a graded group.

If C has a filtration $\cdots \subseteq F_p \subseteq F_{p+1} \subseteq \cdots$, the *filtration level* of an element of C is the unique p for which that element is in $F_p \smallsetminus F_{p-1}$. To compute the spectral sequence associated to the filtration, we cancel edges in increasing order of the amount by which they decrease filtration level. At each stage, this guarantees that the filtration level of y_k equals that of x_k. The complex that remains after we delete all edges that decrease filtration level by k is the E^{k+1} page in the spectral sequence, and the vertices that remain after all edges are deleted is the E^∞ page. In particular, when $C = \widehat{\mathrm{CF}}(S^3, K)$, the filtered complex associated to a knot $K \subset S^3$, the total homology of C is $\widehat{\mathrm{HF}}(S^3; \mathbb{F}) \cong \mathbb{F}$, so a unique vertex survives after all cancellations are complete. The filtration level of this vertex is, by definition, the invariant $\tau(K)$.

More generally, over an arbitrary ring R, we may represent (C, ∂) by a labeled, directed graph, where now we label an edge from x_i to x_j by a_{ij}, often omitting the label when $a_{ij} = 1$. When we cancel an unlabeled edge from x_i to x_j, we replace a zigzag

$$x_k \xrightarrow{a_{kj}} x_j \longleftarrow x_i \xrightarrow{a_{il}} x_l$$

with an edge

$$x_k \xrightarrow{-a_{kl}a_{il}} x_l$$

if no such edge existed previously, and either relabel or delete such an edge if it did exist. Of course, when R is not a field, this procedure is not guaranteed to eliminate all edges or to yield a result that is independent of the choice of the order in which the edges are deleted, but it is still often a useful way to simplify a chain complex.

The same procedure works for type D structures over the torus algebra $\mathcal{A}$, as can be seen by looking at the ordinary differential module obtained by taking the tensor product with $\mathcal{A}$ as above.

Edge cancellation for type A structures is slightly more complicated. We work only with bounded modules for simplicity. Suppose M is a bounded type A structure over $\mathcal{A}$ with a basis $\{x_1, \dots, x_n\}$. As above, we may describe the multiplications using a matrix of formal sums of finite sequences of elements of $\mathcal{A}$, and we may represent the nonzero entries using a labeled graph. If there is an unmarked edge from x_i to x_j (and no other edge), then we may cancel x_i and x_j, replacing a zigzag

$$x_k \xrightarrow{(a_1,\dots,a_p)} x_j \longleftarrow x_i \xrightarrow{(b_1,\dots,b_q)} x_l$$

by an edge

$$x_k \xrightarrow{(a_1,\dots,a_p,b_1,\dots,b_q)} x_l$$

(or eliminating such an edge if one already exists). The $\mathcal{A}_\infty$ module M' described by the resulting graph is then $\mathcal{A}_\infty$ chain homotopic to M. If M is a filtered $\mathcal{A}_\infty$-module and the edge being canceled is filtration-preserving (i.e., x_i and x_j have the same filtration level), then M' is filtered $\mathcal{A}_\infty$ chain homotopic to M. Similar techniques may also be used for bimodules.

The author has written a *Mathematica* package that implements these procedures for modules over the torus algebra, as well as the box tensor product. This package is available online at `http://www.math.columbia.edu/~topology/programs.html`.

3.1.7 $\widehat{\mathrm{CFD}}$ of knot complements

For any knot K, let X_K denote the exterior of K. For $t \in \mathbb{Z}$, let $\mathcal{X}_K^t$ denote the bordered structure on X_K determined by a map $\phi : -F(\mathcal{Z}) \to \partial X_K$ sending h_1 to a t-framed longitude (relative to the Seifert framing) and h_2 to a meridian of K. Lipshitz, Ozsváth, and Thurston [35] give a complete computation of $\widehat{\mathrm{CFD}}(\mathcal{X}_K^t)$ in terms of the knot Floer complex of K, which we now describe.

In the computation that follows, we will need to work with two different framed knot complements, $\mathcal{X}_J^s$ and $\mathcal{X}_K^t$. We first state the results for $\widehat{\mathrm{CFD}}(\mathcal{X}_J^s)$ and then indicate how to modify the notation for $\widehat{\mathrm{CFD}}(\mathcal{X}_K^t)$. Define $r = |2\tau(J) - s|$, and say that $\dim \widehat{\mathrm{HFK}}(S^3, J) = 2n + 1$.

We may find two distinguished bases for $\mathrm{CFK}^-(S^3, J)$: a "vertically reduced" basis $\{\tilde{\xi}_0, \dots, \tilde{\xi}_{2n}\}$, with "vertical arrows" $\tilde{\xi}_{2j-1} \to \tilde{\xi}_{2j}$ of length $k_j \in \mathbb{N}$, and a "horizontally reduced" basis $\{\tilde{\eta}_0, \dots, \tilde{\eta}_{2n}\}$, with "horizontal arrows" $\tilde{\xi}_{2j-1} \to \tilde{\xi}_{2j}$ of length $l_j \in \mathbb{N}$. (See [35, Chapter 10] for the definitions.) Denote the change-of-basis matrices by $(x_{p,q})$ and $(y_{p,q})$, so that

$$\tilde{\xi}_p = \sum_{q=0}^{2n} x_{p,q} \tilde{\eta}_q \quad \text{and} \quad \tilde{\eta}_p = \sum_{q=0}^{2n} y_{p,q} \tilde{\xi}_q. \tag{3.10}$$

In all known instances, the two bases may be taken to be equal as sets (up to a permutation), but it has not been proven that this holds in general.

According to [35, Theorems 10.17, 11.7], the structure of $\widehat{\mathrm{CFD}}(\mathcal{X}_J^t)$ is as follows. The part in idempotent ι_0 (i.e., $\iota_0\widehat{\mathrm{CFD}}(\mathcal{X}_J^s)$) has dimension $2n+1$, with designated bases $\{\xi_0,\dots,\xi_{2n}\}$ and $\{\eta_0,\dots,\eta_{2n}\}$ related by (3.10) without the tildes. The part in idempotent ι_1 (i.e., $\iota_1\widehat{\mathrm{CFD}}(\mathcal{X}_J^s)$) has dimension $r+\sum_{j=1}^n(k_j+l_j)$, with basis

$$\{\gamma_1,\dots,\gamma_r\}\cup\bigcup_{j=1}^n\{\kappa_1^j,\dots,\kappa_{k_j}^j\}\cup\bigcup_{j=1}^n\{\lambda_1^j,\dots,\lambda_{l_j}^j\}.$$

For $j=1,\dots,n$, corresponding to the vertical arrow $\tilde\eta_{2j-1}\to\tilde\eta_{2j}$, there are differentials

$$\xi_{2j}\xrightarrow{\rho_{123}}\kappa_1^j\xrightarrow{\rho_{23}}\cdots\xrightarrow{\rho_{23}}\kappa_{k_j}^j\xleftarrow{\rho_1}\xi_{2j-1}. \tag{3.11}$$

(In other words, $\delta_1(\xi_{2j})$ has a $\rho_{123}\otimes\kappa_1^j$ term, and so on.) We refer to the subspace of $\widehat{\mathrm{CFD}}(\mathcal{X}_J^s)$ spanned by the generators in (3.11) as a *vertical stable chain*. Similarly, corresponding to the horizontal arrow $\eta_{2j-1}\to\eta_{2j}$ of length l_j, there are differentials

$$\eta_{2j-1}\xrightarrow{\rho_3}\lambda_1^j\xrightarrow{\rho_{23}}\cdots\xrightarrow{\rho_{23}}\lambda_{l_j}^j\xrightarrow{\rho_2}\eta_{2j}, \tag{3.12}$$

and the generators here span a *horizontal stable chain*. Finally, the generators $\xi_0,\eta_0,\gamma_1,\dots,\gamma_r$ span the *unstable chain*, with differentials depending on s and $\tau(J)$:

$$\begin{cases}\eta_0\xrightarrow{\rho_3}\gamma_1\xrightarrow{\rho_{23}}\cdots\xrightarrow{\rho_{23}}\gamma_r\xleftarrow{\rho_1}\xi_0 & s<2\tau(J)\\ \xi_0\xrightarrow{\rho_{12}}\eta_0 & s=2\tau(J)\\ \xi_0\xrightarrow{\rho_{123}}\gamma_1\xrightarrow{\rho_{23}}\cdots\xrightarrow{\rho_{23}}\gamma_r\xrightarrow{\rho_2}\eta_0 & s>2\tau(J).\end{cases} \tag{3.13}$$

In some instances, as with the unknot and the figure-eight knot, we may have $\xi_0=\eta_0$.

For $\widehat{\mathrm{CFD}}(\mathcal{X}_K^t)$, we modify the preceding two paragraphs by replacing all lowercase letters with capital letters. Specifically, $\iota_0\widehat{\mathrm{CFD}}(\mathcal{X}_K^t)$ has bases $\{\Xi_0,\dots,\Xi_{2N}\}$ and $\{\mathrm{H}_0,\dots,\mathrm{H}_{2N}\}$ related by change-of-basis matrices $(X_{P,Q})$ and $(Y_{P,Q})$ as in (3.10); $\iota_1\widehat{\mathrm{CFD}}(\mathcal{X}_K^t)$ has basis

$$\{\Gamma_1,\dots,\Gamma_R\}\cup\bigcup_{J=1}^N\{\mathrm{K}_1^J,\dots,\mathrm{K}_{K_J}^J\}\cup\bigcup_{J=1}^N\{\Lambda_1^J,\dots,\Lambda_{L_J}^J\};$$

and the differentials are just as in (3.11), (3.12), and (3.13), suitably modified.[3] In the discussion below, we shall treat $\widehat{\mathrm{CFD}}(\mathcal{X}_K^t)$ as a type D structure over a copy of $\mathcal{A}_\sigma$ in which the elements are referred to as σ_1, σ_2, etc., to facilitate taking the double tensor product.

In Section 3.3, we shall frequently use the following proposition to simplify computations:

Proposition 3.5. *In the matrix entries for the higher maps δ_k for $\widehat{\mathrm{CFD}}(\mathcal{X}_J^s)$, there are no sequences of elements containing $\rho_1 \otimes \rho_2$, $\rho_1 \otimes \rho_{23}$, $\rho_2 \otimes \rho_3$, or $\rho_{12} \otimes \rho_3$.*

Proof. The only instances of ρ_1 in $\widehat{\mathrm{CFK}}(\mathcal{X}_J^s)$ are $\xi_{2j-1} \xrightarrow{\rho_1} \kappa^j_{k_j}$ in the vertical chains and $\xi_0 \xrightarrow{\rho_1} \gamma_r$ in the unstable chain when $s < 2\tau(J)$, and $\delta_1(\kappa^j_{k_j}) = \delta_1(\gamma_r) = 0$. Thus, $\rho_1 \otimes \rho_2$ and $\rho_1 \otimes \rho_{23}$ may not occur in δ_k. Similarly, the only instances of ρ_2 and ρ_{12} are $\lambda^j_{l_j} \xrightarrow{\rho_2} \eta_{2j}$ in the horizontal chains, $\gamma_r \xrightarrow{\rho_2} \eta_0$ in the unstable chain when $s > 2\tau(J)$, and $\xi_0 \xrightarrow{\rho_{12}} \eta_0$ when $s = 2\tau(J)$, and the only instances of ρ_3 are $\eta_{2j-1} \xrightarrow{\rho_3} \lambda^j_1$ in the horizontal chains and $\eta_0 \xrightarrow{\rho_3} \gamma_1$ in the unstable chain when $s < 2\tau(J)$. Thus, no element that is at the head of a ρ_2 or ρ_{12} arrow is also at the tail of a ρ_3 arrow. $\square$

3.2 Direct computation of $\widehat{\mathrm{CFAA}}(Y, B_3)$

As above, let $B = B_1 \cup B_2 \cup B_3 \subset S^3$ denote the Borromean rings. Let Y denote the complement of a neighborhood of $B_1 \cup B_2$; then B_3 is a nulhomologous knot in Y. Let $\partial_L Y$ and $\partial_R Y$ be the boundary components coming from B_1 and B_2, respectively. We define a strongly bordered structure $\mathcal{Y}$ on Y (in the sense of [34, Definition 5.1]) so that the map $\phi_L : F(\mathcal{Z}) \to \partial_L Y$ (resp. $\phi_R : F(\mathcal{Z}) \to \partial_R Y$) takes h_1 to a meridian of B_1 (resp. B_2) and h_2 to a Seifert-framed longitude of B_1 (resp. B_2). It follows that the glued manifold $(\mathcal{Y} \cup_{\partial_L Y} \mathcal{X}_J^s) \cup_{\partial_R Y} \mathcal{X}_K^t$, is S^3, and the image of B_3 is the knot

[3] The reader should take care to distinguish capital eta (H) and kappa (K) from the Roman letters H and K. We find that the mnemonic advantage of using parallel notation for the generators of $\widehat{\mathrm{CFD}}(\mathcal{X}_J^s)$ and $\widehat{\mathrm{CFD}}(\mathcal{X}_K^t)$ outweighs any confusion that may arise.

$D_{J,s}(K,t)$.[4] Thus, we must compute the filtered type AA bimodule $\widehat{\mathrm{CFAA}}(\mathcal{Y}, B_3, 0)$. We do this explicitly using a Heegaard diagram.

Proposition 3.6. *The arced Heegaard diagram $\mathcal{H}$ (with extra basepoint w) shown in Figure 12 determines the pair $(\mathcal{Y}, B_3)$.*

Proof. As in [34, Construction 5.4], by cutting along the arc $\mathbf{z}$, we obtain a bordered Heegaard diagram with a single boundary component, $\mathcal{H}_{dr}$, which we view as rectangle with two tunnels attached. After attaching 2-handles to $\mathcal{H}_{dr} \times [0,1]$ along $\boldsymbol{\beta} \times \{1\}$ and attaching a single 3-handle, we may view the resulting manifold $Y(\mathcal{H}_{dr})$ as $[-1,1] \times \mathbb{R} \times [0,\infty) \subset \mathbb{R}^3$, minus two tunnels in the upper half-plane, plus the point at infinity (Figure 13). The boundary of $Y(\mathcal{H}_{dr})$ is the union of two embedded copies of $F^\circ(\mathcal{Z})$ that are determined by the α arcs on each side; they intersect along a circle A. The extra basepoint w determines a knot C in $Y(\mathcal{H}_{dr})$ with a single point on the boundary: the union of an arc connecting w to z in the complement of the α arcs and an arc connecting z to w in the complement of the β circles, pushed into the interior of $Y(\mathcal{H}_{dr})$ except at z. The curves A and C are both shown in Figure 13.

We obtain Figure 14 from Figure 13 by an isotopy that slides the tunnel on the right underneath the tunnel on the left. The circle A can then be identified with the y-axis plus the point at infinity. To obtain $Y(\mathcal{H})$, we attach a three-dimensional two-handle along A, which can be seen as $[-\epsilon,\epsilon] \times \mathbb{R} \times (-\infty, 0]$ plus the point at infinity. Then $Y(\mathcal{H})$ is the complement of a two-component unlink $(B_1 \cup B_2)$ in S^3, and the knot C inside $Y(\mathcal{H})$ is B_3. When we identify each component of $\partial\Sigma$ with $\mathcal{Z}$, we see that the α arc connecting the points a_1 and a_3 is a meridian, and the α arc connecting a_2 and a_4 is a 0-framed longitude, as in the definition of $\mathcal{Y}$. ∎

If we try to compute $\widehat{\mathrm{CFAA}}(\mathcal{H}, 0)$ directly, we run into difficulties counting the holomorphic curves, largely because there is a 14-sided region that runs over both

[4] Because we are gluing the two boundary components of $\mathcal{Y}$ to separate single-boundary-component bordered manifolds, the choice of framed arc connecting $\partial_L Y$ and $\partial_R Y$ does not affect the final computation of the tensor product, so we suppress all reference to it.

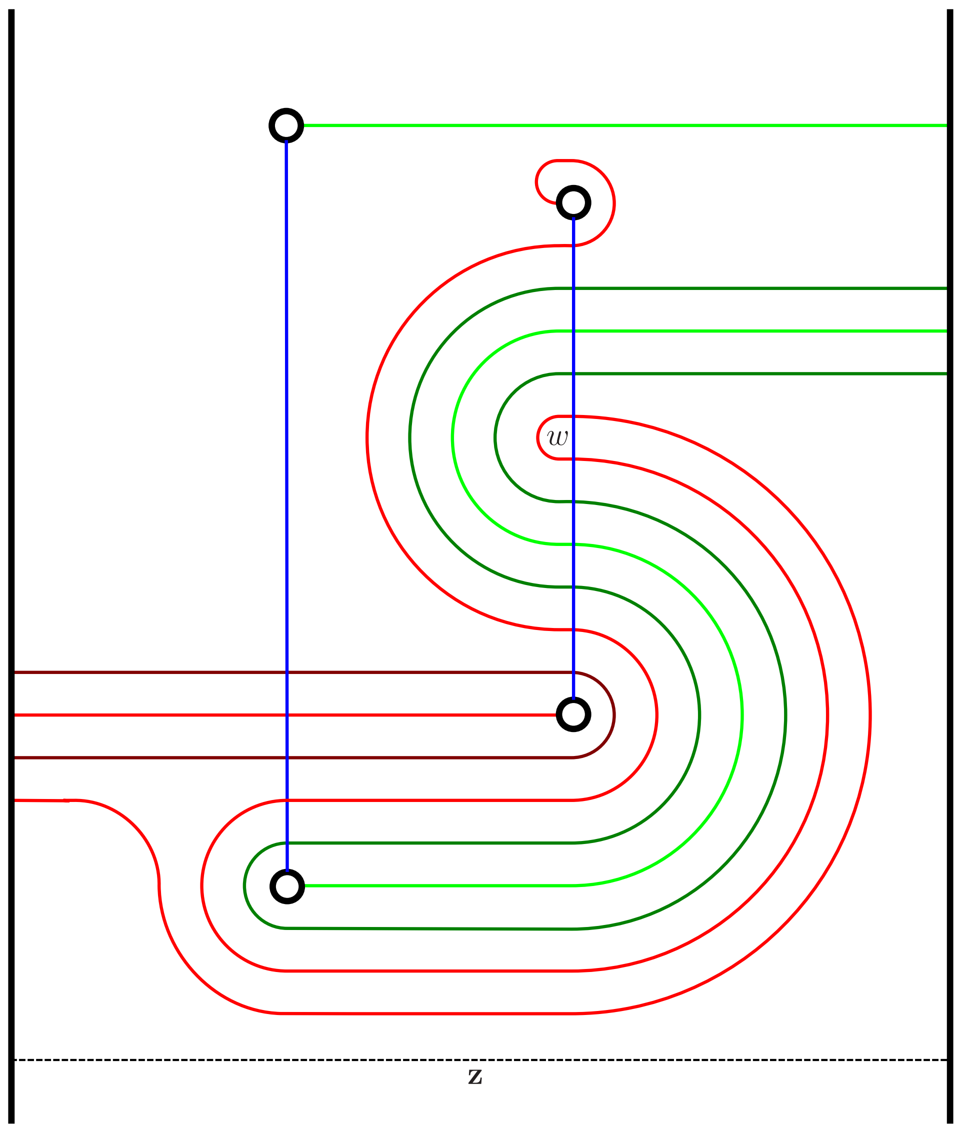

Figure 12: The arced Heegaard diagram $\mathcal{H}$.

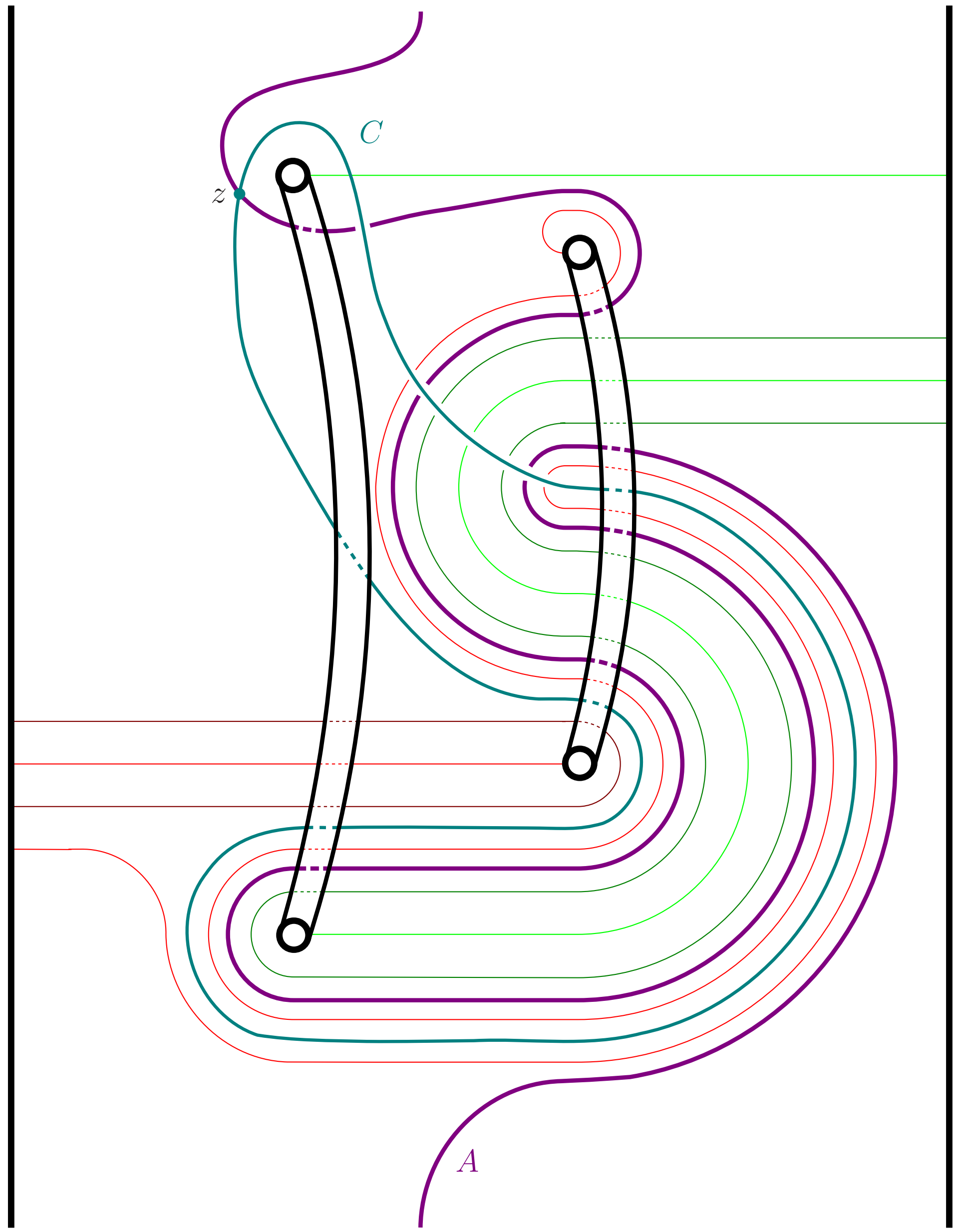

Figure 13: The manifold $Y(\mathcal{H}_{dr})$. The α arcs from $\mathcal{H}$ (the thin red and green curves) and the circle A (purple) sit in the xy-plane, while the knot C (turquoise) sits in the interior of $Y(\mathcal{H}_{dr})$ except at the point z.

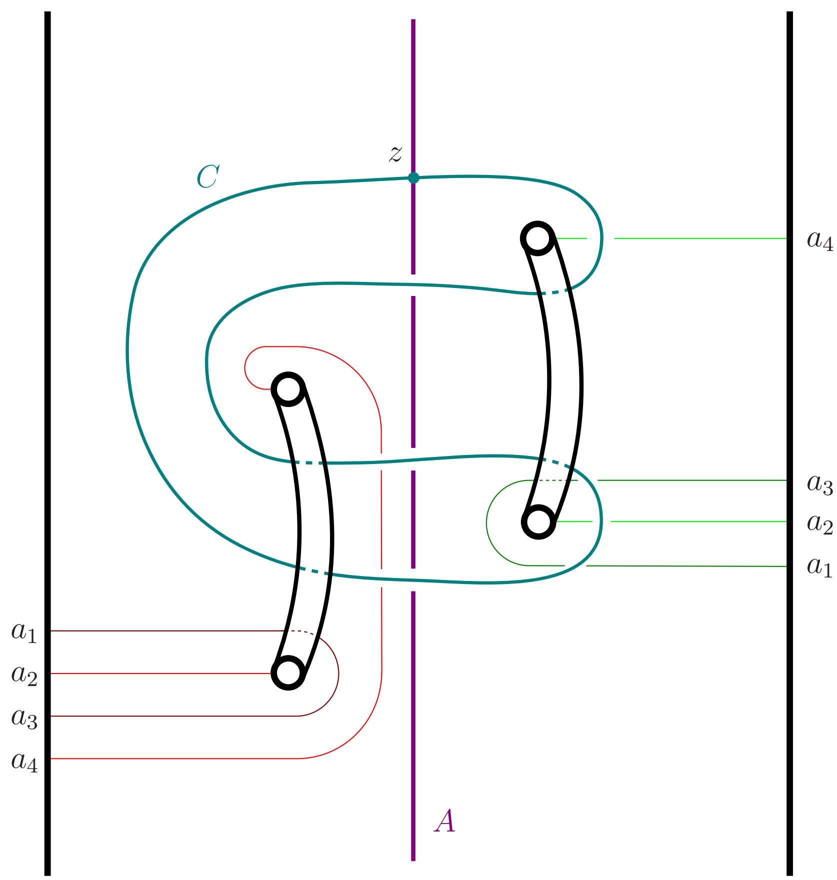

Figure 14: The result of isotoping Figure 13. Each boundary component is identified with $\mathcal{Z}$.

handles and shares edges with itself. Instead, it is easier to perform a sequence of isotopies on the α arcs to obtain the diagram $\mathcal{H}'$ shown in Figure 15. While $\mathcal{H}'$ is not a nice diagram in the sense of Sarkar and Wang [62], the analysis needed to count the relevant holomorphic curves is vastly simpler. Of course, the drawback is that the number of generators is much larger.

By Theorem 3.4, it suffices to compute $\widehat{\mathrm{CFDD}}(\mathcal{H}', 0)$, as described previously. Thus, we identify each component of $\partial\Sigma$ with $-\mathcal{Z}$. We now describe this computation.

In $\mathcal{H}'$, we label the intersection points of the α and β curves $x_1, \dots, x_{52}$, as indicated by the colored numbers in Figure 15.[5] These points are distributed among the various α and β circles as follows:

	β_1	β_2
α_1^L	$x_2, x_4, x_6, x_{10}, x_{11}, x_{15}, x_{22}, x_{29}$	$x_{37}, x_{41}, x_{42}, x_{46}$
α_2^L	x_3, x_5	x_{36}
α_1^R	$x_8, x_{13}, x_{17}, x_{20}, x_{24}, x_{27}, x_{31}, x_{34}$	$x_{39}, x_{44}, x_{48}, x_{51}$
α_2^R	$x_1, x_7, x_9, x_{12}, x_{14}, x_{16}, x_{18}, x_{19}$ $x_{21}, x_{25}, x_{26}, x_{28}, x_{32}, x_{33}, x_{35}$	$x_{38}, x_{40}, x_{43}, x_{45}$ $x_{47}, x_{49}, x_{50}, x_{52}$

The underlying vector space for $\widehat{\mathrm{CFDD}}(\mathcal{H}', 0)$ is generated by the set $\mathfrak{S}(\mathcal{H}', 0)$, consisting pairs of intersection points with one point on each β circle, one point on either α_1^L or α_2^L, and one point on either α_1^R or α_2^R. A simple count shows that there are 245 generators.

The bimodule $\widehat{\mathrm{CFDD}}(\mathcal{H}', 0)$ is a type DD structure over two copies of the torus algebra $\mathcal{A}$. We denote these copies by $\mathcal{A}_\rho$ and $\mathcal{A}_\sigma$, corresponding to the left and right boundary components of $\mathcal{H}'$. In $\mathcal{A}_\sigma$, the Reeb elements are denoted σ_1, σ_2, etc. The idempotents in $\mathcal{A}_\rho$ are denoted ι_0^ρ and ι_1^ρ, and those in $\mathcal{A}_\sigma$ are denoted ι_0^σ and ι_1^σ. The idempotent maps $I_D^\rho : \mathfrak{S}(\mathcal{H}', 0) \to \{\iota_0^\rho, \iota_1^\rho\}$ and $I_D^\sigma : \mathfrak{S}(\mathcal{H}', 0) \to \{\iota_0^\sigma, \iota_1^\sigma\}$ are defined just as in (3.5).

[5]While many authors use different letters to distinguish between intersection points on different α or β curves, we use a single indexing set here in order to facilitate computer calculations.

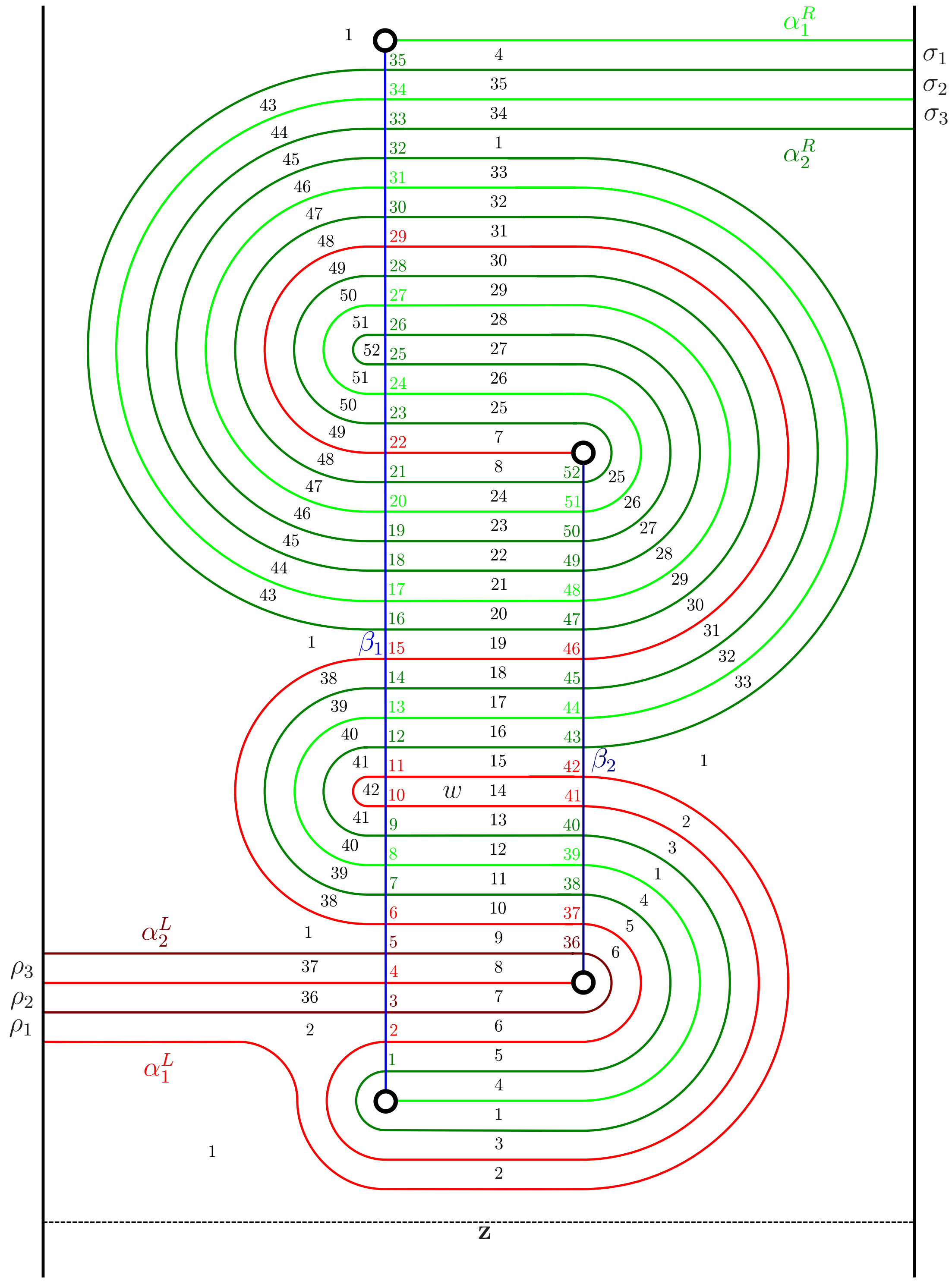

Figure 15: The Heegaard diagram $\mathcal{H}'$, with the boundary labeled consistent with the conventions for type D structures.

Denote the regions of $\Sigma' \smallsetminus (\boldsymbol{\alpha} \cup \boldsymbol{\beta})$ by $R_1, \dots, R_{52}$, as indicated by the black numbers in Figure 15.

For generators $\mathbf{x}$ and $\mathbf{y}$, we may find all the domains in $\pi_2(\mathbf{x}, \mathbf{y})$ by solving the system of linear equations (3.4). The multiplicity of each of the boundary regions (R_2, R_4, R_{34}, R_{35}, R_{36}, and R_{37}) must be 0 or 1; each of the 2^6 possible choices for these multiplicities gives a further set of constraints that guarantees a unique solution. We may then list only those solutions which represent positive classes and which have index 1 for some compatible $\vec{\rho}$, subject to the restrictions of Proposition 3.2. Using *Mathematica* to perform these linear algebra computations, we find some 1,051 domains meeting these requirements.

It would not be feasible to list every single domain and whether or not it supports holomorphic representatives, but we shall describe a number of typical examples, and leave further details to the highly motivated reader.

Bigons and quadrilaterals. In the context of closed Heegaard diagrams, Sarkar and Wang [62] showed that in a Heegaard diagram in which every non-basepointed region is either a bigon or a quadrilateral, the domains with Maslov index 1 are precisely the embedded bigons and quadrilaterals that are embedded in the Heegaard diagram, and these all support support a unique holomorphic representatives. Lipshitz, Ozsváth, and Thurston proved an analogous result for bordered diagrams [35, Proposition 8.4], where now we extend the definition of "quadrilateral" to include a region with boundary consisting of one segment of a β circle, two segments of α arcs, and one segment of $\partial\Sigma$. The only non-basepointed regions in $\mathcal{H}'$ that are not bigons or quadrilaterals are R_2, R_4, R_7, and R_8, which are hexagons. Therefore, any index-1 domain on our list that does not use one of these four regions automatically supports a unique holomorphic representative.

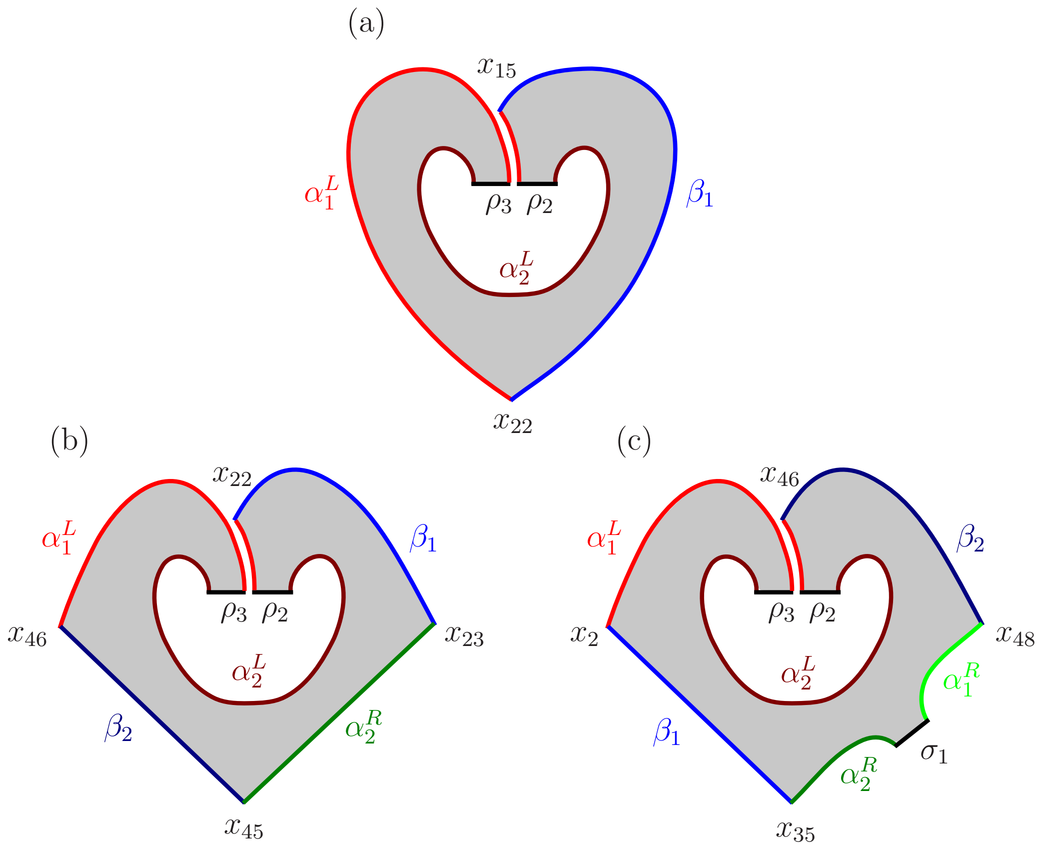

Figure 16: The domains D_1 (a), D_2 (b), and D_3 (c).

Domains contributing ρ_{23}. Consider the domains

$$\begin{aligned}
D_1 &= R_7 + R_8 + R_{19} + \cdots + R_{30} + R_{49} + R_{50} + R_{51} + R_{52} \\
D_2 &= R_7 + R_8 + R_{31} + R_{36} + R_{37} + R_{48} \\
D_3 &= D_2 + R_4 + R_5 + R_{10} + R_{11} + R_{17} + R_{18} + R_{24} + R_{25} + R_{29} + R_{30} + R_{32} \\
&\qquad + R_{38} + R_{39} + R_{47} + R_{49} + R_{50},
\end{aligned}$$

which respectively represent index-1 classes in $\pi_2(x_{15}x_i, x_{22}x_i)$, $\pi_2(x_{22}x_{45}, x_{23}x_{46})$, and $\pi_2(x_{35}x_{46}, x_2x_{48})$, where $x_i \in \beta_2 \cap (\alpha_1^R \cup \alpha_2^R)$ and $i < 47$. (If $i \in \{47, \dots, 52\}$, the index of D_1 is too high.) To obtain a representative of each domain compatible with the sequence $(-\rho_2, -\rho_3)$, as required by Proposition 3.2, we cut along α_1^L all the way to the boundary, as shown in Figure 16. The source curve for D_1 is the disjoint union of two bigons: one with two boundary punctures mapped to the Reeb chords $-\rho_2$ and $-\rho_3$, and one mapped trivially to $\{x_i\} \times [0,1] \times \mathbb{R}$. The source curve for D_2 or D_3 is a quadrilateral, with two boundary punctures on one α edge mapping to $-\rho_2$ and $-\rho_3$ and (for D_3) a boundary puncture on the other α edge mapping to σ_1. It is easy to see that these classes all support holomorphic representatives. Thus, we have differentials $x_{15}x_i \xrightarrow{\rho_{23}\otimes \mathbf{1}} x_{22}x_i$, $x_{22}x_{45} \xrightarrow{\rho_{23}\otimes \mathbf{1}} x_{23}x_{46}$, and $x_{35}x_{46} \xrightarrow{\rho_{23}\otimes \sigma_1} x_2x_{48}$.

On the other hand, let $D_4 = R_7 + R_8 + R_{36} + R_{37}$; this domain represents a class in $\pi_2(x_{21}x_j, x_{23}x_j)$, where $x_j \in \beta_2 \cap (\alpha_1^L \cup \alpha_2^L)$. This domain is illustrated in Figure 17. If $x_j \in \alpha_2^L$, then then this class is excluded for idempotent reasons by Proposition 3.2. On the other hand, if $x_j \in \alpha_1^L$, then the index of this class is 0. Therefore, D_4 cannot count for the differential for any choice of x_j.

Decomposable annuli. Let $A = R_7 + R_8 + R_{48} + R_{49} + R_{30} + R_{31}$; this is the domain for an index-0 annulus in $\pi_2(x_3x_{45}, x_5x_{47})$. Consider the index-1 annuli

$$\begin{aligned}
D_5 &= A + R_{36} \in \pi_2(x_4x_{45}, x_5x_{47}) \\
D_6 &= A + R_{37} \in \pi_2(x_3x_{45}, x_4x_{47}) \\
D_7 &= A + R_{25} + R_{26} + R_{27} + R_{28} + R_{29} + R_{50} + R_{51} + R_{52} \in \pi_2(x_3x_{45}, x_5x_{52}).
\end{aligned}$$

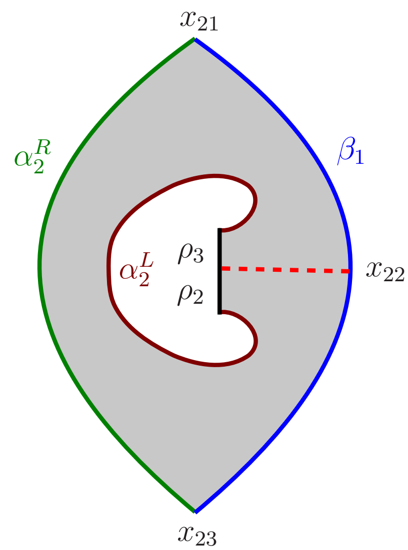

Figure 17: The domain D_4.

each of which is the sum of A with a bigon (possibly with a Reeb chord on the boundary). The mod-2 count of holomorphic representatives of each of these domains depends nontrivially on the choice of complex structure. We claim that either all three domains count for the differential or none of them do. To see this, we use a standard argument in conformal geometry that occurs frequently in computing Heegaard Floer complexes, which we find convenient to state in more generality than is strictly needed for this example. (See, e.g., Ozsváth and Szabó's first paper on Heegaard Floer homology [50].)

Lemma 3.7. *Suppose that a Heegaard diagram contains an annulus A and some or all of the bigons $B_1, \ldots, B_8$ shown in Figure 18, where each of the arcs that cuts into A crosses to the opposite boundary component. Let E_i be the domain $A + B_i$, which has Maslov index* 1*. Then either E_1, E_3, E_6, and E_8 count for the differential and E_2, E_4, E_5, and E_7 do not, or vice versa.*

Proof. Define the *standard annulus* A_0 to be $S^1 \times [0, 1]$, with coordinates (s, t), with the complex structure given by $j\partial_s = \partial_t, j\partial_t = -\partial_s$. Up to rotation in the S^1 factor, there is a unique holomorphic map $U : A_0 \to A$ taking $S^1 \times \{0\}$ to the inner boundary

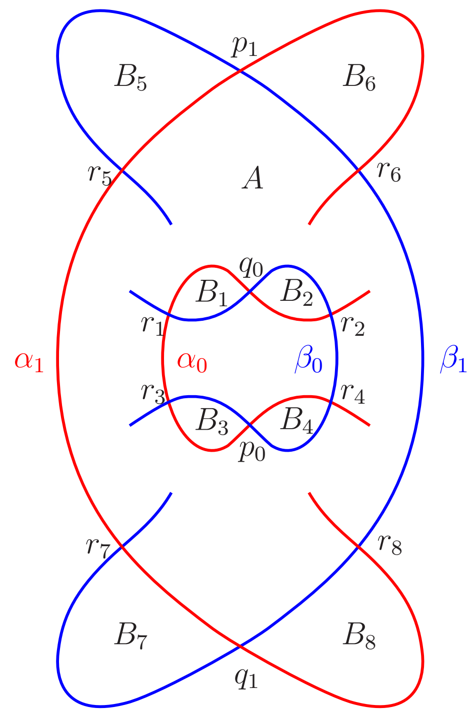

Figure 18: Annuli for which the number of holomorphic representatives depends nontrivially on the choice of complex structure as in Lemma 3.7.

$(A \cap (\alpha_0 \cup \beta_0))$ and $S^1 \times \{1\}$ to the outer boundary $(A \cap (\alpha_1 \cup \beta_1))$. For $i \in \{0, 1\}$, let a_i and b_i denote the inverse images of α_i and β_i, respectively. Define $\Theta_i = \ell(a_i)/\ell(b_i)$, the ratio of the length of the a_i to the length of b_i. For generic choices of the complex structure on Σ, we may assume that $\Theta_0 \neq \Theta_1$.

We consider $E_1 = A + B_1$; the analysis for the other seven cases is extremely similar. The domain E_1 (going from p_0p_1 to r_1q_1) has a one-parameter family of conformal structures, determined by how far we cut into A at r_1. We specify the length of the cut by $c \in \mathbb{R}$, where $c < 0$ corresponds to cutting along α_0 and $c > 0$ corresponds to cutting along β_0. For each value of c, there is a conformal map $u^c : A_0 \to E_1$, unique up to rotation in the S^1 factor. As above, let $a_i^c, b_i^c \subset S^1 \times \{i\}$ be the preimages of α_i and β_i under u^c, and let $\theta_i^c = \ell(a_i^c)/\ell(b_i^c)$. Whenever $\theta_0^c = \theta_1^c$, there is a holomorphic involution A_0 interchanging a_0^c with a_1^c and b_0^c with b_1^c. Thus, the signed count of the zeroes of the function $f(c) = \theta_0^c - \theta_1^c$ equals the signed number of points in the moduli space $\widehat{\mathcal{M}}(E_1)$. We may assume that f is transverse to zero.

Consider the limiting behavior of $f(c)$. As we cut along β_0, the arcs b_0 and a_1 grow in length, approaching all of $S^1 \times \{0\}$ and $S^1 \times \{1\}$, respectively. Thus $\lim_{c\to\infty} \theta_0^c = 0$ and $\lim_{c\to-\infty} \theta_1^c = \infty$, so $\lim_{c\to\infty} f(c) = -\infty$. In the opposite direction, as we cut along α_0, Gromov compactness implies that the maps u^c limit to a broken flowline consisting of holomorphic representatives for B_1 and A, so the limiting values of θ_0^c and θ_1^c are equal the corresponding values for $U : A_0 \to A$. That is, $\lim_{c\to-\infty} f(c) = \Theta_0 - \Theta_1$. By transversality and the intermediate value theorem, we thus see that $\#\widehat{\mathcal{M}}(E_1)$ is odd if and only if $\Theta_0 < \Theta_1$.

For the remaining domains $E_2, \dots, E_8$, we apply the same sort of analysis. As before, we parametrize the cut by $c \in \mathbb{R}$, with $c < 0$ corresponding to cutting along the α circle and $c > 0$ corresponding to cutting along the β circle. The limits are in the following table:

	$\lim_{c\to-\infty} f(c)$ (cutting along α)	$\lim_{c\to\infty} f(c)$ (cutting along β)
E_1, E_3	$\Theta_0 - \Theta_1$	$-\infty$
E_2, E_4	∞	$\Theta_0 - \Theta_1$
E_5, E_7	$\Theta_0 - \Theta_1$	∞
E_6, E_8	$-\infty$	$\Theta_0 - \Theta_1$

Thus, E_1, E_3, E_6, and E_8 count for the differential if and only if $\Theta_0 < \Theta_1$, and E_2, E_4, E_5, and E_7 count otherwise. □

In our Heegaard diagram $\mathcal{H}'$, we identify α_0, β_0, α_1, and β_1 in Figure 18 with α_2^L, β_1, α_2^R, and β_2 in Figure 15, respectively. For the bigons, we may take $B_2 = R_{37}$, $B_4 = R_{36}$, and $B_7 = R_{25} + R_{26} + R_{27} + R_{28} + R_{29} + R_{50} + R_{51} + R_{52}$, so that the domains D_5, D_6, and D_7 have the forms of E_4, E_2, and E_7, respectively. (For D_5 and D_6, the source surface should actually be $A_0' = A_0 \setminus (p, 0)$, where p is some point in S^1, and the puncture is sent to the Reeb chord ρ_2 or ρ_3. The analysis is exactly the same, however.) By Lemma 3.7, either all three of these domains count for the differential or none of them do, depending on the value of $\Theta_0 - \Theta_1$. If we arrange that $\Theta_0 < \Theta_1$, we see that none of these domains count.

Moreover, the other annuli in $\mathcal{H}'$ with Maslov index 0 are obtained by adding rectangular strips (e.g., $R_6 + R_9$ or $R_{24} + R_{25} + R_{47} + R_{50} + R_{29} + R_{32}$) to this one, and we may easily arrange that the values of $\Theta_0 - \Theta_1$ for all of these annuli are arbitrarily close together. Therefore, the annuli obtained by adding rectangular strips to D_5, D_6, and D_7 also do not count for the differential.

More annuli. Let $D_8 = R_2 + R_6 + R_7 + R_8 + R_{14} + R_{36} + R_{37} + R_{42}$, which determines an annulus in $\pi_2(x_{21}x_{36}, x_{23}x_{37})$ with a single ρ_{123} chord on one boundary component (Figure 19(a)). Let $c \in \mathbb{R}$ represent the cut parameter at x_{36}, where $c < 0$ corresponds to cutting along α_2^L and $c > 0$ corresponds to cutting along β_2. As above, for each

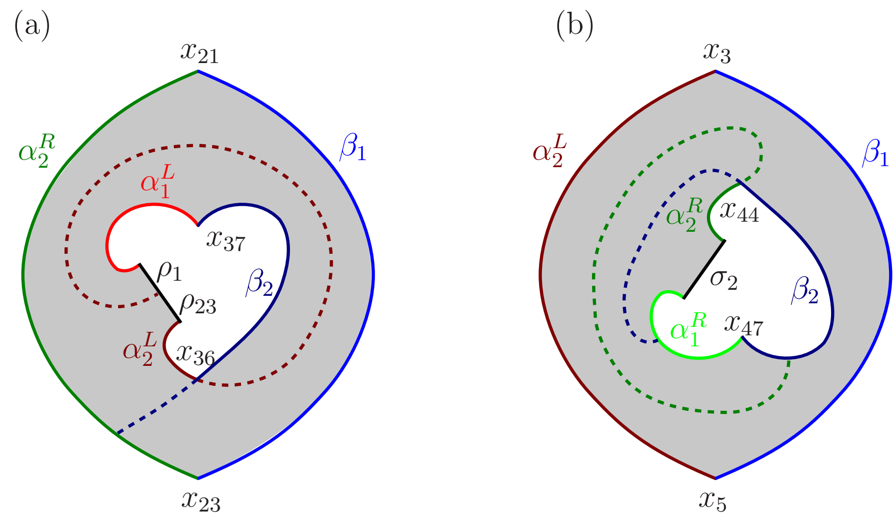

Figure 19: The domains D_9 (a) and D_9 (b).

value of c there is a unique holomorphic map u^c from the source annulus A_0' taking $(S^1 \setminus p) \times \{0\}$ to $\alpha_1^L \cup \alpha_2^L \cup \beta_2$, the puncture $(p, 0)$ to the Reeb chord ρ_{123}, and $(S^1 \times \{1\})$ to $\alpha_2^R \cup \beta_1$. With notation as in the proof of Lemma 3.7, we must consider the limits of $f(c) = \theta_0^c - \theta_1^c$ as $c \to \pm\infty$. As we cut along β_2, the arcs $b_0^c = (u^c)^{-1}(\beta_2)$ and $a_1^c = (u^c)^{-1}(\alpha_2^R)$ become arbitrarily long relative to their complements, so

$$\lim_{c\to\infty} f(c) = \lim_{c\to\infty} \theta_0^c - \lim_{c\to\infty} \theta_1^c = 0 - \infty = -\infty.$$

As we cut along α_2^L out toward the puncture, the arc a_0^c becomes arbitrarily long relative to b_0^c, while the ratio of the lengths of a_1^c and b_1^c approaches some finite value Θ, so

$$\lim_{c\to-\infty} f(c) = \lim_{c\to-\infty} \theta_0^c - \lim_{c\to-\infty} \theta_1^c = \infty - \Theta = \infty.$$

By transversality, we see that f always has an odd number of zeroes, so the class given by D_8 always counts for the differential.

Next, consider the domain

$$\begin{aligned} D_9 = R_7 + R_8 + R_{20} + R_{24} + R_{25} + R_{29} + R_{30} \\ + R_{31} + R_{32} + R_{35} + R_{43} + R_{47} + R_{48} + R_{49} + R_{50}, \end{aligned}$$

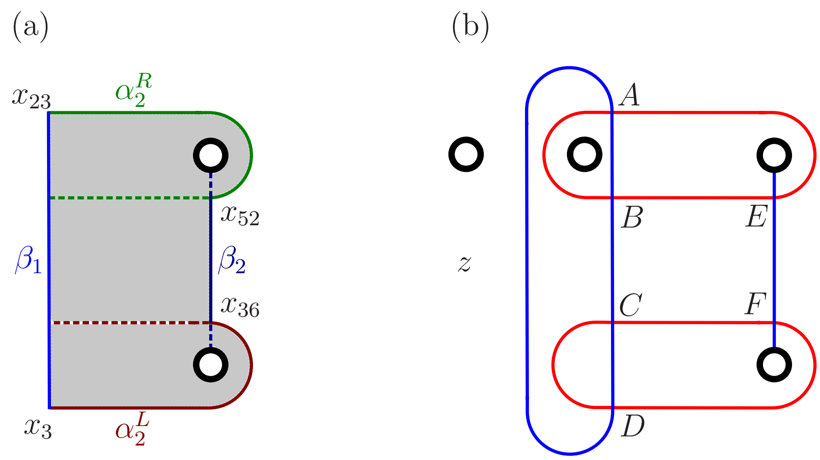

Figure 20: (a) The genus-1 domain D_{11}. (b) A Heegaard diagram for $S^1 \times S^2$ containing a domain biholomorphic to D_{11}.

which represents an annulus in $\pi_2(x_3x_{44}, x_5x_{47})$ with a single σ_2 Reeb chord (Figure 19(b)). Once again, we specify the cut parameter at x_{47} by $c \in \mathbb{R}$ and consider the limiting behavior of a function $f(c)$ defined as in previous examples. In the as $c \to \pm\infty$, the domain decomposes into a bigon $B_\pm$ with a single boundary puncture and an annulus $A_\pm$ with Maslov index 0, so by Gromov compactness, $\lim_{c\to\pm\infty} f(c) = \Theta_0^\pm - \Theta_1^\pm$, where $\Theta_0^\pm$ and $\Theta_1^\pm$ are the conformal angle ratios of $A_\pm$ as in the proof of Lemma 3.7. As mentioned previously, we may assume that $\Theta_0^+ - \Theta_1^+$ and $\Theta_0^- - \Theta_1^-$ are arbitrarily close together; in particular, they have the same sign. Thus, D_9 does not count for the differential. A similar argument applies for

$$D_{10} = R_2 + R_6 + R_7 + R_8 + R_9 + R_{14} + R_{30} + R_{31} + R_{42} + R_{48} + R_{49}.$$

Genus-1 classes. Let $D_{11} = R_7 + R_8 + \cdots + R_{24}$ (Figure 20(a)), which determines a class in $\pi_2(x_3x_{52}, x_{23}x_{36})$ represented by an embedded punctured torus. Determining whether domains with positive genus support holomorphic representatives is often one of the biggest difficulties in computing Heegaard Floer homology directly. In this case, the trick is to notice that the genus-2 Heegaard diagram for $S^1 \times S^2$ shown in Figure 20(b) has a domain (connecting the generators DE and AF) that is biholomorphic to D_{11}. By counting the remaining disks in this diagram, it is easy to see that the toroidal domain must count in order for the homology to be correct. Therefore, D_5 must also support a holomorphic representative. The same analysis applies to any domain of the form $\sum_{i=a}^{b} R_i$, where $4 \leq a \leq 7$ and $24 \leq b \leq 33$, provided that a and b are chosen such that the two α segments of the boundary do not lie on the same α curve. A similar analysis also works for the domain

$$D_{12} = R_5 + R_6 + R_7 + R_8 + R_9 + R_{10} + R_{18} + R_{30} + R_{31} + R_{48} + R_{49}$$

and others like it.

Next, consider the domains

$$\begin{aligned} D_{13} &= R_8 + \cdots + R_{24} \in \pi_2(x_4 x_{47}, x_{22} x_{47}) \\ D_{14} &= R_7 + \cdots + R_{19} + R_{30} + R_{31} + R_{48} + R_{49} \in \pi_2(x_3 x_{45}, x_{16} x_{36}) \\ D_{15} &= R_8 + R_{20} + R_{21} + R_{22} + R_{23} + R_{24} + R_{37} \in \pi_2(x_{16} x_{36}, x_{22} x_{47}). \end{aligned}$$

The domains D_{13} and D_{15} obviously do count for the differential: D_{13} is an annulus that always has a holomorphic representative (by a standard argument), and D_{15} is a rectangle with a single Reeb chord. The domain D_{14}, however, is a punctured torus. Notice that $D_6 + D_{13}$ and $D_{14} + D_{15}$ both determine the same homology class in $\pi_2(x_3 x_{45}, x_{22} x_{47})$, with index 2. More precisely, we there is a one-parameter family of disks limiting in one direction to the broken flowline $D_6 * D_{13}$ and in the other direction to $D_{14} * D_{15}$, which can be seen explicitly by varying the cut parameter at x_{47}. It follows that D_{14} counts for the differential if and only if D_6 does. By our assumption above, D_{14} does not count.

Miscellaneous domains. Let $D_{16} = R_7 + 2R_8 + R_9 + R_{10} + \cdots + R_{24} + R_{31} + R_{37} + R_{48}$; this is a domain from $x_3 x_{45}$ to $x_{23} x_{46}$. Because the region R_8, which as drawn in Figure 15 goes over one of the handles, is used twice, it is a little bit tricky to see what the source surface should be; the only possibility is indicated in Figure 21. Topologically, this is an immersed annulus with one boundary component having two α and two β

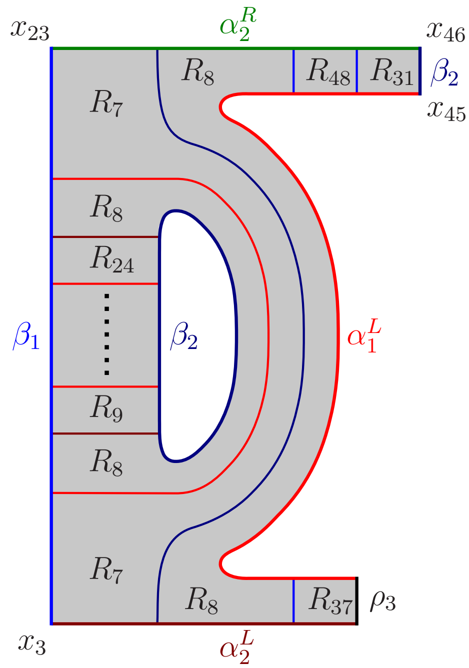

Figure 21: The only possible source surface for the domain D_{16}, which does not satisfy the correct boundary conditions.

segments (and a single Reeb chord), and the other component consisting of all of β_2, so it does not satisfy the necessary boundary conditions. Thus, D_{16} cannot count for the differential.

By inspecting the long list of the index-1 domains in $\mathcal{H}'$, we see that they all fall into one of the classes just described. We may thus sort the list into those that support holomorphic representatives and those that do not. Using this list, we may then record the differential on $\widehat{\mathrm{CFDD}}(\mathcal{H}', 0)$ as a 245×245 matrix with entries in $\mathcal{A}_\rho \otimes \mathcal{A}_\sigma$, although for obvious reasons we do not record this matrix here.

By counting the multiplicity of w in each domain (whether it counts for the differential or not), we can determine the relative Alexander gradings of all of the generators. We find that the generators of $\widehat{\mathrm{CFDD}}(\mathcal{H}', 0)$ all fall into three consecutive gradings, which for now we arbitrarily declare to be -1, 0, and 1. In the end, after we evaluate all tensor products, the symmetry of $\widehat{\mathrm{CFK}}(S^3, D_{J,s}(K, t))$ will show that this was the correct choice. We do not explicitly list all of the gradings here, however.

We may then use the edge cancellation algorithm explained in Subsection 3.1.6 to simplify $\widehat{\mathrm{CFDD}}(\mathcal{H}', 0)$, canceling only edges that preserve the filtration level. By abuse of notation, we denote the resulting module by $\widehat{\mathrm{CFDD}}(\mathcal{Y}, B_3, 0)$.

Theorem 3.8. *The type DD structure $\widehat{\mathrm{CFDD}}(\mathcal{Y}, B_3, 0)$ has a basis $\{y_1, \dots, y_{19}\}$ with the following properties:*

1. *The Alexander gradings of the basis elements are:*

$$A(y_i) = \begin{cases} -1 & i = 1 \\ 0 & i = 2, \dots, 10 \\ 1 & i = 11, \dots, 19. \end{cases}$$

2. *The associated idempotents in $\mathcal{A}_\rho$ and $\mathcal{A}_\sigma$ of the generators are:*

	ι_0^ρ	ι_1^ρ
ι_0^σ	$y_4, y_5, y_7, y_{11}, y_{13}, y_{17}, y_{19}$	$y_8, y_{10}, y_{14}, y_{16}$
ι_1^σ	y_3, y_6, y_{12}, y_{18}	y_1, y_2, y_9, y_{15}

3. *The differential is given by*

$$\delta_1(y_i) = \sum_{j=1}^{19} a_{ij} \otimes y_j,$$

where (a_{ij}) is the following matrix:

$$
\left(\begin{array}{c|ccccccccc|ccccccccc}
0 & 0 & 0 & 0 & 0 & 0 & 0 & 0 & 0 & 0 & 0 & 0 & 0 & 0 & 0 & 0 & 0 & 0 & 0 \\
\hline
1 & 0 & 0 & 0 & 0 & 0 & 0 & \sigma_2 & 0 & 0 & 0 & 0 & 0 & 0 & 0 & 0 & 0 & 0 & 0 \\
\rho_1 & 0 & 0 & 0 & 0 & 0 & 0 & 0 & 0 & 0 & 0 & 0 & 0 & 0 & 0 & 0 & 0 & 0 & 0 \\
\rho_1\sigma_{123} & \rho_1\sigma_3 & \sigma_3 & 0 & 0 & 0 & 0 & 0 & 0 & 0 & 0 & 0 & 0 & 0 & 0 & 0 & 0 & 0 & 0 \\
0 & \rho_3\sigma_{123}+\rho_{123}\sigma_3 & 0 & 0 & 0 & \sigma_3 & 0 & 0 & \rho_3\sigma_{123} & \rho_3 & 0 & 0 & 0 & 0 & 0 & 0 & 0 & 0 & 0 \\
\rho_{123} & 0 & 0 & 0 & 0 & 0 & \sigma_2 & 0 & \rho_3 & 0 & 0 & 0 & 0 & 0 & 0 & 0 & 0 & 0 & 0 \\
0 & 0 & 0 & 0 & 0 & 0 & 0 & \rho_3 & 0 & 0 & 0 & 0 & 0 & 0 & 0 & 0 & 0 & 0 & 0 \\
0 & 0 & \rho_2\sigma_1 & 0 & 0 & 0 & 0 & 0 & 0 & 0 & 0 & 0 & 0 & 0 & 0 & 0 & 0 & 0 & 0 \\
0 & 0 & \rho_2 & 0 & 0 & 0 & 0 & \sigma_2 & 0 & 0 & 0 & 0 & 0 & 0 & 0 & 0 & 0 & 0 & 0 \\
\sigma_{123} & 0 & 0 & \rho_2 & 0 & 0 & 0 & 0 & \sigma_3 & 0 & 0 & 0 & 0 & 0 & 0 & 0 & 0 & 0 & 0 \\
\hline
0 & \rho_1\sigma_1 & \sigma_1 & 0 & 0 & 0 & 0 & \rho_1 & \rho_1\sigma_1 & 0 & 0 & 0 & 0 & 0 & 0 & 0 & 0 & 0 & 0 \\
0 & \rho_1 & 1 & 0 & 0 & 0 & 0 & 0 & 0 & 0 & \sigma_2 & 0 & 0 & 0 & 0 & 0 & 0 & 0 & 0 \\
0 & 0 & \sigma_{123} & 1 & 0 & 0 & 0 & 0 & 0 & 0 & 0 & \sigma_3 & 0 & 0 & 0 & 0 & 0 & 0 & 0 \\
0 & 0 & 0 & 0 & 1 & 0 & 0 & 0 & 0 & 0 & 0 & 0 & 0 & 0 & \sigma_3 & 0 & 0 & 0 & \rho_3 \\
0 & \rho_{123} & 0 & 0 & 0 & 1 & 0 & 0 & 0 & 0 & 0 & 0 & 0 & 0 & 0 & \sigma_2 & 0 & \rho_3 & 0 \\
0 & 0 & 0 & 0 & 0 & 0 & 1 & \rho_{123} & 0 & 0 & 0 & 0 & 0 & 0 & 0 & 0 & \rho_3 & 0 & 0 \\
0 & 0 & 0 & 0 & 0 & 0 & 0 & 1 & 0 & 0 & \rho_2 & 0 & 0 & 0 & 0 & 0 & 0 & 0 & 0 \\
0 & 0 & 0 & 0 & 0 & 0 & 0 & 0 & 1 & 0 & 0 & \rho_2 & 0 & 0 & 0 & 0 & \sigma_2 & 0 & 0 \\
0 & \sigma_{123} & 0 & 0 & 0 & 0 & 0 & 0 & \sigma_{123} & 1 & 0 & 0 & \rho_2 & 0 & 0 & 0 & 0 & \sigma_3 & 0
\end{array}\right)
$$

The block decomposition indicates the filtration levels.

Finally, to compute $\widehat{\mathrm{CFAA}}(\mathcal{Y}, B_3, 0)$, we use the AA identity bimodule described in Theorem 3.4:

$$\widehat{\mathrm{CFAA}}(\mathcal{Y}, B_3, 0) \simeq \widehat{\mathrm{CFAA}}(\mathbb{I}, 0) \boxtimes_{\mathcal{A}_\sigma} (\widehat{\mathrm{CFAA}}(\mathbb{I}, 0) \boxtimes_{\mathcal{A}_\rho} \widehat{\mathrm{CFDD}}(\mathcal{Y}, B_3, 0)).$$

We evaluate this tensor product using our *Mathematica* package. The filtration on $\widehat{\mathrm{CFDD}}(\mathcal{Y}, B_3, 0)$ induces a filtration on $\widehat{\mathrm{CFAA}}(\mathcal{Y}, B_3, 0)$, and we again use the edge cancellation procedure to reduce the number of generators.

Theorem 3.9. *The filtered AA-module $\widehat{\mathrm{CFAA}}(\mathcal{Y}, B_3, 0)$ has a basis*

$$\{a_1, \dots, a_5, b_1, \dots, b_6, c_1, d_1, \dots, d_4, e_1, e_2, e_3\}$$

with the following properties:

1. *The Alexander gradings of the basis elements are:*

$$\begin{aligned} A(c_1) &= -1 \\ A(a_i) = A(d_i) &= 0 \\ A(b_i) = A(e_i) &= 1. \end{aligned}$$

2. *The associated idempotents in $\mathcal{A}_\rho$ and $\mathcal{A}_\sigma$ of the generators are:*

	ι_0^ρ	ι_1^ρ
ι_0^σ	$a_1, a_3, a_4, b_1, b_3, b_4, b_6$	d_1, d_3, e_1, e_3
ι_1^σ	a_2, a_5, b_2, b_5	c_1, d_2, d_4, e_2

3. *The A_∞ multiplications are presented in the matrices that follow. For $x, y \in \{a, b, c, d, e\}$, the entry in the i^{th} row and j^{th} column of the matrix M_{xy} records the multiplications taking x_i to y_j, as described in Subsection 3.1.1. The matrices M_{ab}, M_{cb}, M_{cd}, M_{ce}, M_{db}, and M_{de} are necessarily zero because of the Alexander grading.*

$$M_{aa} = \begin{pmatrix} 0 & \sigma_1 & \sigma_{12} & \rho_{12} & \sigma_{123}\rho_{12} + \sigma_1\rho_3\rho_2\rho_{12} \\ 0 & 0 & \sigma_2 & 0 & \sigma_{23}\rho_{12} + \rho_{12} \\ 0 & 0 & 0 & 0 & \sigma_3\rho_{12} \\ 0 & 0 & 0 & 0 & \sigma_1 \\ 0 & 0 & 0 & 0 & 0 \end{pmatrix}$$

$$M_{ac} = \begin{pmatrix} \sigma_{123}\rho_{123} + \sigma_{123}\sigma_{23}\rho_{123} + \sigma_3\sigma_2\sigma_1\rho_{123} + \sigma_1\sigma_{23}\rho_3\rho_2\rho_{123} \\ \quad + \sigma_{123}\sigma_{23}\rho_3\rho_2\rho_1 + \sigma_3\sigma_2\sigma_1\rho_3\rho_2\rho_1 + \sigma_1\sigma_{23}\rho_3\rho_2\rho_3\rho_2\rho_1 \\ \sigma_{23}\rho_{123} + \rho_3\rho_2\rho_1 + \sigma_{23}\sigma_{23}\rho_{123} + \sigma_{23}\sigma_{23}\rho_3\rho_2\rho_1 \\ \sigma_3\sigma_{23}\rho_{123} + \sigma_3\rho_3\rho_2\rho_1 + \sigma_3\sigma_{23}\rho_3\rho_2\rho_1 \\ \sigma_{123}\rho_3 + \sigma_3\sigma_2\sigma_1\rho_3 \\ \sigma_{23}\rho_3 \end{pmatrix}$$

$$M_{ad} = \begin{pmatrix} \rho_1 & 0 & \begin{array}{l}\sigma_{12}\rho_{123} + \sigma_{123}\sigma_2\rho_{123} + \sigma_{12}\rho_3\rho_2\rho_1 + \sigma_1\sigma_2\rho_3\rho_2\rho_{123} \\ \quad + \sigma_{123}\sigma_2\rho_3\rho_2\rho_1 + \sigma_1\sigma_2\rho_3\rho_2\rho_3\rho_2\rho_1\end{array} & \sigma_{123}\rho_1 + \sigma_1\rho_3\rho_2\rho_1 \\ 0 & \rho_1 & \sigma_2\rho_{123} + \sigma_{23}\sigma_2\rho_{123} + \sigma_2\rho_3\rho_2\rho_1 + \sigma_{23}\sigma_2\rho_3\rho_2\rho_1 & \sigma_{23}\rho_1 \\ 0 & 0 & \sigma_3\sigma_2\rho_{123} + \sigma_3\sigma_2\rho_3\rho_2\rho_1 + \rho_1 & \sigma_3\rho_1 \\ 0 & 0 & \sigma_{12}\rho_3 & 0 \\ 0 & 0 & \sigma_2\rho_3 & 0 \end{pmatrix}$$

$$M_{ba} = \begin{pmatrix} 1 & 0 & 0 & \sigma_3\sigma_2\rho_{123}\rho_2 + \sigma_3\sigma_2\rho_3\rho_2\rho_1\rho_2 & \sigma_{123}\rho_3\rho_2\rho_{12} + \sigma_1\rho_3\rho_2\rho_3\rho_2\rho_{12} \\ 0 & 1 & 0 & 0 & \rho_3\rho_2\rho_{12} + \sigma_{23}\rho_3\rho_2\rho_{12} \\ 0 & 0 & 1 & 0 & \sigma_3\rho_3\rho_2\rho_{12} \\ 0 & 0 & 0 & 1 + \sigma_3\sigma_2\rho_3\rho_2 & \sigma_{123} \\ 0 & 0 & 0 & 0 & 1 + \sigma_{23} \\ 0 & 0 & 0 & 0 & \sigma_3 \end{pmatrix}$$

$$M_{bb} = \begin{pmatrix} 0 & \sigma_1 & \sigma_{12} & \rho_{12} & 0 & 0 \\ 0 & 0 & \sigma_2 & 0 & \rho_{12} & 0 \\ 0 & 0 & 0 & 0 & 0 & \rho_{12} \\ 0 & 0 & 0 & 0 & \sigma_1 & \sigma_{12} \\ 0 & 0 & 0 & 0 & 0 & \sigma_2 \\ 0 & 0 & 0 & 0 & 0 & 0 \end{pmatrix}$$

$$M_{bc} = \begin{pmatrix} \begin{array}{l} \sigma_3\sigma_2\sigma_{123}\rho_{123}\rho_{23} + \sigma_{123}\sigma_{23}\rho_3\rho_2\rho_{123} + \sigma_{123}\rho_3\rho_2\rho_3\rho_2\rho_1 + \sigma_1\sigma_{23}\rho_3\rho_2\rho_3\rho_2\rho_{123} \\ \qquad + \sigma_3\sigma_2\sigma_3\sigma_2\sigma_1\rho_{123}\rho_{23} + \sigma_3\sigma_2\sigma_{123}\rho_3\rho_2\rho_1\rho_{23} + \sigma_{123}\sigma_{23}\rho_3\rho_2\rho_3\rho_2\rho_1 \\ \qquad + \sigma_1\sigma_{23}\rho_3\rho_2\rho_3\rho_2\rho_3\rho_2\rho_1 + \sigma_3\sigma_2\sigma_3\sigma_2\sigma_1\rho_3\rho_2\rho_1\rho_{23} \end{array} \\ \sigma_{23}\rho_3\rho_2\rho_{123} + \rho_3\rho_2\rho_3\rho_2\rho_1 + \sigma_{23}\sigma_{23}\rho_3\rho_2\rho_{123} + \sigma_{23}\sigma_{23}\rho_3\rho_2\rho_3\rho_2\rho_1 \\ \sigma_3\sigma_{23}\rho_3\rho_2\rho_{123} + \sigma_3\rho_3\rho_2\rho_3\rho_2\rho_1 + \sigma_3\sigma_{23}\rho_3\rho_2\rho_3\rho_2\rho_1 \\ \sigma_3\sigma_2\sigma_{123}\rho_3\rho_{23} + \sigma_3\sigma_2\sigma_3\sigma_2\sigma_1\rho_3\rho_{23} \\ 0 \\ 0 \end{pmatrix}$$

$$M_{bd} = \begin{pmatrix} 0 & \sigma_{123}\rho_{123} + \sigma_{123}\rho_3\rho_2\rho_1 & \begin{array}{l} \sigma_3\sigma_2\sigma_{12}\rho_{123}\rho_{23} + \sigma_{123}\sigma_2\rho_3\rho_2\rho_{123} \\ \quad + \sigma_1\sigma_2\rho_3\rho_2\rho_3\rho_2\rho_{123} + \sigma_3\sigma_2\sigma_{12}\rho_3\rho_2\rho_1\rho_{23} \\ \quad + \sigma_{123}\sigma_2\rho_3\rho_2\rho_3\rho_2\rho_1 + \sigma_1\sigma_2\rho_3\rho_2\rho_3\rho_2\rho_3\rho_2\rho_1 \end{array} & \begin{array}{l} \sigma_{123}\rho_{123} + \sigma_3\sigma_2\sigma_1\rho_{123} \\ \quad + \sigma_1\rho_3\rho_2\rho_3\rho_2\rho_1 \\ \quad + \sigma_3\sigma_2\sigma_1\rho_3\rho_2\rho_1 \end{array} \\ 0 & \sigma_{23}\rho_{123} + \sigma_{23}\rho_3\rho_2\rho_1 & \begin{array}{l} \sigma_2\rho_3\rho_2\rho_{123} + \sigma_{23}\sigma_2\rho_3\rho_2\rho_{123} + \sigma_2\rho_3\rho_2\rho_3\rho_2\rho_1 \\ \quad + \sigma_{23}\sigma_2\rho_3\rho_2\rho_3\rho_2\rho_1 \end{array} & \sigma_{23}\rho_{123} + \rho_3\rho_2\rho_1 \\ 0 & \sigma_3\rho_{123} + \sigma_3\rho_3\rho_2\rho_1 & \begin{array}{l} \rho_3\rho_2\rho_1 + \sigma_3\sigma_2\rho_3\rho_2\rho_{123} \\ \quad + \sigma_3\sigma_2\rho_3\rho_2\rho_3\rho_2\rho_1 + \rho_{123} \end{array} & \sigma_3\rho_{123} \\ 0 & \sigma_{123}\rho_3 & \sigma_3\sigma_2\sigma_{12}\rho_3\rho_{23} & \sigma_{123}\rho_3 + \sigma_3\sigma_2\sigma_1\rho_3 \\ 0 & \sigma_{23}\rho_3 & 0 & \sigma_{23}\rho_3 \\ 0 & \sigma_3\rho_3 & \rho_3 & \sigma_3\rho_3 \end{pmatrix}$$

$$M_{be} = \begin{pmatrix} \rho_1 & 0 & 0 \\ 0 & \rho_1 & 0 \\ 0 & 0 & \rho_1 \\ 0 & 0 & 0 \\ 0 & 0 & 0 \\ 0 & 0 & 0 \end{pmatrix}$$

$$M_{cc} = (0)$$

$$M_{da} = \begin{pmatrix} 0 & 0 & 0 & \rho_2 & 0 \\ 0 & 0 & 0 & 0 & \rho_2 \\ 0 & 0 & 0 & 0 & 0 \\ 0 & 0 & 0 & 0 & \rho_2 \end{pmatrix}$$

$$M_{dc} = \begin{pmatrix} \sigma_{123}\rho_{23} + \sigma_3\sigma_2\sigma_1\rho_{23} + \sigma_{123} \\ \sigma_{23}\rho_{23} + \sigma_{23} \\ \sigma_3 \\ 1 + \sigma_{23}\rho_{23} \end{pmatrix}$$

$$M_{dd} = \begin{pmatrix} 0 & \sigma_1 & \sigma_{12}\rho_{23} + \sigma_{12} & 0 \\ 0 & 0 & \sigma_2\rho_{23} + \sigma_2 & 0 \\ 0 & 0 & 0 & 0 \\ 0 & 0 & \sigma_2\rho_{23} & 0 \end{pmatrix}$$

$$M_{ea} = \begin{pmatrix} 0 & 0 & 0 & \sigma_3\sigma_2\rho_{23}\rho_2 & 0 \\ 0 & 0 & 0 & 0 & 0 \\ 0 & 0 & 0 & 0 & 0 \end{pmatrix}$$

$$M_{eb} = \begin{pmatrix} 0 & 0 & 0 & \rho_2 & 0 & 0 \\ 0 & 0 & 0 & 0 & \rho_2 & 0 \\ 0 & 0 & 0 & 0 & 0 & \rho_2 \end{pmatrix}$$

$$M_{ec} = \begin{pmatrix} \sigma_3\sigma_2\sigma_{123}\rho_{23}\rho_{23} \\ 0 \\ 0 \end{pmatrix}$$

$$M_{ed} = \begin{pmatrix} 1 & \sigma_{123}\rho_{23} & \sigma_3\sigma_2\sigma_{12}\rho_{23}\rho_{23} & \sigma_{123}\rho_{23} + \sigma_3\sigma_2\sigma_1\rho_{23} + \sigma_{123} \\ 0 & 1 + \sigma_{23}\rho_{23} & 0 & \sigma_{23}\rho_{23} + \sigma_{23} \\ 0 & \sigma_3\rho_{23} & 1 + \rho_{23} & \sigma_3\rho_{23} + \sigma_3 \end{pmatrix}$$

$$M_{ee} = \begin{pmatrix} 0 & \sigma_1 & \sigma_{12} \\ 0 & 0 & \sigma_2 \\ 0 & 0 & 0 \end{pmatrix}$$

Because we are ultimately interested in the tensor product of $\widehat{\mathrm{CFAA}}(\mathcal{Y}, B_3, 0)$ with $\widehat{\mathrm{CFD}}(\mathcal{X}_J^s)$ and $\widehat{\mathrm{CFD}}(\mathcal{X}_K^t)$, we may disregard any higher multiplication that uses sequences of algebra elements that cannot occur in these type D structures. Specifically, by Proposition 3.5, we may disregard any sequence containing $\rho_2\rho_3$, $\rho_1\rho_2$, $\rho_1\rho_{23}$, $\sigma_2\sigma_3$, $\sigma_1\sigma_2$, or $\sigma_1\sigma_{23}$. Accordingly, for the discussion that follows, we may replace M_{ac}, M_{ad}, M_{ba}, M_{bc}, and M_{bd} with the following:

$$M'_{ac} = \begin{pmatrix} \sigma_{123}\rho_{123} + \sigma_{123}\sigma_{23}\rho_{123} + \sigma_3\sigma_2\sigma_1\rho_{123} + \sigma_{123}\sigma_{23}\rho_3\rho_2\rho_1 + \sigma_3\sigma_2\sigma_1\rho_3\rho_2\rho_1 \\ \sigma_{23}\rho_{123} + \rho_3\rho_2\rho_1 + \sigma_{23}\sigma_{23}\rho_{123} + \sigma_{23}\sigma_{23}\rho_3\rho_2\rho_1 \\ \sigma_3\sigma_{23}\rho_{123} + \sigma_3\rho_3\rho_2\rho_1 + \sigma_3\sigma_{23}\rho_3\rho_2\rho_1 \\ \sigma_{123}\rho_3 + \sigma_3\sigma_2\sigma_1\rho_3 \\ \sigma_{23}\rho_3 \end{pmatrix}$$

$$M'_{ad} = \begin{pmatrix} \rho_1 & 0 & \sigma_{12}\rho_{123} + \sigma_{123}\sigma_2\rho_{123} + \sigma_{12}\rho_3\rho_2\rho_1 + \sigma_{123}\sigma_2\rho_3\rho_2\rho_1 & \sigma_{123}\rho_1 + \sigma_1\rho_3\rho_2\rho_1 \\ 0 & \rho_1 & \sigma_2\rho_{123} + \sigma_{23}\sigma_2\rho_{123} + \sigma_2\rho_3\rho_2\rho_1 + \sigma_{23}\sigma_2\rho_3\rho_2\rho_1 & \sigma_{23}\rho_1 \\ 0 & 0 & \sigma_3\sigma_2\rho_{123} + \sigma_3\sigma_2\rho_3\rho_2\rho_1 + \rho_1 & \sigma_3\rho_1 \\ 0 & 0 & \sigma_{12}\rho_3 & 0 \\ 0 & 0 & \sigma_2\rho_3 & 0 \end{pmatrix}$$

$$M'_{ba} = \begin{pmatrix} 1 & 0 & 0 & \sigma_3\sigma_2\rho_{123}\rho_2 & \sigma_{123}\rho_3\rho_2\rho_{12} \\ 0 & 1 & 0 & 0 & \rho_3\rho_2\rho_{12} + \sigma_{23}\rho_3\rho_2\rho_{12} \\ 0 & 0 & 1 & 0 & \sigma_3\rho_3\rho_2\rho_{12} \\ 0 & 0 & 0 & 1 + \sigma_3\sigma_2\rho_3\rho_2 & \sigma_{123} \\ 0 & 0 & 0 & 0 & 1 + \sigma_{23} \\ 0 & 0 & 0 & 0 & \sigma_3 \end{pmatrix}$$

$$M'_{bc} = \begin{pmatrix} \sigma_3\sigma_2\sigma_{123}\rho_{123}\rho_{23} + \sigma_{123}\sigma_{23}\rho_3\rho_2\rho_{123} \\ \sigma_{23}\rho_3\rho_2\rho_{123} + \sigma_{23}\sigma_{23}\rho_3\rho_2\rho_{123} \\ \sigma_3\sigma_{23}\rho_3\rho_2\rho_{123} \\ \sigma_3\sigma_2\sigma_{123}\rho_3\rho_{23} \\ 0 \\ 0 \end{pmatrix}$$

$$M'_{bd} = \begin{pmatrix} 0 & \sigma_{123}\rho_{123} + \sigma_{123}\rho_3\rho_2\rho_1 & \sigma_3\sigma_2\sigma_{12}\rho_{123}\rho_{23} + \sigma_{123}\sigma_2\rho_3\rho_2\rho_{123} & \begin{matrix} \sigma_{123}\rho_{123} + \sigma_3\sigma_2\sigma_1\rho_{123} \\ + \sigma_3\sigma_2\sigma_1\rho_3\rho_2\rho_1 \end{matrix} \\ 0 & \sigma_{23}\rho_{123} + \sigma_{23}\rho_3\rho_2\rho_1 & \sigma_2\rho_3\rho_2\rho_{123} + \sigma_{23}\sigma_2\rho_3\rho_2\rho_{123} & \sigma_{23}\rho_{123} + \rho_3\rho_2\rho_1 \\ 0 & \sigma_3\rho_{123} + \sigma_3\rho_3\rho_2\rho_1 & \rho_3\rho_2\rho_1 + \sigma_3\sigma_2\rho_3\rho_2\rho_{123} + \rho_{123} & \sigma_3\rho_{123} \\ 0 & \sigma_{123}\rho_3 & \sigma_3\sigma_2\sigma_{12}\rho_3\rho_{23} & \sigma_{123}\rho_3 + \sigma_3\sigma_2\sigma_1\rho_3 \\ 0 & \sigma_{23}\rho_3 & 0 & \sigma_{23}\rho_3 \\ 0 & \sigma_3\rho_3 & \rho_3 & \sigma_3\rho_3 \end{pmatrix}$$

3.3 Evaluation of the tensor product

Using the computation of $\widehat{\mathrm{CFAA}}(\mathcal{Y}, B_3, 0)$ given in the previous section, we may now compute the double tensor product

$$(\widehat{\mathrm{CFAA}}(\mathcal{Y}, B_3, 0) \boxtimes_{\mathcal{A}_\rho} \widehat{\mathrm{CFD}}(\mathcal{X}_J^s)) \boxtimes_{\mathcal{A}_\sigma} \widehat{\mathrm{CFD}}(\mathcal{X}_K^t).$$

In what follows, we evaluate the tensor product over $\mathcal{A}_\rho$ and simplify the resulting filtered type A module before evaluating the tensor product over $\mathcal{A}_\sigma$. Then we use the edge cancellation algorithm to compute $\tau(D_{J,s}(K,t))$.

As discussed above, we assume from now on that $s \le 2\tau(J)$.

3.3.1 Tensor product over $\mathcal{A}_\rho$

Let $\mathcal{V}$ denote the bordered solid torus obtained by gluing together $\mathcal{Y}$ and $\mathcal{X}_J^s$, and let $D_{J,s}$ denote the image of the knot B_3 in the union. By the gluing theorem, $\widehat{\mathrm{CFA}}(\mathcal{V}, D_{J,s}) \simeq \widehat{\mathrm{CFAA}}(\mathcal{Y}, B_3, 0) \boxtimes_{\mathcal{A}_\rho} \widehat{\mathrm{CFD}}(\mathcal{X}_J^s)$. We shall describe this tensor product as a direct sum of subspaces corresponding to the stable and unstable chains in $\widehat{\mathrm{CFD}}(\mathcal{X}_J^s)$. This decomposition will not be a direct sum of $\mathcal{A}_\infty$ modules, but we will be able to keep track of the few multiplications that do not respect the decomposition, and ultimately they will not affect the computation of $\tau(D_{J,s}(K,t))$.

The generators of $\iota_1\widehat{\mathrm{CFD}}(\mathcal{X}_J^s)$ all lie in the interiors of the chains, so the corresponding generators of the tensor product can be grouped in a natural way, but it is not obvious *a priori* how to divide up the generators coming from $\iota_0\widehat{\mathrm{CFD}}(\mathcal{X}_J^s)$. Consider the two specified bases for $\iota_0\widehat{\mathrm{CFD}}(\mathcal{X}_J^s)$: $\{\eta_0, \dots, \eta_{2n}\}$ and $\{\xi_0, \dots, \xi_{2n}\}$. Depending on the structure of the unstable chain, the generators ξ_i have outgoing arrows labeled ρ_1, ρ_{12}, or ρ_{123}, while the η_i have outgoing arrows labeled ρ_3 and incoming arrows labeled ρ_2 or ρ_{12}. Accordingly, we should try to pair the generators of $\widehat{\mathrm{CFAA}}(\mathcal{Y}, B_3, 0)\iota_0$ with the ξ_i or η_i depending on which of these two conditions they satisfy. If we consider only the $\mathcal{A}_\infty$ maps in $\widehat{\mathrm{CFAA}}(\mathcal{Y}, B_3, 0)$ that use a single element of $\mathcal{A}_\rho$, we notice that each of the generators $a_1, \dots, a_5$ and $b_1, \dots, b_6$ satisfies exactly one such condition. Specifically, define the following subspaces of

$\widehat{\mathrm{CFAA}}(\mathcal{Y}, B_3, 0) \boxtimes_{\mathcal{A}_\rho} \widehat{\mathrm{CFD}}(\mathcal{X}^s_J)$:

$$\begin{aligned}
P^j_{\mathrm{vert}} &= \langle a_4, a_5, b_4, b_5, b_6 \rangle \boxtimes \langle \xi_{2j-1}, \xi_{2j} \rangle \\
&\qquad + \langle c_1, d_1, d_2, d_3, d_4, e_1, e_2, e_3 \rangle \boxtimes \left\langle \kappa^j_i \mid 1 \leq i \leq k_j \right\rangle \\
P^j_{\mathrm{hor}} &= \langle a_1, a_2, a_3, b_1, b_2, b_3 \rangle \boxtimes \langle \eta_{2j-1}, \eta_{2j} \rangle \\
&\qquad + \langle c_1, d_1, d_2, d_3, d_4, e_1, e_2, e_3 \rangle \boxtimes \left\langle \lambda^j_i \mid 1 \leq i \leq l_j \right\rangle \\
P_{\mathrm{unst}} &= \langle a_4, a_5, b_4, b_5, b_6 \rangle \boxtimes \langle \xi_0 \rangle \\
&\qquad + \langle a_1, a_2, a_3, b_1, b_2, b_3 \rangle \boxtimes \langle \eta_0 \rangle \\
&\qquad + \langle c_1, d_1, d_2, d_3, d_4, e_1, e_2, e_3 \rangle \boxtimes \langle \lambda_i \mid 1 \leq i \leq r \rangle .
\end{aligned} \tag{3.14}$$

We thus obtain a direct sum decomposition of $\widehat{\mathrm{CFAA}}(\mathcal{Y}, B_3, 0) \boxtimes_{\mathcal{A}_\rho} \widehat{\mathrm{CFD}}(\mathcal{X}^s_J)$ as a vector space:

$$\widehat{\mathrm{CFAA}}(\mathcal{Y}, B_3, 0) \boxtimes_{\mathcal{A}_\rho} \widehat{\mathrm{CFD}}(\mathcal{X}^s_J) = \bigoplus_{j=1}^{n} P^j_{\mathrm{vert}} \oplus \bigoplus_{j=1}^{n} P^j_{\mathrm{hor}} \oplus P_{\mathrm{unst}}. \tag{3.15}$$

By inspecting the matrices M_{xy}, we see that any $\mathcal{A}_\infty$ multiplication on the tensor product that comes from a multiplication in $\widehat{\mathrm{CFAA}}(\mathcal{Y}, B_3, 0)$ that uses at most one element of $\mathcal{A}_\rho$ preserves this decomposition. These multiplications are illustrated in Figures 22 through 25. In these and subsequent figures, the dashed arrows represent repeated sections. For instance, the dashed arrow from $e_1\kappa^j_1$ to $d_2\kappa^j_{k_j}$ in Figure 22 means that there are multiplications $e_1\kappa^j_i \xrightarrow{\sigma_{123}} d_2\kappa^j_{i+1}$ for each $i = 1, \ldots, k_j - 1$. The Alexander grading is indicated by horizontal position, increasing from left to right.

In addition, there are a few more multiplications that preserve the splitting, coming from multiplications in $\widehat{\mathrm{CFAA}}(\mathcal{Y}, B_3, 0)$ that use sequences like $\rho_3\rho_2$, $\rho_3\rho_{23}$, or $\rho_{23}\rho_{23}$. These multiplications are not shown in Figures 22 through 25. They are as follows:

- In P^j_{vert}, when $k_j > 1$, there are multiplications

$$\begin{aligned}
&b_1\xi_{2j} \xrightarrow{\sigma_3\sigma_2\sigma_{12}} d_3\kappa^j_2 &\qquad& b_1\xi_{2j} \xrightarrow{\sigma_3\sigma_2\sigma_{123}} c_1\kappa^j_2 \\
&e_1\kappa^j_i \xrightarrow{\sigma_3\sigma_2\sigma_{12}} d_3\kappa^j_{i+2} && e_1\kappa^j_i \xrightarrow{\sigma_3\sigma_2\sigma_{123}} c_1\kappa^j_{i+2} \quad (i = 1, \ldots, k_j - 2).
\end{aligned} \tag{3.16}$$

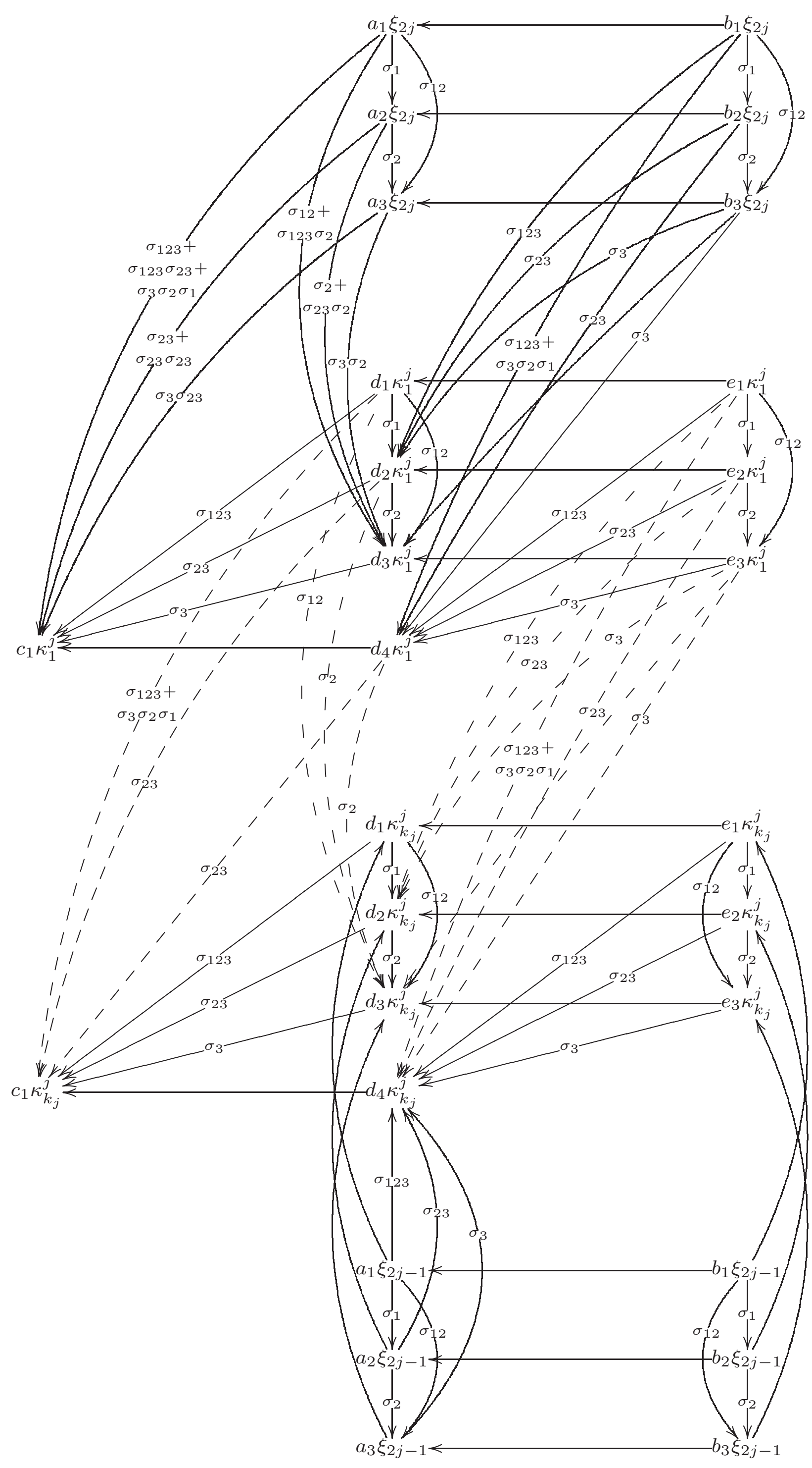

Figure 22: The subspace P^j_{vert}, corresponding to a vertical stable chain $\xi_{2j} \xrightarrow{\rho_{123}} \kappa^j_1 \xrightarrow{\rho_{23}} \cdots \xrightarrow{\rho_{23}} \kappa^j_{k_j} \xleftarrow{\rho_1} \xi_{2j-1}$.

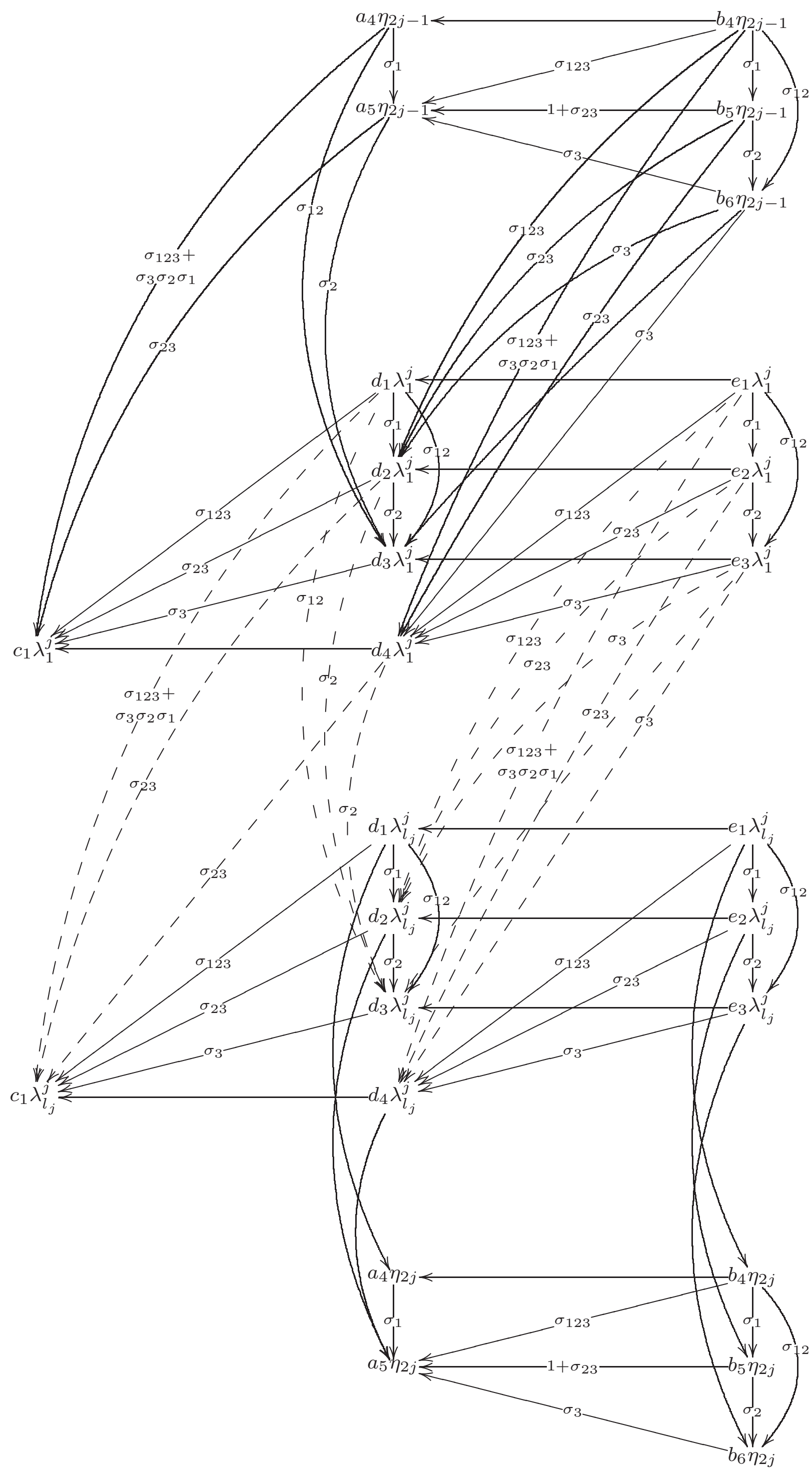

Figure 23: The subspace P^j_{hor}, corresponding to a horizontal stable chain $\eta_{2j-1} \xrightarrow{\rho_3} \lambda_1^j \xrightarrow{\rho_{23}} \cdots \xrightarrow{\rho_{23}} \lambda_{l_j}^j \xrightarrow{\rho_2} \eta_{2j}$.

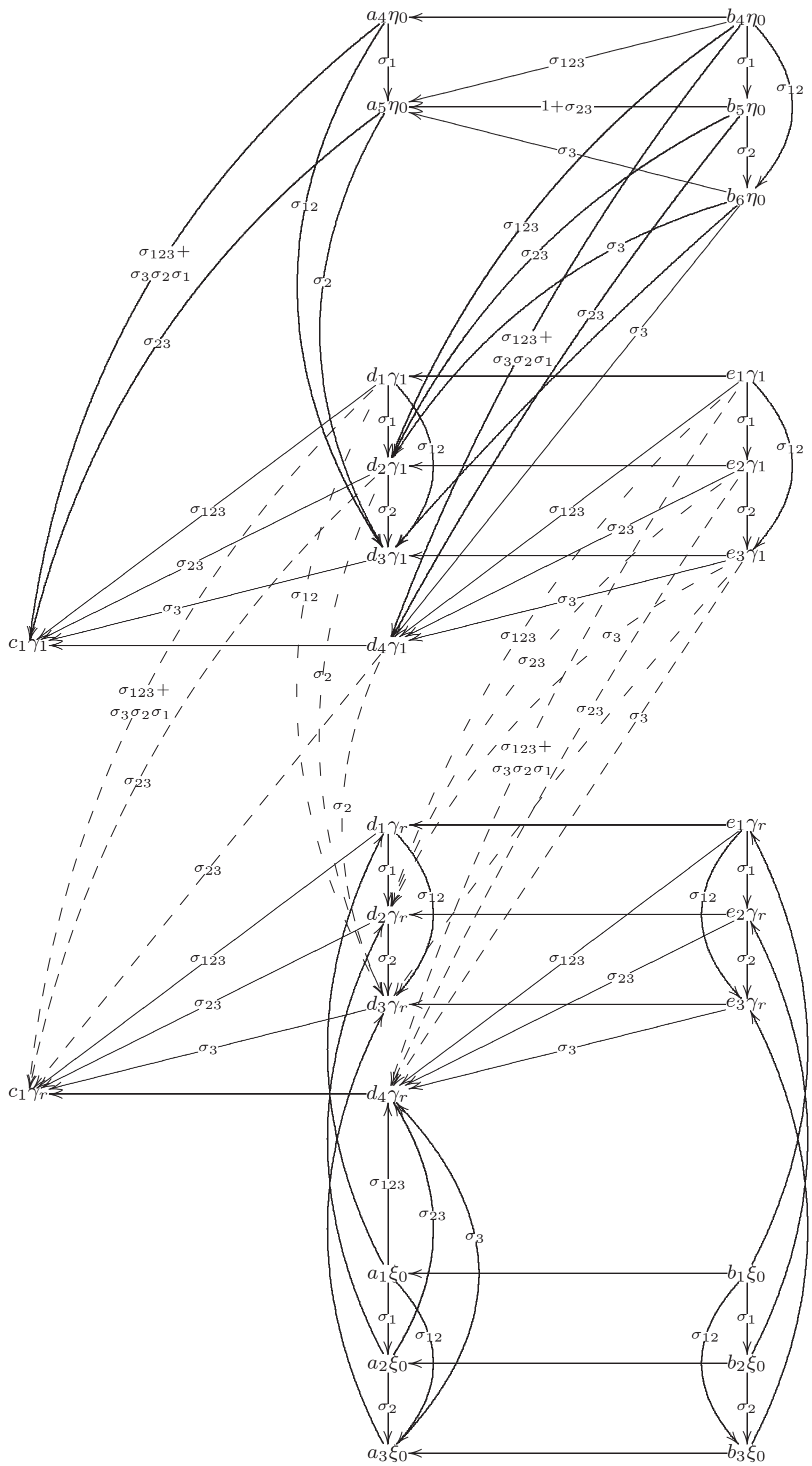

Figure 24: The subspace P_{unst} when $s < 2\tau(J)$, corresponding to the unstable chain $\eta_0 \xrightarrow{\rho_3} \gamma_1 \xrightarrow{\rho_{23}} \cdots \xrightarrow{\rho_{23}} \gamma_s \xleftarrow{\rho_1} \xi_0$.

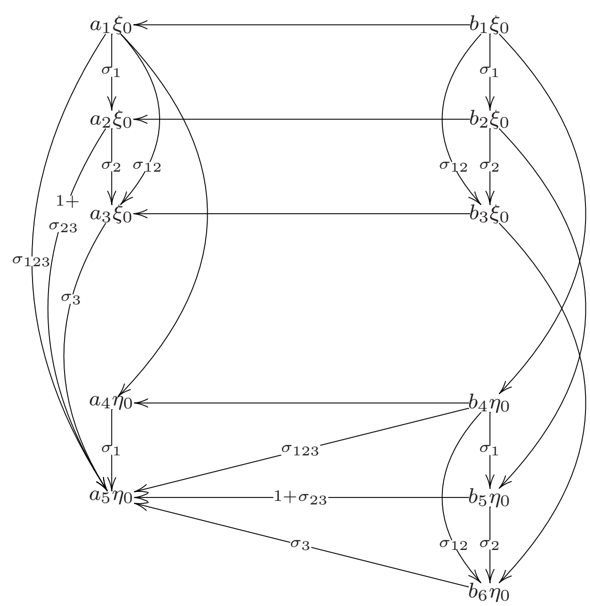

Figure 25: The subspace P_{unst} when $s = 2\tau(J)$, corresponding to the unstable chain $\xi_0 \xrightarrow{\rho_{12}} \eta_0$.

- In P^j_{hor}, when $l_j = 1$, there is a multiplication $b_4\eta_{2j-1} \xrightarrow{\sigma_3\sigma_2} a_4\eta_{2j}$. When $l_j > 1$, there are multiplications

$$\begin{aligned} &b_4\eta_{2j-1} \xrightarrow{\sigma_3\sigma_2\sigma_{12}} d_3\lambda^j_2 && b_4\eta_{2j-1} \xrightarrow{\sigma_3\sigma_2\sigma_{123}} c_1\lambda^j_2 \\ &e_1\lambda^j_{l_j-1} \xrightarrow{\sigma_3\sigma_2} a_4\eta_{2j} \\ &e_1\lambda^j_i \xrightarrow{\sigma_3\sigma_2\sigma_{12}} d_3\lambda^j_{i+2} && e_1\lambda^j_i \xrightarrow{\sigma_3\sigma_2\sigma_{123}} c_1\lambda^j_{i+2} \quad (i = 1, \dots, l_j - 2). \end{aligned} \tag{3.17}$$

- In P_{unst} in the case when $s < 2\tau(J) - 1$, there are multiplications

$$\begin{aligned} &b_4\eta_0 \xrightarrow{\sigma_3\sigma_2\sigma_{12}} d_3\gamma_2 && b_4\eta_0 \xrightarrow{\sigma_3\sigma_2\sigma_{123}} c_1\gamma_2 \\ &e_1\gamma_i \xrightarrow{\sigma_3\sigma_2\sigma_{12}} d_3\gamma_{i+2} && e_1\gamma_i \xrightarrow{\sigma_3\sigma_2\sigma_{123}} c_1\gamma_{i+2} \quad (i = 1, \dots, r - 2). \end{aligned} \tag{3.18}$$

Finally, we must consider the multiplications in the tensor product that do not respect the splitting in (3.15). These arise from sequences of arrows in $\widehat{\mathrm{CFD}}(\mathcal{X}^s_J)$ that involve multiple stable or unstable chains, and they depend on the change-of-basis coefficients relating $\{\eta_0, \dots, \eta_{2n}\}$ and $\{\xi_0, \dots, \xi_{2n}\}$.

For instance, if $\eta_{2j} = \xi_{2h}$ (where $j, h \in \{1, \dots, n\}$), then $\widehat{\mathrm{CFD}}(\mathcal{X}^s_J)$ contains a string of arrows of the form

$$\eta_{2j-1} \xrightarrow{\rho_3} \lambda^j_1 \xrightarrow{\rho_{23}} \cdots \xrightarrow{\rho_{23}} \lambda^j_{l_j} \xrightarrow{\rho_2} \eta_{2j} \xrightarrow{\rho_{123}} \kappa^h_1 \xrightarrow{\rho_{23}} \cdots \xrightarrow{\rho_{23}} \kappa^h_{k_h}.$$

Any multiplication in $\widehat{\mathrm{CFAA}}(\mathcal{Y}, B_3, 0)$ that uses a contiguous subsequence of

$$\rho_3, \underbrace{\rho_{23}, \dots, \rho_{23}}_{l_j-1 \text{ times}}, \rho_2, \rho_{123}, \underbrace{\rho_{23}, \dots, \rho_{23}}_{k_h-1 \text{ times}}$$

contributes a nonzero multiplication in the tensor product that need not respect the splitting. Similarly, if $\eta_{2j} = \xi_{2h-1}$, then the same is true for contiguous subsequences of

$$\rho_3, \underbrace{\rho_{23}, \dots, \rho_{23}}_{l_j-1 \text{ times}}, \rho_2, \rho_1.$$

Similar sequences may also occur near the unstable chain, where we take ξ_0 instead of ξ_{2h-1} or ξ_{2h}. By Proposition 3.5, these are the only such sequences that occur. More generally, if the coefficient of ξ_p in η_{2j} is nonzero, we obtain multiplications that do not respect the splitting in (3.15). We make this notion more precise below.

By inspecting the matrices M_{xy}, we see that the only sequences of this form that actually occur in $\widehat{\mathrm{CFAA}}(\mathcal{Y}, B_3, 0)$ are $\rho_3\rho_2\rho_{123}$, $\rho_3\rho_2\rho_{12}$, and $\rho_3\rho_2\rho_1$, which occur in the first three rows of M_{ac}, M_{ad}, M_{ba}, M_{bc}, and M_{bd}. Accordingly, the only multiplications that do not preserve the splitting arise when there is a horizontal edge $\eta_{2j-1} \to \eta_{2j}$ of length 1, and they act on the elements $a_i \boxtimes \eta_{2j-1}$ and $b_i \boxtimes \eta_{2j-1}$ $(i = 1, 2, 3)$.

Notice that there are no multiplications into or out of any of the subspaces P^j_{hor}. Therefore, each P^j_{hor} is actually a direct summand (as an $\mathcal{A}_\infty$ submodule) of $\widehat{\mathrm{CFA}}(\mathcal{V}, D_{J,s})$, as is $P = \bigoplus_{j=1}^n P^j_{\mathrm{vert}} \oplus P_{\mathrm{unst}}$. This implies that the tensor product $\widehat{\mathrm{CFA}}(\mathcal{V}, D_{J,s}) \boxtimes \widehat{\mathrm{CFD}}(\mathcal{X}^t_K)$ (whose total homology, ignoring the filtration, is $\widehat{\mathrm{HF}}(S^3) \cong \mathbb{F}$) will also split as a direct sum. We shall eventually see that the direct summand coming from P contributes $\mathbb{F}$ to the total homology, which means that each summand coming from P^j_{hor} is acyclic and thus does not affect the computation of $\tau(D_{J,s}(K,t))$. Therefore, we shall henceforth ignore the submodules P^j_{hor}.

It is preferable to describe all of the multiplications that do not respect the splitting in terms of the bases specified in (3.14). Recall that $(x_{p,q})$ and $(y_{p,q})$ are the change-of-basis matrices, so that $\xi_p = \sum_{q=0}^{2n} x_{p,q}\eta_q$ and $\eta_p = \sum_{q=0}^{2n} y_{p,q}\xi_q$. Let $\mathfrak{j}$ denote the set $\{j \in \{1, \dots, n\} \mid l_j = 1\}$. For each $p \in \{0, \dots, 2n\}$ and $h \in \{1, \dots, n\}$, each $j \in \mathfrak{j}$ for which $x_{p,2j-1} = 1$ and $y_{2j,2h-1} = 1$ contributes multiplications (which we will specify shortly) from $a_i\xi_p$ and/or $b_i\xi_p$ $(i = 1, 2, 3)$ into P^h_{vert} via the sequence $\rho_3\rho_2\rho_{123}$. Of course, multiple values of j may satisfy this criterion, but they all contribute the same multiplications, so we really only care about the count of such j modulo 2. That is, define $u_{p,h} = \sum_{j\in\mathfrak{j}} x_{p,2j-1}y_{2j,2h-1}$; there are multiplications from $a_i\xi_p$ and $b_i\xi_p$ into P^h_{vert} iff $u_{p,h} = 1$.

Similarly, each j for which $x_{p,2j-1} = 1$ and $y_{2j,2h}$ $(h = 1, \dots, n)$ contributes multiplications via $\rho_3\rho_2\rho_1$, so define $v_{p,h} = \sum_{j\in\mathfrak{j}} x_{p,2j-1}y_{2j,2h}$. Finally, we set $w_p = \sum_{j\in\mathfrak{j}} x_{p,2j-1}y_{2h,0}$; this determines whether there are additional multiplications from

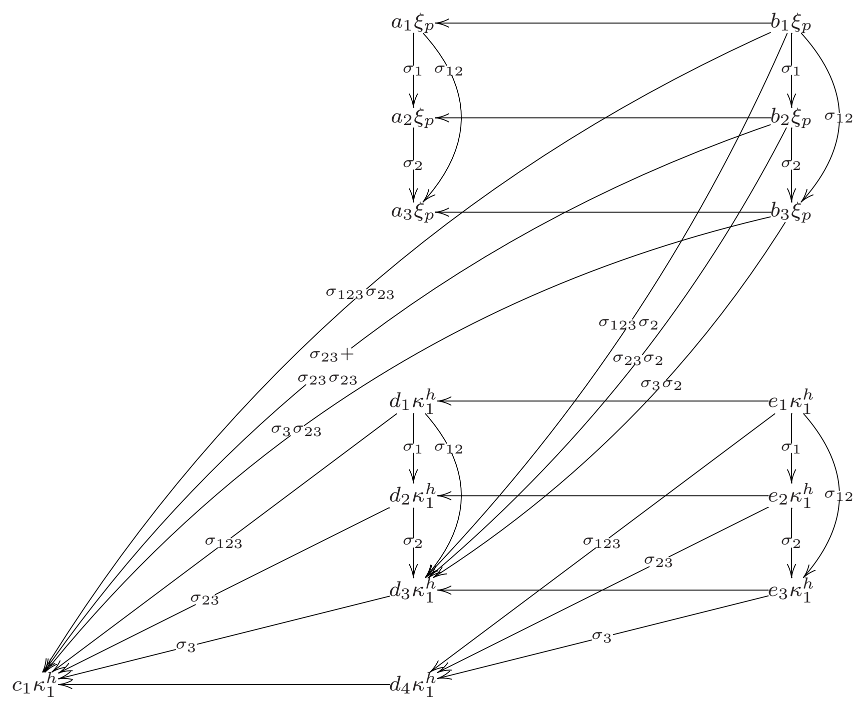

Figure 26: Multiplications coming from a sequence $\rho_3\rho_2\rho_{123}$ when $u_{p,h} = 1$.

$a_i\xi_p$ and $b_i\xi_p$ into the unstable chain via $\rho_3\rho_2\rho_1$, $\rho_3\rho_2\rho_{12}$, or $\rho_3\rho_2\rho_{123}$, according to whether $s < 2\tau(J)$, $s = 2\tau(J)$ or $s > 2\tau(K)$, respectively (although we are ignoring the third case).

We now specify these multiplications:

- If $u_{p,h} = 1$, the sequence $\rho_3\rho_2\rho_{123}$ provides the multiplications shown in Figure 26.

- If $v_{p,h} = 1$, the sequence $\rho_3\rho_2\rho_1$ provides the multiplications shown in Figure 27.

- If $s < 2\tau(J)$ and $w_p = 1$, the sequence $\rho_3\rho_2\rho_1$ provides the multiplications shown in Figure 27, where we replace $\kappa^h_{k_h}$ by γ_r.

- Finally, if $s = 2\tau(K)$ and $w_p = 1$, the sequence $\rho_3\rho_2\rho_{12}$ provides the following

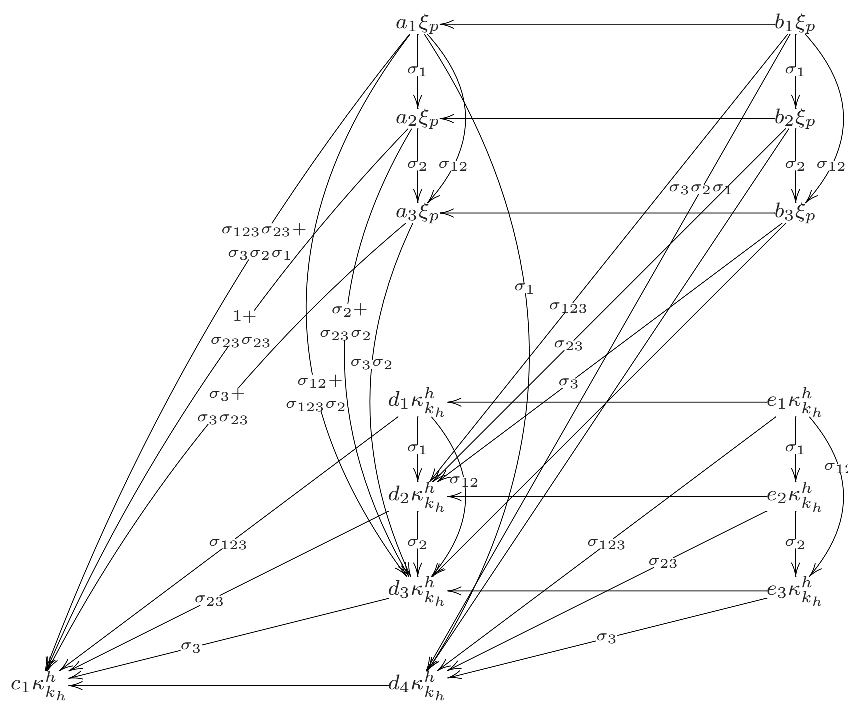

Figure 27: Multiplications coming from a sequence $\rho_3\rho_2\rho_1$ when $v_{p,h} = 1$. If $w_p = 1$ and $s < 2\tau(K)$, we obtain the same multiplications by replacing $\kappa^h_{k_h}$ by γ_r.

multiplications:

$$\begin{aligned}
a_1\xi_p &\xrightarrow{\sigma_1} a_5\eta_0 \\
b_1\xi_p &\xrightarrow{\sigma_{123}} a_5\eta_0 \\
b_2\xi_p &\xrightarrow{1+\sigma_{23}} a_5\eta_0 \\
b_3\xi_p &\xrightarrow{\sigma_3} a_5\eta_0.
\end{aligned} \tag{3.19}$$

3.3.2 Simplification of $\widehat{\mathrm{CFA}}(\mathcal{V}, D_{J,s})$

Next, we may simplify $\widehat{\mathrm{CFA}}(\mathcal{V}, D_{J,s})$ by canceling unmarked edges that preserve the filtration level. In order to keep track of additional edges that may appear, we must look carefully at the order of cancellation. As mentioned above, we ignore the direct summands P^j_{hor}. Define $P^0 = P_{\mathrm{unst}}$ and $P^j = P^j_{\mathrm{vert}}$.

Assume first that $s < 2\tau(J)$.

For each $j \in \{1, \dots, n\}$, in P^j, we may cancel the differentials $b_1\xi_{2j-1} \to e_1\kappa^j_{k_j}$, $b_2\xi_{2j-1} \to e_2\kappa^j_{k_j}$, $b_2\xi_{2j-1} \to e_2\kappa^j_{k_j}$, and $a_1\xi_{2j-1} \to d_1\kappa^j_{k_j}$. Since the targets of those arrows do not lie at the heads of any other arrows, no additional arrows are introduced. Similarly, in P^0, cancel $b_1\xi_0 \to e_1\gamma_r$, $b_2\xi_0 \to e_2\gamma_r$, $b_2\xi_0 \to e_2\gamma_r$, and $a_1\xi_0 \to d_1\gamma_r$.

Next, we cancel the differentials $a_2\xi_{2j-1} \to d_2\kappa^j_{k_j}$ and $a_2\xi_0 \to d_2\gamma_r$. Because of the edge $a_2\xi_{2j-1} \xrightarrow{\sigma_{23}} d_4\kappa^j_{k_j}$, canceling $a_2\xi_{2j-1} \to d_2\kappa^j_{k_j}$ introduces new multiplications:

$$\begin{aligned}
e_1\kappa^j_{k_j-1} &\xrightarrow{\sigma_{123}\sigma_2} a_3\xi_{2j-1} & \qquad e_1\kappa^j_{k_j-1} &\xrightarrow{\sigma_{123}\sigma_{23}} d_4\kappa^j_{k_j} \\
e_2\kappa^j_{k_j-1} &\xrightarrow{\sigma_{23}\sigma_2} a_3\xi_{2j-1} & \qquad e_2\kappa^j_{k_j-1} &\xrightarrow{\sigma_{23}\sigma_{23}} d_4\kappa^j_{k_j} \\
e_3\kappa^j_{k_j-1} &\xrightarrow{\sigma_3\sigma_2} a_3\xi_{2j-1} & \qquad e_3\kappa^j_{k_j-1} &\xrightarrow{\sigma_3\sigma_{23}} d_4\kappa^j_{k_j}.
\end{aligned} \tag{3.20}$$

(If $k_j = 1$, then replace $e_i\kappa^j_{k_j-1}$ by $b_i\xi_{2j}$ in (3.20).) We shall examine the effects of these cancellations on the edges that do not respect the splitting momentarily.

Next, because of the edge $a_3\xi_{2j-1} \xrightarrow{\sigma_3} d_4\kappa^j_{k_j}$, canceling $a_3\xi_{2j-1} \to d_3\kappa^j_{k_j}$ removes the edge $e_3\kappa^j_{k_j-1} \xrightarrow{\sigma_3} d_4\kappa^j_{k_j}$ and adds edges

$$\begin{aligned} d_1\kappa^j_{k_j-1} &\xrightarrow{\sigma_{12}\sigma_3} d_4\kappa^j_{k_j} \\ d_2\kappa^j_{k_j-1} &\xrightarrow{\sigma_2\sigma_3} d_4\kappa^j_{k_j} \\ d_4\kappa^j_{k_j-1} &\xrightarrow{\sigma_2\sigma_3} d_4\kappa^j_{k_j} \\ e_1\kappa^j_{k_j-2} &\xrightarrow{\sigma_3\sigma_2\sigma_{12}\sigma_3} d_4\kappa^j_{k_j}. \end{aligned} \tag{3.21}$$

Because we will ultimately tensor with $\widehat{\mathrm{CFD}}(X^t_K)$, in which the sequences $\sigma_2\sigma_3$ and $\sigma_{12}\sigma_3$ do not appear, we may disregard these four edges. We also eliminate the edge $e_3\kappa^j_{k_j-1} \xrightarrow{\sigma_3} d_4\kappa^j_{k_j-1}$. The same thing occurs in P^0 when we cancel $a_3\xi_0 \to d_3\gamma_r$.

Let Q^j denote the module resulting from P^j after the cancellations just described. The multiplications on Q^j are shown in Figures 28 and 29 and equations (3.16) and (3.18).

Now we keep track of what these cancellations do to the edges that do not respect the splitting, as shown in Figures 26 and 27.

If $u_{p,j} = 1$, then there are edges from $b_i\xi_p$ to $d_3\kappa^j_1$, as shown in Figure 26. If $k_j = 1$, then canceling $a_3\xi_{2j-1} \to d_3\kappa^j_1$ will introduce new multiplications coming from $b_i\xi_p$, but all of these multiplications involve $\sigma_2\sigma_3$ or $\sigma_{12}\sigma_3$ and may thus be disregarded. Also, when $p = 2m+1$ or $p = 0$ these edges are eliminated when we cancel $b_i\xi_{2m+1} \to e_i\kappa^m_{k_m}$ or $b_i\xi_0 \to e_i\gamma_r$, respectively.

If $v_{p,j} = 1$, when we cancel $a_2\xi_{2j-1} \to d_2\kappa^j_{k_j}$, we obtain multiplications

$$\begin{aligned} b_1\xi_p &\xrightarrow{\sigma_{123}\sigma_2} a_3\xi_{2j-1} \qquad & b_1\xi_p &\xrightarrow{\sigma_{123}\sigma_{23}} d_4\kappa^j_{k_j} \\ b_2\xi_p &\xrightarrow{\sigma_{23}\sigma_2} a_3\xi_{2j-1} \qquad & b_2\xi_p &\xrightarrow{\sigma_{23}\sigma_{23}} d_4\kappa^j_{k_j} \\ b_3\xi_p &\xrightarrow{\sigma_3\sigma_{23}} d_4\kappa^j_{k_j} \qquad & b_3\xi_p &\xrightarrow{\sigma_3\sigma_2} a_3\xi_{2j-1} \end{aligned} \tag{3.22}$$

in addition to the ones already appearing in Figure 27. When we then cancel

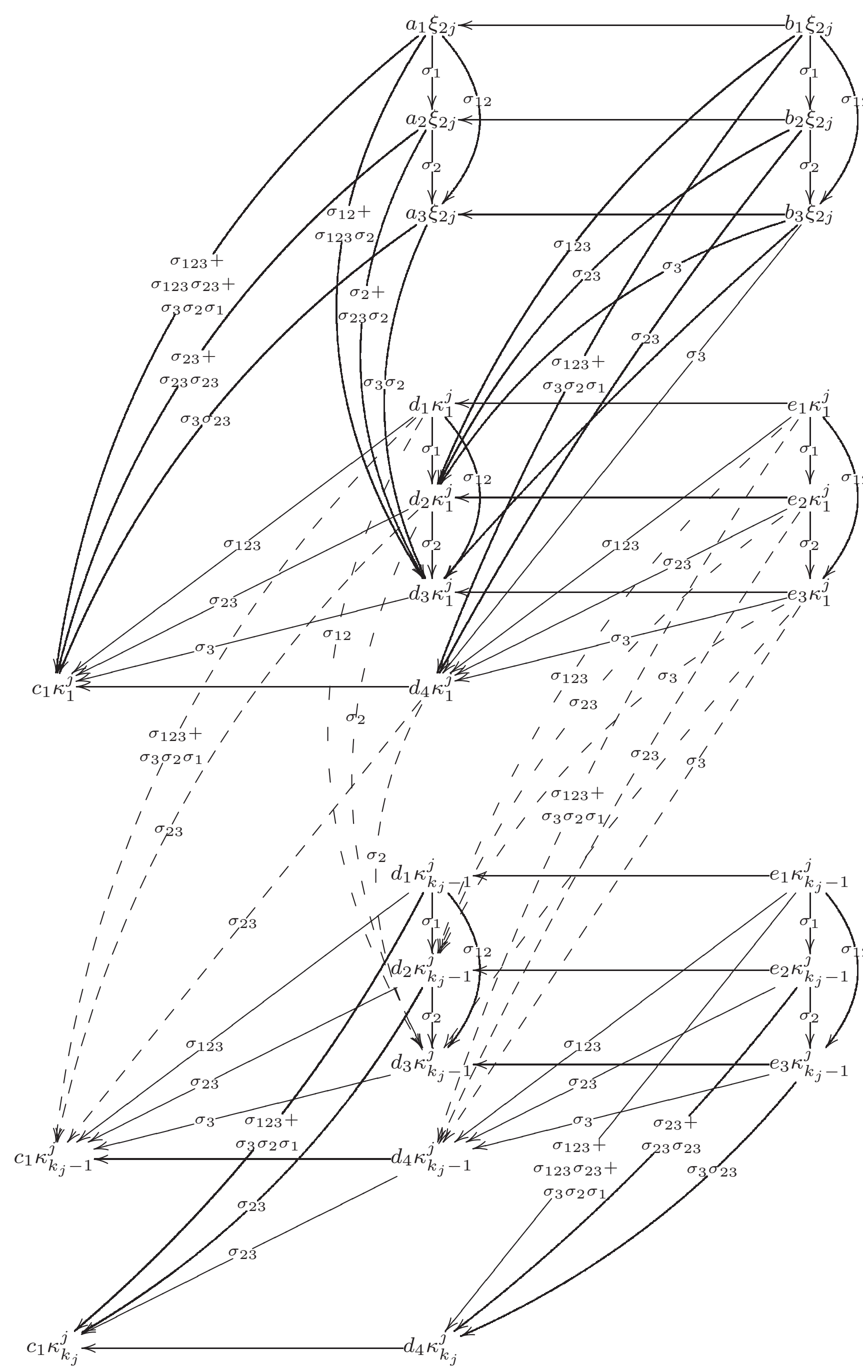

Figure 28: The subspace Q^j ($j > 0$) obtained from P^j_{vert} by canceling edges.

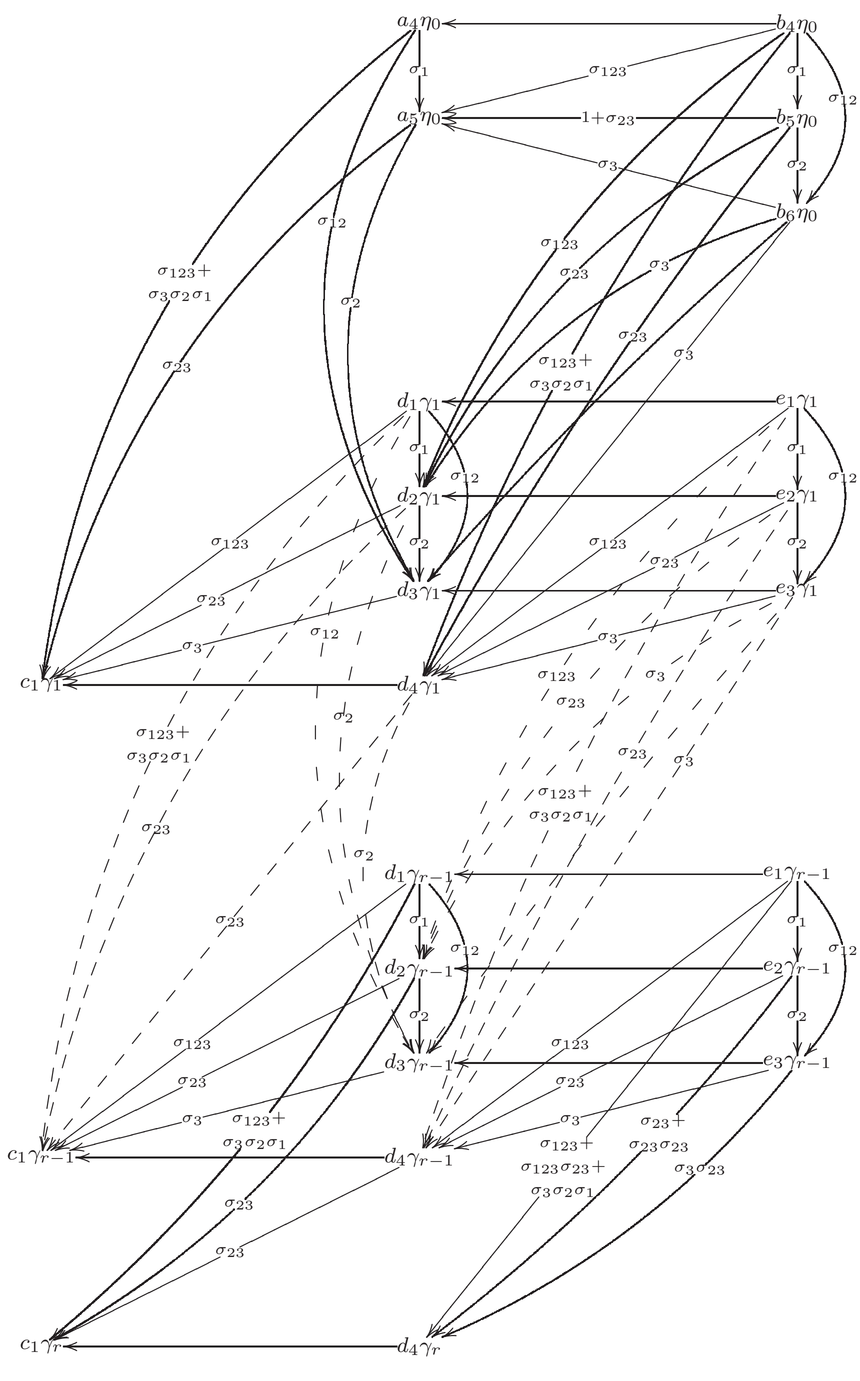

Figure 29: The subspace Q^0 obtained from P_{unst} by canceling edges, when $s < 2\tau(J)$.

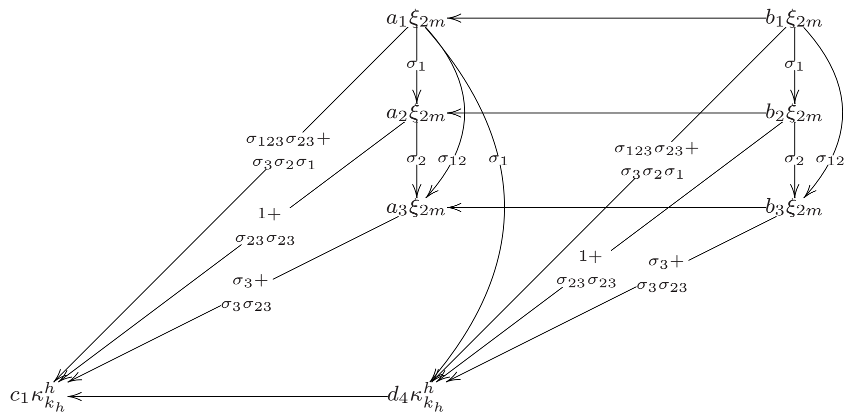

Figure 30: Reduced form of Figure 27 when $p = 2m$, $m > 0$.

$a_3\xi_{2j-1} \to d_3\kappa^j_{k_j}$, we obtain new multiplications:

$$\begin{aligned}
a_1\xi_p &\xrightarrow{\sigma_{12}\sigma_3+\sigma_{123}\sigma_2\sigma_3} d_4\kappa^j_{k_j} \\
a_2\xi_p &\xrightarrow{\sigma_2\sigma_3+\sigma_{23}\sigma_2\sigma_3} d_4\kappa^j_{k_j} \\
a_3\xi_p &\xrightarrow{\sigma_3\sigma_2\sigma_3} d_4\kappa^j_{k_j} \\
b_3\xi_p &\xrightarrow{\sigma_3} d_4\kappa^j_{k_j}
\end{aligned} \tag{3.23}$$

Most of these may be disregarded by Proposition 3.5. If $p = 2m$ for $m > 0$, the resulting reduced form of Figure 27 is shown in Figure 30. On the other hand, if $p = 2m+1$, we also cancel the edges $a_i\xi_{2m+1} \to d_i\kappa^m_{k_m}$ and $b_i\xi_{2m+1} \to e_i\kappa^m_{k_m}$, introducing the multiplications shown in Figure 31. Similarly, if $p = 0$, we cancel the edges $a_i\xi_0 \to d_i\gamma_r$ and $b_i\xi_0 \to e_i\gamma_r$, introducing similar multiplications.

We now return to the case where $s = 2\tau(J)$. In P_{unst}, the edges $a_1\xi_0 \to a_4\eta_0$, $b_1\xi_0 \to b_4\eta_0$, $b_2\xi_0 \to b_5\eta_0$, and $b_3\xi_0 \to b_6\eta_0$ cancel, and since their targets do not have any other incoming edges, no new multiplications are introduced. The only three remaining generators are $a_2\xi_0$, $a_3\xi_0$, and $a_5\eta_0$, all in filtration level 0, with the

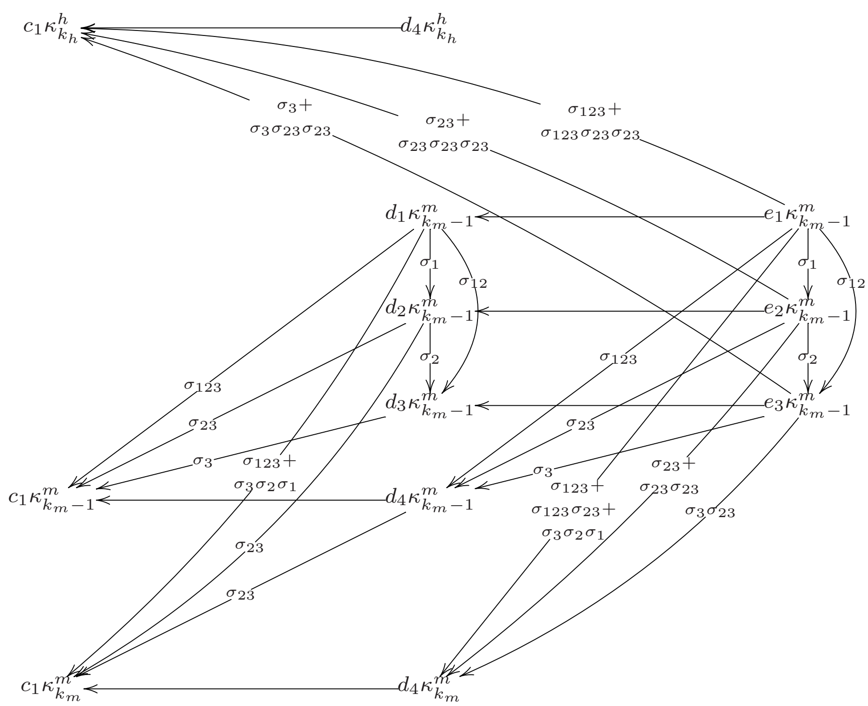

Figure 31: Reduced form of Figure 27 in the case where $p = 2m + 1$ (or $p = 0$, replacing $\kappa^m_{k_m-1}$ by γ_{r-1} and $\kappa^m_{k_m}$ by γ_r).

following multiplications:

$$\begin{tikzcd} & a_3\xi_0 \arrow[dr, "\sigma_3"] & \\ a_2\xi_0 \arrow[ur, "\sigma_2"] \arrow[rr, "1+\sigma_{23}"] & & a_5\eta_0 \end{tikzcd} \tag{3.24}$$

As above, $a_2\xi_0$ and $a_3\xi_0$ may have some outgoing edges, and $a_5\eta_0$ may have some incoming ones. The rest of the argument goes through unchanged.

3.3.3 Tensor product over $\mathcal{A}_\sigma$

Let $Q = \bigoplus_{j=0}^n Q^j$, with multiplications as described in the previous subsection. We consider the tensor product $Q \boxtimes_{\mathcal{A}_\sigma} \widehat{\mathrm{CFD}}(\mathcal{X}_K^t)$. Again, the goal is to obtain a decomposition of the tensor product according to the stable and unstable chains in $\widehat{\mathrm{CFD}}(\mathcal{X}_K^t)$.

It is convenient to give the generators of Q^j new names, somewhat similar to the notation used in [30, Section 4]. For $j = 1, \ldots, n$ and $i = 1, \ldots, k_j - 1$, define:

$$\begin{array}{llll} A^j = a_1\xi_{2j} & A'^j = b_1\xi_{2j} & E_i^j = d_1\kappa_i^j & E_i'^j = e_1\kappa_i^j \\ B^j = a_2\xi_{2j} & B'^j = b_2\xi_{2j} & F_i^j = d_2\kappa_i^j & F_i'^j = e_2\kappa_i^j \\ C^j = a_3\xi_{2j} & C'^j = b_3\xi_{2j} & G_i^j = d_3\kappa_i^j & G_i'^j = e_3\kappa_i^j \\ D^j = c_1\kappa_{k_j}^j & D'^j = d_4\kappa_{k_j}^j & H_i^j = c_1\kappa_i^j & H_i'^j = d_4\kappa_i^j \end{array}$$

When $s < 2\tau(J)$, for $i = 1, \ldots, r-1$, define:

$$\begin{array}{llll} A^0 = a_4\eta_0 & A'^0 = b_4\eta_0 & E_i^0 = d_1\gamma_i & E_i'^0 = e_1\gamma_i \\ B^0 = a_5\eta_0 & B'^0 = b_5\eta_0 & F_i^0 = d_2\gamma_i & F_i'^0 = e_2\gamma_i \\ & C'^0 = b_6\eta_0 & G_i^0 = d_3\gamma_i & G_i'^0 = e_3\gamma_i \\ D^0 = c_1\gamma_r & D'^0 = d_4\gamma_r & H_i^0 = c_1\gamma_i & H_i'^0 = d_4\gamma_i \end{array}$$

Also, for notational convenience, define $k_0 = r$.

We divide up the generators of the subspaces Q^j by Alexander grading and idempotent:

	$A=-1$	$A=0$	$A=1$
ι_0^σ		A^j, C^j, E_i^j, G_i^j	$A'^j, C'^j, E_i'^j, G_i'^j$
ι_1^σ	D^j, H_i^j	$B^j, D'^j, F_i^j, H_i'^j$	$B'^j, F_i'^j$

In Figures 28 and 29, notice that of the generators in idempotent ι_0, A^j, A'^j, E_i^j, and $E_i'^j$ have outgoing edges labeled σ_1, σ_{12}, and σ_{123}, while C^j, C'^j, G_i^j, and $G_i'^j$ have outgoing edges labeled σ_3 and incoming edges labeled σ_2 and σ_{12}. Accordingly, it makes sense to associate the former with the vertical chains and the latter with the horizontal chains. That is, for each $J \in \{1, \dots, N\}$ and $j \in \{0, \dots, n\}$, define:

$$\begin{aligned} Z_{\text{vert}}^{J,j} &= \left\langle A^j, A'^j, E_i^j, E_i'^j \right\rangle \boxtimes \langle \Xi_{2J-1}, \Xi_{2J} \rangle \\ &\quad + \left\langle B^j, B'^j, D^j, D'^j, F_i^j, F_i'^j, H_i^j, H_i'^j \right\rangle \boxtimes \left\langle \mathrm{K}_I^J \mid 1 \le I \le K_J \right\rangle \\ Z_{\text{hor}}^{J,j} &= \left\langle C^j, C'^j, G_i^j, G_i'^j \right\rangle \boxtimes \langle \mathrm{H}_{2J-1}, \mathrm{H}_{2J} \rangle \\ &\quad + \left\langle B^j, B'^j, D^j, D'^j, F_i^j, F_i'^j, H_i^j, H_i'^j \right\rangle \boxtimes \left\langle \Lambda_I^J \mid 1 \le I \le L_J \right\rangle \\ Z_{\text{unst}}^{j} &= \left\langle A^j, A'^j, E_i^j, E_i'^j \right\rangle \boxtimes \langle \Xi_0 \rangle \\ &\quad + \left\langle C^j, C'^j, G_i^j, G_i'^j \right\rangle \boxtimes \langle \mathrm{H}_0 \rangle \\ &\quad + \left\langle B^j, B'^j, D^j, D'^j, F_i^j, F_i'^j, H_i^j, H_i'^j \right\rangle \boxtimes \langle \Gamma_i \mid 1 \le I \le R \rangle . \end{aligned} \tag{3.25}$$

Then, as a vector space,

$$Q \boxtimes \widehat{\mathrm{CFD}}(\mathcal{X}_K^t) = \bigoplus_{\substack{J=1,\dots,N \\ j=0,\dots,n}} Z_{\text{vert}}^{J,j} \oplus \bigoplus_{\substack{J=1,\dots,N \\ j=0,\dots,n}} Z_{\text{hor}}^{J,j} \oplus \bigoplus_{j=0}^{n} Z_{\text{unst}}^{j}. \tag{3.26}$$

For fixed J, we write $Z_{\text{vert}}^{J,*} = \bigoplus_{j=0}^n Z_{\text{vert}}^{J,j}$, and so on.

As before, it is easy to verify that the differentials on the tensor product coming from m_1 and m_2 multiplications in Figures 28 and 29 respect the splitting (3.26). These differentials are illustrated in Figures 32 through 36. Note that we obtain slightly different differentials depending on whether $j = 0$ or $j > 0$. The double-dotted arrows correspond to the dashed arrows in Figures 22 through 25: for instance, in Figure 32, the double-dotted arrow from $E_1'^j \Xi_{2J}$ to $H_{k_j-1}'^j \mathrm{K}_1^J$ really means that there are differentials $E_i'^j \Xi_{2J} \to H_{i+1}'^j \mathrm{K}_1^J$ for $i = 1, \dots, k_j - 2$.

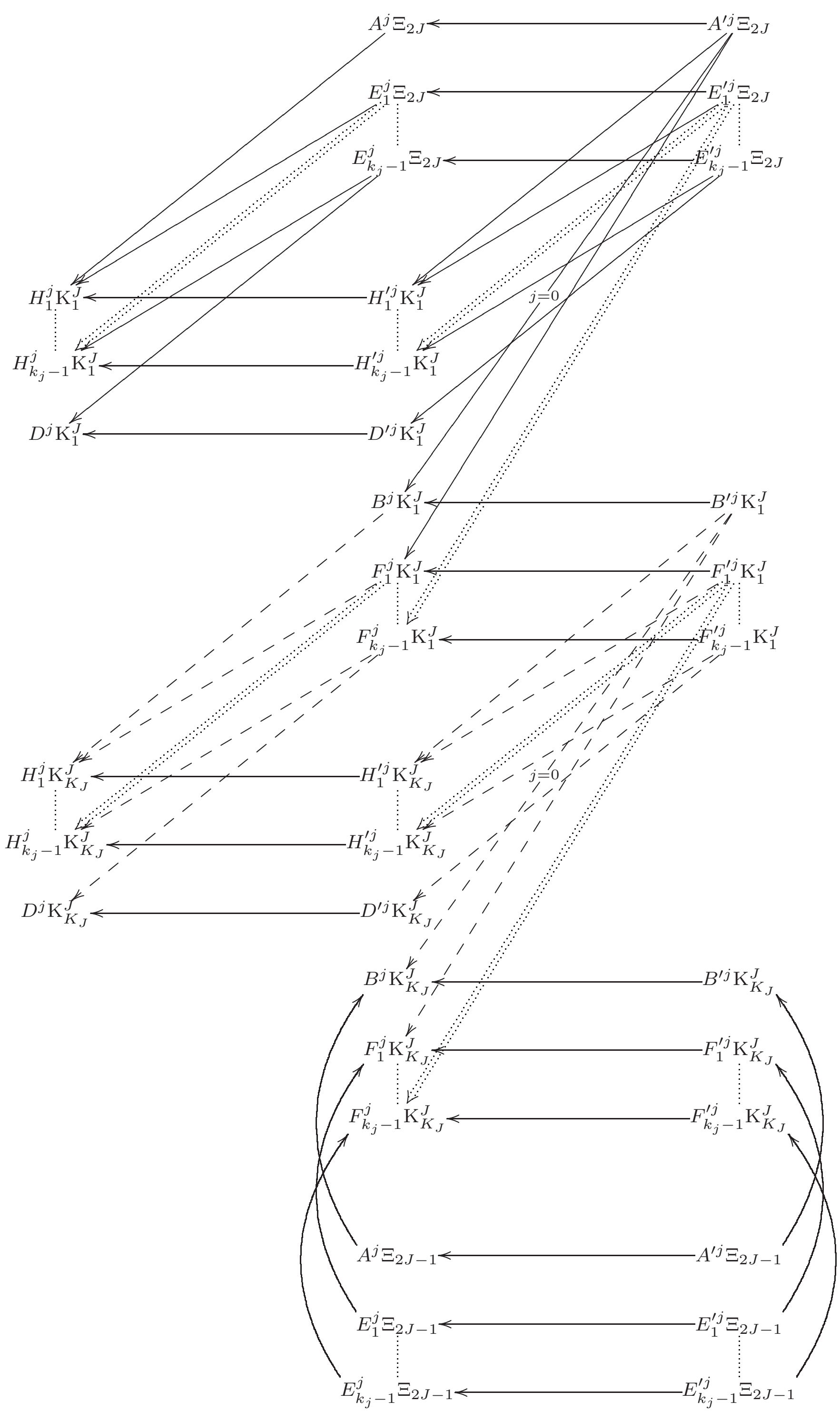

Figure 32: The subspace $Z_{\mathrm{vert}}^{J,j}$, corresponding to a vertical stable chain $\Xi_{2J} \xrightarrow{\sigma_{123}} \mathrm{K}_1^J \xrightarrow{\sigma_{23}} \cdots \xrightarrow{\sigma_{23}} \mathrm{K}_{K_J}^J \xleftarrow{\sigma_1} \Xi_{2J-1}$.

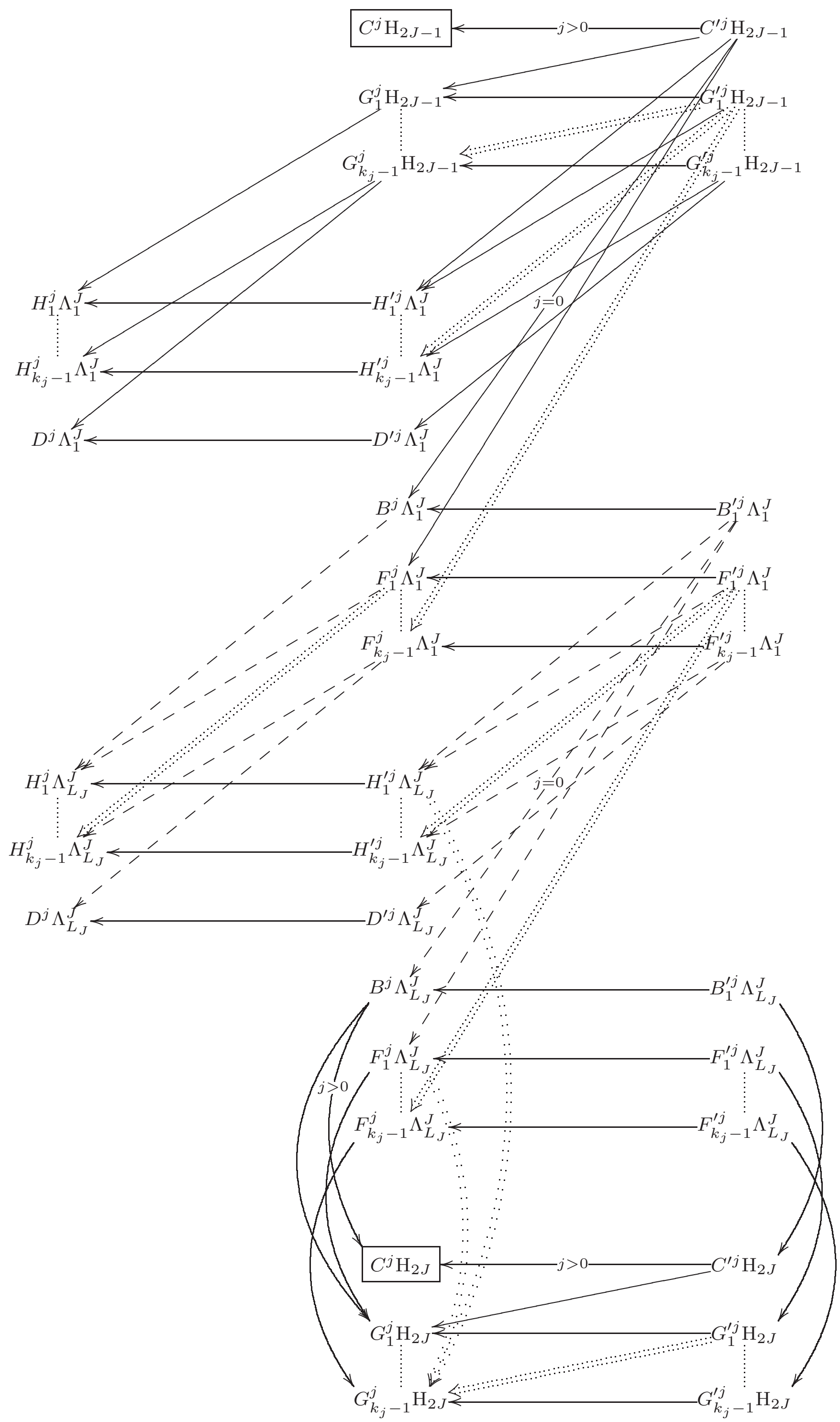

Figure 33: The subspace $Z_{\mathrm{hor}}^{J,j}$, corresponding to a horizontal stable chain $\mathrm{H}_{2J-1} \xrightarrow{\sigma_3} \Lambda_1^J \xrightarrow{\sigma_{23}} \cdots \xrightarrow{\sigma_{23}} \Lambda_{L_J}^J \xrightarrow{\sigma_2} \mathrm{H}_{2J}$.

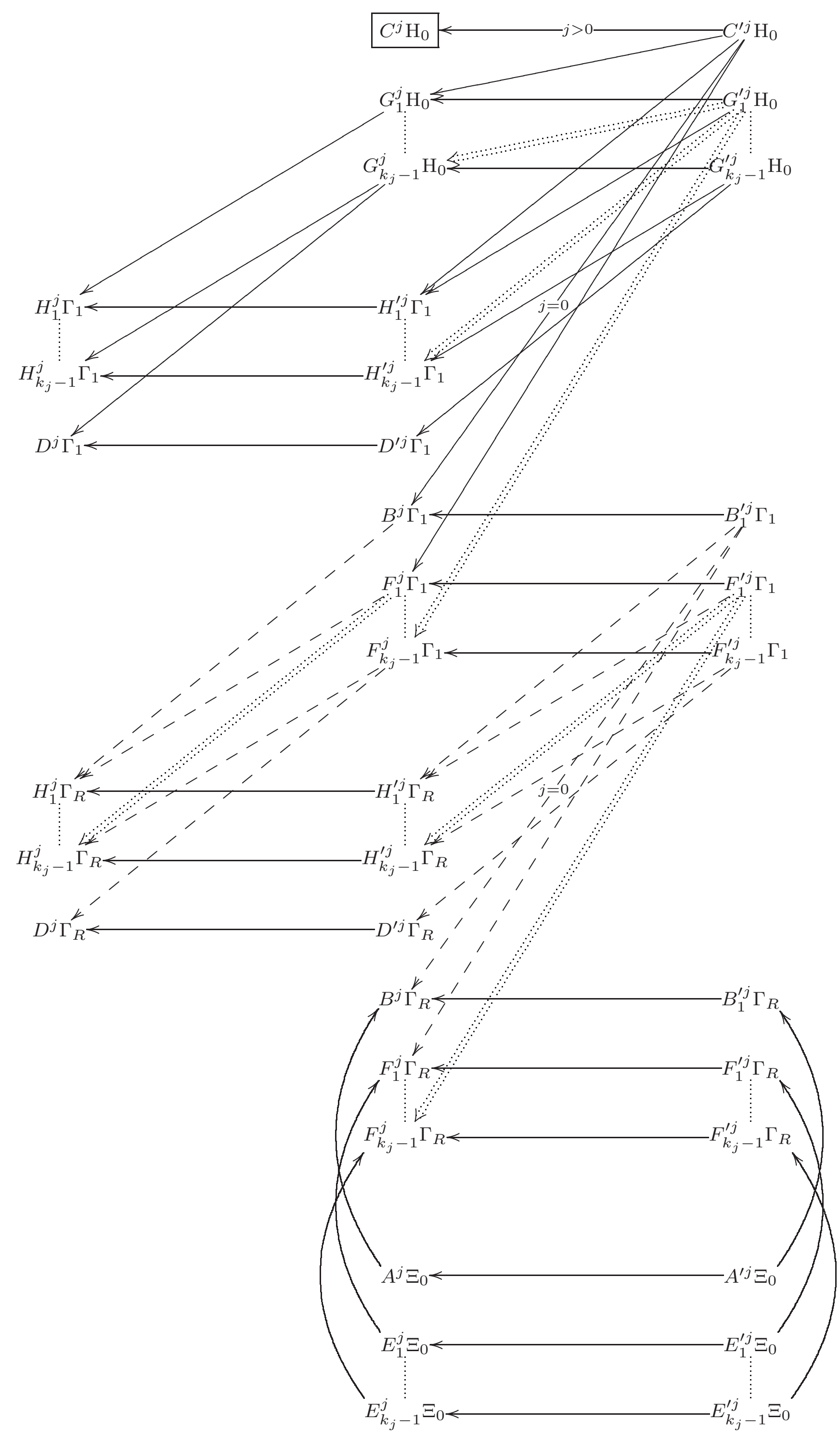

Figure 34: The subspace Z^j_{unst} when $t < 2\tau(K)$, corresponding to the unstable chain $\mathrm{H}_0 \xrightarrow{\sigma_3} \Gamma_1 \xrightarrow{\sigma_{23}} \cdots \xrightarrow{\sigma_{23}} \Gamma_R \xleftarrow{\sigma_1} \Xi_0$.

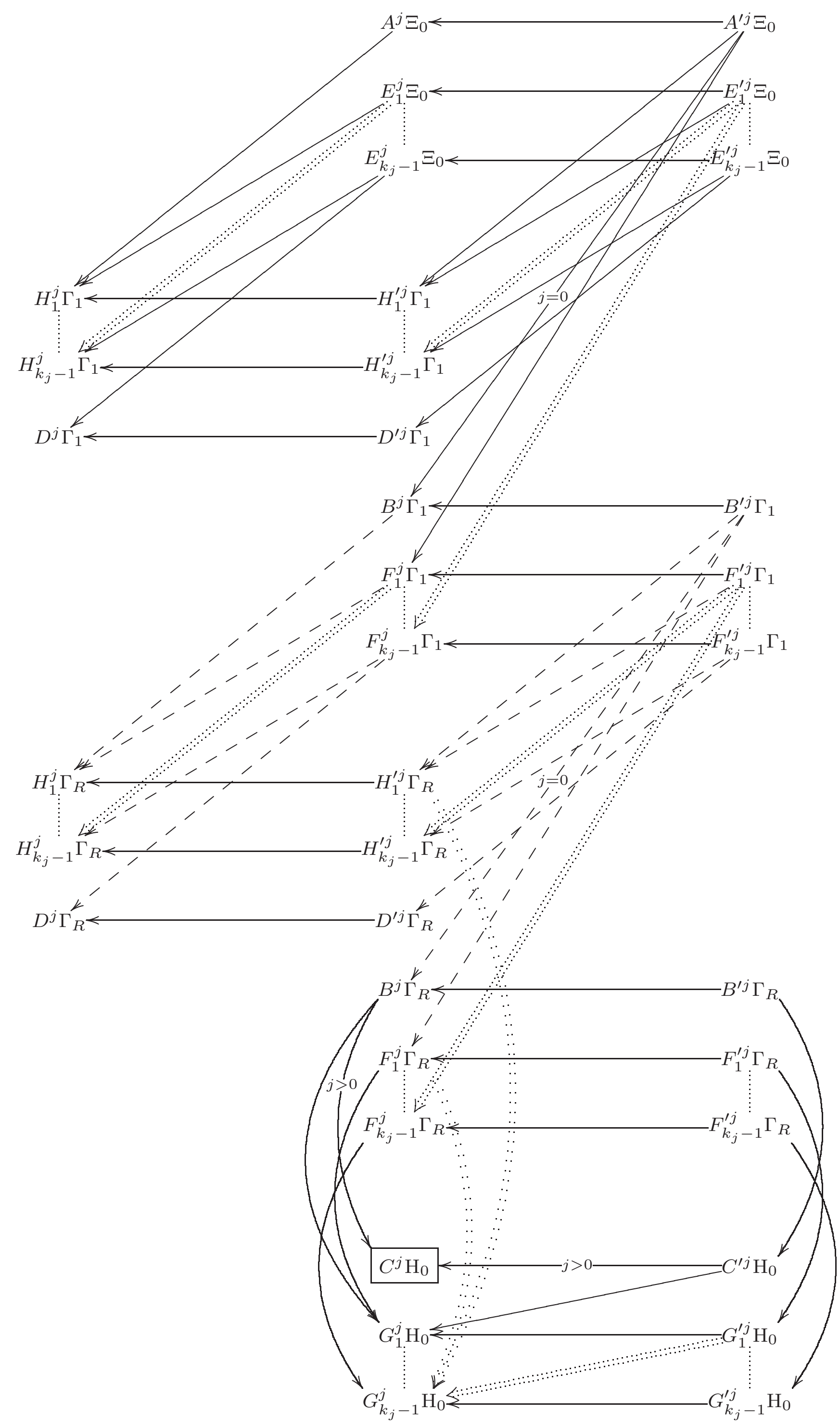

Figure 35: The subspace Z^j_{unst} when $t > 2\tau(K)$, corresponding to the unstable chain $\Xi_0 \xrightarrow{\sigma_{123}} \Gamma_1 \xrightarrow{\sigma_{23}} \cdots \xrightarrow{\sigma_{23}} \Gamma_R \xrightarrow{\sigma_2} \mathrm{H}_0$.

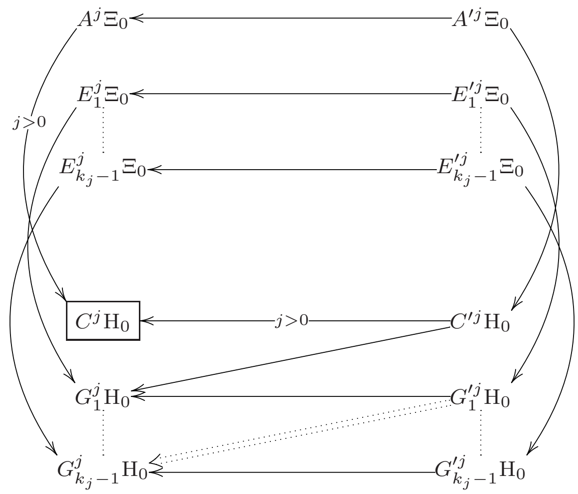

Figure 36: The subspace Z^j_{unst} when $t = 2\tau(K)$, corresponding to the unstable chain $\Xi_0 \xrightarrow{\sigma_{12}} \mathrm{H}_0$.

Next, we must consider the differentials coming from the remaining multiplications on Q. First, we look at differentials that respect the splitting. If $k_j > 1$, the relevant multiplications on Q^j are:

$$\begin{array}{llll}
A^j \xrightarrow{\sigma_{123}\sigma_2} G_1^j & B^j \xrightarrow{\sigma_{23}\sigma_2} G_1^j & C^j \xrightarrow{\sigma_3\sigma_2} G_1^j & \text{if } j > 0 \\
A'^j \xrightarrow{\sigma_{123}\sigma_{23}} D'^j & B'^j \xrightarrow{\sigma_{23}\sigma_{23}} D'^j & C'^j \xrightarrow{\sigma_3\sigma_{23}} D'^j & \text{if } k_j = 1 \\
E'^j_{k_j-1} \xrightarrow{\sigma_{123}\sigma_{23}} D'^j & F'^j_{k_j-1} \xrightarrow{\sigma_{23}\sigma_{23}} D'^j & G'^j_{k_j-1} \xrightarrow{\sigma_3\sigma_{23}} D'^j & \text{if } k_j > 1.
\end{array}$$

Therefore:

- In $Z^{J,j}_{\text{vert}}$, if $K_J > 1$, there are differentials $E'^j_{k_j-1}\Xi_{2J} \to D'^j\mathrm{K}^J_2$ and $F'^j_{k_j-1}\mathrm{K}^J_I \to D'^j\mathrm{K}^J_{I+2}$.

- In $Z^{J,j}_{\text{hor}}$, if $K_J > 1$, there are differentials $G'^j_{k_j-1}\mathrm{H}_{2J-1} \to D'^j\Lambda^J_2$ and $F'^j_{k_j-1}\Lambda^J_I \to D'^j\Lambda^J_{I+2}$. Additionally, when $j > 0$, there are differentials $C^j\mathrm{H}_{2J-1} \to G^j_1\mathrm{H}_{2J}$ if $K_J = 1$, and $B^j\Lambda^J_{K_J-1} \to G^j_1\mathrm{H}_{2J}$ if $K_J > 1$.

- In Z^j_{unst}, if $t < 2\tau(K)-1$, there are differentials $G'^j_{k_j-1}\mathrm{H}_0 \to D'^j\Gamma_2$ and $F'^j_{k_j-1}\Gamma_I \to$

$D'^j\Gamma_{I+2}$. If $t = 2\tau(K)+1$, there are differentials $A^j\Xi_0 \to G_1^j\mathrm{H}_0$ for $j > 0$. If $t > 2\tau(K)+1$, there are differentials $E'^j_{k_{j-1}}\Xi_0 \to D'^j\Gamma_2$ and $F'^j_{k_{j-1}}\Gamma_I \to D'^j\Gamma_{I+2}$ for all j, and $B^j\Gamma_{R-1} \to G_1^j\mathrm{H}_0$ for $j > 0$.

Next, we may have some differentials that preserve the decomposition

$$\bigoplus_J Z^{J,*}_{\mathrm{vert}} \oplus \bigoplus_J Z^{J,*}_{\mathrm{hor}} \oplus Z^*_{\mathrm{unst}}$$

but which come from the multiplications on Q that do not preserve the splitting $Q = \bigoplus_{j=0}^n Q^j$, shown in Figures 26, 30, and 31. The resulting differentials are shown in Table 1. In each line that involves expressions like K_I^J, Λ_I^J, and Γ_I, we assume that K_J, L_J, or R is sufficiently large for the indices to make sense and that I ranges over appropriate bounds. The symbol * denotes both primed and unprimed symbols; thus, for instance, the notation $A^{*j}\Xi_{2J} \to D^{*h}\mathrm{K}_2^J$ means that there are differentials $A^j\Xi_{2J} \to D^h\mathrm{K}_2^J$ and $A'^j\Xi_{2J} \to D'^h\mathrm{K}_2^J$. Additionally, note that if $k_h = 1$, then we replace H_1^h by D^h where it appears; if $k_j = 1$, we replace $E'^j_{k_j-1}$, $F'^j_{k_j-1}$, and $G'^j_{k_j-1}$ by A'^j, B'^j, and C'^j, respectively.

Notice that almost all of the differentials in Table 1 drop the filtration level by a nonzero amount. The two exceptions are $A^j\Xi_{2J-1} \to D'^h\mathrm{K}^J_{K_J}$ and $A^j\Xi_0 \to D'^h\Gamma_R$ in the second column.

Finally, we must look at differentials that do not respect the splitting at all. Notice that the sequence $\sigma_3\sigma_2\sigma_1$ occurs several times in Figures 28 and 29, and the sequences $\sigma_3\sigma_2\sigma_{12}$ and $\sigma_3\sigma_2\sigma_{123}$ occur in Equations (3.16) and (3.18), and these are the only such sequences that appear. More precisely, in Q^j with $k_j > 1$, we have the following

	$u_{2j,h}=1,\ j,h>0$	$v_{2j,h}=1,\ j>0$	$v_{2j-1,h}=1$ or $w_h=1$
Z^J_{vert}	$A'^j\Xi_{2J}\to H^h_1\mathrm{K}^J_2$ $B'^j\mathrm{K}^J_I\to H^h_1\mathrm{K}^J_{I+1}$ $B'^j\mathrm{K}^J_I\to H^h_1\mathrm{K}^J_{I+2}$	$A^{*j}\Xi_{2J}\to D^{*h}\mathrm{K}^J_2$ $B^{*j}\mathrm{K}^J_I\to D^{*h}\mathrm{K}^J_I$ $B^{*j}\mathrm{K}^J_I\to D^{*h}\mathrm{K}^J_{I+2}$ $A^j\Xi_{2J-1}\to D'^h\mathrm{K}^J_{K_J}$	$E'^j_{k_j-1}\Xi_{2J}\to D^h\mathrm{K}^J_1$ $E'^j_{k_j-1}\Xi_{2J}\to D^h\mathrm{K}^J_3$ $F'^j_{k_j-1}\mathrm{K}^J_I\to D^h\mathrm{K}^J_{I+1}$ $F'^j_{k_j-1}\mathrm{K}^J_I\to D^h\mathrm{K}^J_{I+3}$
Z^J_{hor}	If $L_J=1$: $C'^j\mathrm{H}_{2J-1}\to G^h_1\mathrm{H}_{2J-1}$ If $L_J>1$: $C'^j\mathrm{H}_{2J-1}\to H^h_1\Lambda^J_2$ $B'^j\Lambda^J_I\to H^h_1\Lambda^J_{I+1}$ $B'^j\Lambda^J_I\to H^h_1\Lambda^J_{I+2}$ $B'^j\Lambda^J_{K_J-1}\to G^h_1\mathrm{H}_{2J-1}$	$C^{*j}\mathrm{H}_{2J-1}\to D^{*J}\Lambda^J_1$ $C^{*j}\mathrm{H}_{2J-1}\to D^{*J}\Lambda^J_2$ $B^{*j}\Lambda^J_I\to D^{*h}\Lambda^J_I$ $B^{*j}\Lambda^J_I\to D^{*h}\Lambda^J_{I+2}$	$G'^j_{k_j-1}\mathrm{H}_{2J-1}\to D^h\Lambda^J_1$ $G'^j_{k_j-1}\mathrm{H}_{2J-1}\to D^h\Lambda^J_3$ $F'^j_{k_j-1}\Lambda^J_I\to D^h\Lambda^J_{I+1}$ $F'^j_{k_j-1}\Lambda^J_I\to D^h\Lambda^J_{I+3}$
Z_{unst}, $t<2\tau(K)$	$C'^j\mathrm{H}_0\to H^h_1\Gamma_2$ $B'^j\Gamma_I\to H^h_1\Gamma_{I+1}$ $B'^j\Gamma_I\to H^h_1\Gamma_{I+2}$	$C^{*j}\mathrm{H}_0\to D^{*J}\Gamma_1$ $C^{*j}\mathrm{H}_0\to D^{*J}\Gamma_2$ $B^{*j}\Gamma_I\to D^{*h}\Gamma_I$ $B^{*j}\Gamma_I\to D^{*h}\Gamma_{I+2}$ $A^j\Xi_0\to D'^h\Gamma_R$	$G'^j_{k_j-1}\mathrm{H}_0\to D^h\Gamma_1$ $G'^j_{k_j-1}\mathrm{H}_0\to D^h\Gamma_3$ $F'^j_{k_j-1}\Gamma_I\to D^h\Gamma_{I+1}$ $F'^j_{k_j-1}\Gamma_I\to D^h\Gamma_{I+3}$
Z_{unst}, $t>2\tau(K)$	If $R=1$: $A'^j\Xi_0\to G^h_1\mathrm{H}_0$ If $R>1$: $A'^j\Xi_0\to H^h_1\Gamma_2$ $B'^j\Gamma_I\to H^h_1\Gamma_{I+1}$ $B'^j\Gamma_I\to H^h_1\Gamma_{I+2}$ $B'^j\Gamma_{R-1}\to G^h_1\mathrm{H}_0$	$A^{*j}\Xi_0\to D^{*h}\Gamma_2$ $B^{*j}\Gamma_I\to D^{*h}\Gamma_I$ $B^{*j}\Gamma_I\to D^{*h}\Gamma_{I+2}$	$E'^j_{k_j-1}\Xi_0\to D^h\Gamma_1$ $E'^j_{k_j-1}\Xi_0\to D^h\Gamma_3$ $F'^j_{k_j-1}\Gamma_I\to D^h\Gamma_{I+1}$ $F'^j_{k_j-1}\Gamma_I\to D^h\Gamma_{I+3}$

Table 1: Differentials arising from the multiplications in Figures 26, 30, and 31.

multiplications:

$$\begin{array}{rlrll}
A^j \xrightarrow{\sigma_3\sigma_2\sigma_1} H_1^j & & A'^j \xrightarrow{\sigma_3\sigma_2\sigma_1} H_1'^j & & \\
E_i^j \xrightarrow{\sigma_3\sigma_2\sigma_1} H_{i+1}^j & & E_i'^j \xrightarrow{\sigma_3\sigma_2\sigma_1} H_{i+1}'^j & & (i=1,\dots,k_j-2) \\
E_{k_j-1}^j \xrightarrow{\sigma_3\sigma_2\sigma_1} D^j & & E_{k_j-1}'^j \xrightarrow{\sigma_3\sigma_2\sigma_1} D'^j & & \\
A'^j \xrightarrow{\sigma_3\sigma_2\sigma_{12}} G_2^j & & A'^j \xrightarrow{\sigma_3\sigma_2\sigma_{123}} H_2^j & & \\
E_i'^j \xrightarrow{\sigma_3\sigma_2\sigma_{12}} G_{i+2}^j & & E_i'^j \xrightarrow{\sigma_3\sigma_2\sigma_{123}} H_{i+2}^j & & (i=1,\dots,k_j-3) \\
& & E_{k_j-2}'^j \xrightarrow{\sigma_3\sigma_2\sigma_{123}} D^j & &
\end{array} \tag{3.27}$$

If $k_j = 1$, then we simply have $A^j \xrightarrow{\sigma_3\sigma_2\sigma_1} D^j$ and $A'^j \xrightarrow{\sigma_3\sigma_2\sigma_1} D'^j$. Finally, from Figure 30, if $v_{2j,h} = 1$, then there are multiplications $A^j \xrightarrow{\sigma_3\sigma_2\sigma_1} D^h$ and $A'^j \xrightarrow{\sigma_3\sigma_2\sigma_1} D'^h$.

Notice that all of these multiplications come out of A^j, A'^j, E_i^j, or $E_i'^j$, all of which are paired with $\{\Xi_0, \dots, \Xi_{2N}\}$ rather than $\{\mathrm{H}_0, \dots, \mathrm{H}_{2N}\}$ in (3.25). It follows that each group $Z_{\text{hor}}^{J,*}$ is actually a direct summand as a chain complex. We shall see that the generator of the total homology comes from $\bigoplus_J Z_{\text{vert}}^{J,*} \oplus Z_{\text{unst}}^*$, so we may ignore each of these summands. Furthermore, if we define $U_{P,M}$, $V_{P,M}$, and W_P analogously to $u_{p,h}$, $v_{p,m}$, and w_p above, then we obtain differentials from $A^j\Xi_P$, $A'^j\Xi_P$, $E_i^j\Xi_P$, and/or $E_i'^j\Xi_P$ to elements of Z_{vert}^M and Z_{unst} whenever $U_{P,M}$, $V_{P,M}$, or W_P is nonzero. Specifically:

- If $V_{P,M} = 1$, then there are differentials

$$\begin{array}{rlrll}
A^j\Xi_P \to H_1^j \mathrm{K}_{K_M}^M & & A'^j\Xi_P \to H_1'^j \mathrm{K}_{K_M}^M & & \\
E_i^j\Xi_P \to H_{i+1}^j \mathrm{K}_{K_M}^M & & E_i'^j\Xi_P \to H_{i+1}'^j \mathrm{K}_{K_M}^M & & (i=1,\dots,k_j-2) \\
E_{k_j-1}^j\Xi_P \to D^j \mathrm{K}_{K_M}^M & & E_{k_j-1}'^j\Xi_P \to D'^j \mathrm{K}_{K_M}^M & &
\end{array} \tag{3.28}$$

  if $k_j > 1$, and $A^j\Xi_P \to D^j\mathrm{K}_{K_M}^M$ and $A'^j\Xi_P \to D'^j\mathrm{K}_{K_M}^M$ if $k_j = 1$. Also, if $v_{2j,h} = 1$, then there are differentials $A^j\Xi_P \to D^h\mathrm{K}_{K_M}^M$ and $A'^j\Xi_P \to D'^h\mathrm{K}_{K_M}^M$.

  Similarly, if $W_P = 1$ and $t < 2\tau(K)$, then we obtain similar differentials going into Z_{unst}, replacing $\mathrm{K}_{K_M}^M$ by Γ_R.

- If $U_{P,M} = 1$, then there are differentials

$$\begin{aligned} A'^j \Xi_P &\to H_2^j \mathrm{K}_1^M \\ E_i'^j \Xi_P &\to H_{i+2}^j \mathrm{K}_1^M \ (i = 1, \dots, k_j - 3) \\ E_{k_j-2}'^j \Xi_P &\to D^j \mathrm{K}_1^M. \end{aligned} \tag{3.29}$$

  Similarly, if $W_P = 1$ and $t > 2\tau(K)$, then we obtain similar differentials going into Z_{unst}, replacing K_1^M by Γ_1.

- Finally, if $W_P = 1$ and $t = 2\tau(K)$, there are differentials

$$\begin{aligned} A'^j \Xi_P &\to G_2^j \mathrm{H}_0 \\ E_i'^j \Xi_P &\to G_{i+2}^j \mathrm{H}_0 \ (i = 1, \dots, k_j - 3) \end{aligned} \tag{3.30}$$

3.3.4 Computation of $\tau(D_{J,s}(K,t))$

We now describe the edge cancellations that occur in each of the pieces. Recall that we must cancel edges in increasing order of the amount by which they drop filtration level. We shall see that a single generator survives. The filtration level of this generator, by definition, is $\tau(D_{J,s}(K,t))$.

We start by canceling the filtration-preserving edges in $Z_{\mathrm{vert}}^{J,j}$. Note that there are are no other edges into $B'^j \mathrm{K}_{K_J}^J$ or $F_i'^j \mathrm{K}_{K_J}^J$, so eliminating the edges coming from these does not introduce any new edges. If $V_{2J-1}, M = 1$, or if $W_{2J-1} = 1$ and $t < 2\tau(K)$, then canceling the edges $A^j \Xi_{2J-1} \to B^j \mathrm{K}_{K_J}^J$ and $E_i^j \to F_k^j \mathrm{K}_{K_J}^J$ introduces some new edges, which all reduce filtration level by 2. Note also that the filtration-preserving edges $A^j \Xi_{2j-1} \to D'^h \mathrm{K}_{K_J}^J$ $(j > 0)$ in Table 1 are eliminated, since $B^j \mathrm{K}_{K_j}^J$ has no other incoming edges when $j > 0$.

In Z_{unst}^j, when $t < 2\tau(K)$, we perform the same cancellations as in $Z_{\mathrm{vert}}^{J,j}$, *mutatis mutandis*. When $t > 2\tau(K)$, there are $2k_j$ filtration-preserving edges to cancel when $j > 0$ (namely, $B^{*j}\Gamma^R \to C^{*j}\mathrm{H}_0$ and $F_i^{*j}\Gamma^R \to G_i^{*j}\mathrm{H}_0$ for $i = 1, \dots, k_j - 1$), but only $2k_0 - 1$ such edges in Z_{unst}^0, since the generator $C_0\mathrm{H}_0$ does not exist. Thus, the generator $B^0\Gamma^R$ survives after these cancellations. Also, note that canceling

$B^j\Gamma^R \to C^j\mathrm{H}_0$ and $F_i^j\Gamma^R \to G_i^j\mathrm{H}_0$ may introduce some new differentials using the arrows in Table 1, but they all filtration level by 2.

When $t = 2\tau(K)$, the only generator in Z^0_{unst} that survives is $A^0\Xi_0$. Notice, however, that by (3.28), there is a differential $A^0\Xi_0 \to H_1^0\mathrm{K}^M_{K_M}$ for any M with $V_{0,M} = 1$. All the generators of Z^j_{unst} for $j > 0$ are canceled.

We have now canceled all edges that preserve the filtration level, so we now begin canceling differentials that drop filtration level by 1. Specifically, in $Z^{J,j}_{\text{vert}}$, cancel every horizontal edge $X' \to X$, starting at the top of Figure 32 and working down. We use the following key observations:

- If X is in filtration level 0 and X' is in level 1, then X has no other incoming edges, since by induction we have already eliminated everything above X and X', and Table 1 and Equations (3.28) and (3.29) contain no differentials that go into $A^j\Xi_{2J}$, $E_i^j\Xi_{2J}$, $B^j\mathrm{K}^J_I$, or $F_i^j\mathrm{K}^J_I$ from elsewhere.

- If X is in filtration level -1 and X' is in level 0, then X' has no other outgoing edges, since Table 1 and Equations (3.28) and (3.29) contain no differentials that go out of $H_i'^j\mathrm{K}^J_I$ or $D'^j\mathrm{K}^J_I$.

Thus, we can completely cancel $Z^{J,j}_{\text{vert}}$.

If $t = 2\tau(K)$, we have now eliminated all generators except $A^0\Xi_0$, which is in filtration level 0, so $\tau(D_{J_s}(K,t)) = 0$ when $s < 2\tau(J)$ and $t = 2\tau(K)$.

If $t > 2\tau(K)$, we proceed with Z^j_{unst} just as with $Z^{J,j}_{\text{vert}}$. When $j > 0$, all generators in cancel; when $j = 0$, the one surviving generator is $B^0\Gamma_R$, which is in filtration level 0. Thus, $\tau(D_{J_s}(K,t)) = 0$ when $s < 2\tau(J)$ and $t > 2\tau(K)$.

If $t < 2\tau(K)$, when $j > 0$, we start by canceling $C'^j\mathrm{H}_0 \to C^j\mathrm{H}_0$ and proceeding downward in Figure 34, as before, eliminating all generators. When $j = 0$, we start by canceling $G_1'^j\mathrm{H}_0 \to G_1^j\mathrm{H}_0$ and proceed downward, and we thus see that the only surviving generator is $C'^j\mathrm{H}_0$, which is in filtration level 1. Thus, $\tau(D_{J_s}(K,t)) = 1$ when $s < 2\tau(J)$ and $t < 2\tau(K)$.

Finally, we must return to the case where $s = 2\tau(J)$. Recall that Q_0 in this case consists of three generators, all in filtration level 0, as in (3.24). For $j > 0$, the definitions of $Z^{J,j}_{\mathrm{vert}}$, $Z^{J,j}_{\mathrm{hor}}$, and Z^{j}_{unst} go through the same way, and we see again that all of the resulting generators eventually cancel. It follows that the surviving generator must be in filtration level 0, so $\tau(D_{J,s}(K,t)) = 0$ whenever $s = 2\tau(K)$. $\square$

3.4 Other results regarding $D_{J,s}(K,t)$

Prior to Hedden's complete computation of $\widehat{\mathrm{HFK}}$ and τ of all twisted Whitehead doubles [20], Livingston and Naik [39] used the formal properties of τ to understand the asymptotic behavior of τ for large values of the twisting parameter:

Theorem 3.10. *Suppose ν is any homomorphism from the smooth knot concordance group to $\mathbb{Z}$ with the properties that $|\nu(K)| \le g_4(K)$ and $\nu(T_{p,q}) = (p-1)(q-1)/2$, where $p, q > 0$ and $T_{p,q}$ denotes the (p,q) torus knot. Then for any knot K, there exists $t_\nu(K) \in \mathbb{Z}$ such that*

$$\nu(Wh_+(K,t)) = \begin{cases} 1 & t \le t_\nu(K) \\ 0 & t > t_\nu(K) \end{cases}$$

and $TB(K) \le t_\nu(K) < -TB(-K)$ (where $TB(K)$ denotes the maximal Thurston-Bennequin number of K).

Two invariants satisfying the hypotheses of Theorem 3.10 are $\tau(K)$ and $-s(K)/2$, a renormalization of Rasmussen's concordance invariant $s(K)$ [55]. Around the same time, Hedden and Ording [21] proved that these two invariants are not equal by showing that $\tau(Wh_+(T_{2,3},2)) = 0$ while $s(Wh_+(T_{2,3},2)) = -2$, disproving a conjecture of Rasmussen. Later, Hedden [20] showed that $t_\tau(K) = 2\tau(K) - 1$ for any knot K. Finding a general formula for the s invariant of Whitehead doubles remains an open question.

We may extend the techniques of Livingston and Naik to study knots of the form $D_{J,s}(K,t)$ as well.

Proposition 3.11. *Let ν be an invariant satisfying the hypotheses of Theorem 3.10, and fix knots J and K.*

1. *If $s \leq TB(J)$ and $t \leq TB(K)$, then $\nu(D_{J,s}(K,t)) = 1$. If $s \geq -TB(-J)$ and $t \geq -TB(-K)$, then $\nu(D_{J,s}(K,t)) = -1$.*

2. *For fixed s (resp. t), the function $t \mapsto \nu(D_{J,s}(K,t))$ (resp. $s \mapsto \nu(D_{J,s}(K,t))$) is non-increasing and has as its image either $\{-1,0\}$, $\{0\}$, or $\{0,1\}$.*

Proof. The proof is very similar to that of [39, Theorem 2].

When $s \leq TB(J)$ and $t \leq TB(K)$, the annuli $A(J,s)$ and $A(K,t)$ are quasipositive, so $D_{J,s}(K,t)$ is a strongly quasipositive knot with genus 1, and hence $\nu(D_{J,s}(K,t)) = 1$ as in [36]. Mirroring gives the second half of (1).

The non-increasing statement in (2) follows from the fact that $D_{J,s}(K,t)$ is obtained from $D_{J,s-1}(K,t)$ or $D_{J,s}(K,t-1)$ by changing a positive crossing to a negative crossing, which can only preserve or decrease ν [36]. Also, since $D_{J,s}(K,t)$ is related to $D_{J,s'}(K,t)$ or $D_{J,s}(K,t')$ (for any s' or t') by a *band modification*, each of the two functions can assume at most two values, either -1 and 0 or 0 and -1. Finally, we rule out the possibility that either of the functions in (1) is constant and nonzero. Suppose, without loss of generality, that $\nu(D_{J,s}(K,t)) = 1$ for a fixed s and all t. In particular, $\nu(D_{J,s}(K,-TB(-K))) = 1$. On the other hand, $\nu(D_{J,-TB(-J)}(K,-TB(-K))) = -1$, which contradicts the fact that the image of the function $s \mapsto \nu(D_{J,s}(K,-TB(-K)))$ contains at most two consecutive integers. $\square$

On the other hand, the behavior of $\nu(D_{J,s}(K,t)$ for small s and t (specifically, when $TB(J) < s < -TB(-J)$ or $TB(K) < t < -TB(-K)$) may be more complicated than the simple behavior of τ given by Theorem 1.1.

In another direction, we may also look for instances when $D_{J,s}(K,t)$ is actually smoothly slice. The following proposition generalizes Casson's argument [25,

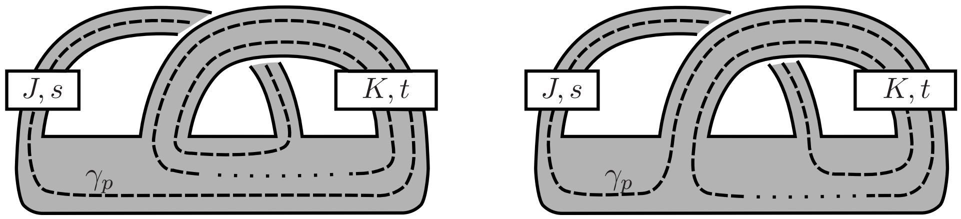

Figure 37: The Seifert surface F with the curve γ_p, in the cases where $p < 0$ (left) and $p > 0$ (right).

page 227] that the $p(p+1)$-twisted positive Whitehead double of the $(p, p+1)$ torus knot is smoothly slice. For an oriented knot K and relatively prime integers p, q, let $C_{p,q}(K)$ denote the (p, q)-cable of K. (Note that $C_{p,q}(K)^r = C_{-p,-q}(K) = C_{p,q}(K^r)$ and $\overline{C_{p,q}(K)} = C_{p,-q}(\bar{K})$.)

Proposition 3.12. *Let K be any knot, and let $p, t \in \mathbb{Z}$. If J is any knot that is smoothly concordant to $-C_{p,pt\pm1}(K)$, then $D_{J,-p(pt\pm1)}(K, t)$ is smoothly slice.*

Proof. Let F be the Seifert surface for $D_{J,s}(K, t)$ shown in Figure 37, and let γ_p be a curve that winds once around the band tied into J and p times around the band tied into K, as indicated. The knot type of γ_p is $C_{p,pt+1}(K)$, and the surface framing on γ_p is $s + p + p^2t$. Thus, if J is smoothly concordant to $-C_{p,pt+1}(K)$ and $s = -p(pt+1)$, we may surger F along γ_p in D^4 along a smooth slice disk for $J \# C_{p,pt+1}(K)$, resulting in a smooth slice disk for $D_{J,s}(K, t)$.

If we reverse the crossing between the two bands of F, we obtain the result with the opposite signs. □

Proposition 3.12 is quite interesting in light of very recent work of Hom [23], who found a general formula for the τ invariant of all cable knots in terms of p, q, $\tau(K)$, and an invariant $\epsilon(K) \in \{-1, 0, 1\}$ that depends solely on the knot Floer complex of K. She proved:

Theorem 3.13. *Let K be a knot, and let $p > 0$. Then:*

- *If* $\epsilon(K) = 1$*, then* $\tau(C_{p,q}(K)) = p\tau(K) + \frac{1}{2}(p-1)(q-1)$ *for all* q*.*
- *If* $\epsilon(K) = -1$*, then* $\tau(C_{p,q}(K)) = p\tau(K) + \frac{1}{2}(p-1)(q+1)$ *for all* q*.*
- *If* $\epsilon(K) = 0$*, then* $\tau(K) = 0$*, and*

$$\tau(C_{p,q}(K)) = \begin{cases} \frac{1}{2}(p-1)(q+1) & q < 0 \\ \frac{1}{2}(p-1)(q-1) & q > 0. \end{cases}$$

We may use Theorem 3.13 to compute the value of τ for the cable knots appearing in Proposition 3.12, where we take $t = 2\tau(K)$.

Corollary 3.14. *For any knot* K*, if either* $\epsilon(K) \geq 0$ *and* $p > 0$*, or* $\epsilon(K) \leq 0$ *and* $p < 0$*, there exists a knot* J *such that* $D_{J,2\tau(J)-p}(K, 2\tau(K))$ *is smoothly slice, while* $\tau(D_{J,2\tau(J)-p}(K, 2\tau(K) - \frac{p}{|p|})) \neq 0$*.*

Proof. Suppose that $\epsilon(K) = 1$ and $p > 0$. Set $J = -C_{p,2p\tau(K)+1}(K)$, so that:

$$\begin{aligned} 2\tau(J) - p &= -2\tau(C_{p,2p\tau(K)+1}(K)) - p \\ &= -2p\tau(K) - (p-1)(2p\tau(K)) - p \\ &= -2p^2\tau(K) - p \\ &= -p(2p\tau(K) + 1). \end{aligned}$$

By Proposition 3.12, $D_{J,2\tau(J)-p}(K, 2\tau(K))$ is smoothly slice. On the other hand, $\tau(D_{J,2\tau(J)-p}(K, 2\tau(K) - 1) = 1$ by Theorem 1.1. The case where $\epsilon(K) = -1$ and $p < 0$ follows by mirroring, since $\epsilon(\bar{K}) = -\epsilon(K)$. Finally, if $\epsilon(K) = 0$, we set $J = -C_{p,1}(K)$ if $p > 0$ and $J = -C_{-p,-1}$ if $p < 0$. □

Theorem 1.1 says that the set $\{(s,t) \in \mathbb{Z}^2 \mid D_{J,s}(K,t) = 0\}$ always has the same shape for any J and K, up to translation: the union of the second and fourth quadrants of the $\mathbb{Z}^2$ lattice, including both axes. Corollary 3.14 implies that any point on the boundary of this region may be realized by a smoothly slice knot $D_{J,s}(K,t)$ for suitable choices of J and K.

Finally, recall that the main idea of the proof of Theorem 1.1 is that only the form of the unstable chains in $\widehat{\mathrm{CFD}}(\mathcal{X}_J^s)$ and $\widehat{\mathrm{CFD}}(\mathcal{X}_K^t)$ matters for the computation of of $\tau(D_{J,s}(K,t))$. Petkova [54] and Hom [23] have observed similar behavior in using bordered Heegaard Floer homology to compute $\tau(C_{p,q}(K))$. The invariant $\epsilon(K)$ defined by Hom describes the structure of the part of $\widehat{\mathrm{CFD}}(\mathcal{X}_K^t)$ "near" the unstable chain. Specifically, when we take vertically and horizontally reduced bases $\{\tilde{\xi}_0, \dots, \tilde{\xi}_{2n}\}$ and $\{\tilde{\eta}_0, \dots, \tilde{\eta}_{2n}\}$ for $\mathrm{CFK}^-(K)$, we may arrange that $\tilde{\xi}_0 = \tilde{\eta}_i$ for some i. The cases $\epsilon(K) = 1$, $\epsilon(K) = -1$, and $\epsilon(K) = 0$ correspond, respectively, to whether i is even and positive, odd and positive, or zero. Within each case, Hom showed that only the form of the unstable chain matters for computing $\tau(C_{p,q}(K))$. Hom, Petkova, Hedden, and the author are presently investigating how to extend this idea to study the behavior of τ for arbitrary satellite knots.

Chapter 4

Heegaard Floer homology of cyclic branched covers

In this chapter, we present some of our work regarding the Heegaard Floer homology of cyclic branched covers, particularly with a view towards computing concordance obstructions.

Given a knot $K \subset S^3$ and $m \in \mathbb{N}$, let $p_m \colon \Sigma_m(K) \to S^3$ denote the m-fold cyclic branched cover of S^3 with downstairs branch set K, and let $\tilde{K}_m = p_m^{-1}(K)$. The Heegaard Floer homology of $\Sigma_m(K)$ and the knot Floer homology of $\tilde{K}_m$ have been the subject of extensive research, especially in the case where $m = 2$.

The main fact that distinguishes double branched covers is the *skein exact triangle*. Suppose K_0 and K_1 are obtained as the two resolutions of a crossing in a diagram of K, as in Figure 38. (Necessarily, one of these is a two-component link.) The manifolds

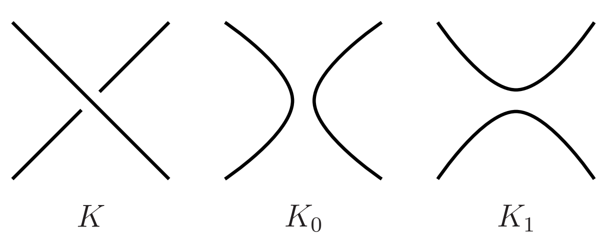

Figure 38: The 0- and 1- resolutions of a crossing.

$\Sigma_2(K_0)$ and $\Sigma_2(K_1)$ are then obtained as 0- and 1-surgery, respectively, on a certain framed knot $\gamma \subset \Sigma_2(K)$. Therefore, there is an exact sequence

$$\cdots \to \widehat{\mathrm{HF}}(\Sigma_2(K)) \to \widehat{\mathrm{HF}}(\Sigma_2(K_0)) \to \widehat{\mathrm{HF}}(\Sigma_2(K_1)) \to \widehat{\mathrm{HF}}(\Sigma_2(K)) \to \dots. \tag{4.1}$$

Using this sequence, Ozsváth and Szabó [52] showed that the double branched cover of a quasi-alternating knot or link is always an L-space.[1] Moreover, by iterating the exact sequence at all of the crossings of a diagram for K, they showed that there is a spectral sequence converging to $\widehat{\mathrm{HF}}(\Sigma_2(K))$ whose E_2 page is the reduced Khovanov homology of the mirror of K. Generalizations and applications of this spectral sequence have been one of the most active subjects of research in Floer homology in recent years; see, e.g., [17, 18, 3, 22, 57].

To describe the concordance obstructions arising from branched covers, we briefly recall some facts about a more powerful variant of Heegaard Floer homology, known as HF^+. We use $\mathbb{F} = \mathbb{F}_2$ coefficients for simplicity. For an oriented 3-manifold Y, the invariant $\mathrm{HF}^+(Y)$ is an $\mathbb{F}[U]$-module that splits as a direct sum

$$\mathrm{HF}^+(Y) = \bigoplus_{\mathfrak{s} \in \mathrm{Spin}^c(Y)} \mathrm{HF}^+(Y, \mathfrak{s}).$$

Henceforth we assume Y is a rational homology sphere. Then $\mathrm{HF}^+(Y)$ has an absolute $\mathbb{Q}$-grading, restricting to a relative $\mathbb{Z}$-grading on each summand $\mathrm{HF}^+(Y, \mathfrak{s})$, such that multiplication by U has degree -2. For each spin^c structure $\mathfrak{s}$, the summand $\mathrm{HF}^+(Y, \mathfrak{s})$ is isomorphic to a copy of $\mathbb{F}[U, U^{-1}]/U\mathbb{F}[U]$ plus a finitely generated group. The *correction term* $d(Y, \mathfrak{s}) \in \mathbb{Q}$ is defined as the grading of the lowest-degree generator element of $\mathbb{F}[U, U^{-1}]/U\mathbb{F}[U]$. The correction terms satisfy the following three properties:

[1] The set of *quasi-alternating links*, $\mathcal{Q}$, is characterized by the following properties: (1) the unknot is in $\mathcal{Q}$; (2) if K, K_0, and K_1 are related as in Figure 38 and satisfy $\det(K) = \det(K_0) + \det(K_1)$, and K_0 and K_1 are in $\mathcal{Q}$, then K is in $\mathcal{Q}$. A rational homology sphere Y is an *L-space* if $\widehat{\mathrm{HF}}(Y, \mathfrak{s}) = \mathbb{Z}$ for each $\mathfrak{s} \in \mathrm{Spin}^c(Y)$.

1. For any $Y, \mathfrak{s}$, $d(-Y, \mathfrak{s}) = -d(Y, \mathfrak{s})$.
2. If $\mathfrak{s}_1 \in \mathrm{Spin}^c(Y_1)$ and $\mathfrak{s}_2 \in \mathrm{Spin}^c(Y_2)$, then $d(Y_1 \# Y_2, \mathfrak{s}_1 \# \mathfrak{s}_2) = d(Y_1, \mathfrak{s}_1) + d(Y_2, \mathfrak{s}_2)$.
3. If $\bar{\mathfrak{s}}$ is the conjugate spin^c structure of $\mathfrak{s}$, then $d(Y, \bar{\mathfrak{s}}) = d(Y, \mathfrak{s})$.

Finally, there is an exact sequence

$$\cdots \to \widehat{\mathrm{HF}}_*(Y, \mathfrak{s}) \xrightarrow{\iota} \mathrm{HF}^+_*(Y, \mathfrak{s}) \xrightarrow{U} \mathrm{HF}^+_{*-2}(Y, \mathfrak{s}) \to \widehat{\mathrm{HF}}_{*-1}(Y, \mathfrak{s}) \to \dots.$$

It follows that Y is an L-space if and only if $\mathrm{HF}^+(Y, \mathfrak{s}) \cong \mathbb{F}[U, U^{-1}]/U\mathbb{F}[U]$ for all $\mathfrak{s} \in \mathrm{Spin}^c(Y)$, and if so, the grading of the generator of $\widehat{\mathrm{HF}}(Y, \mathfrak{s})$ is $d(Y, \mathfrak{s})$.

The (hat) knot Floer homology of a nulhomologous knot $K \subset Y$ splits as a direct sum

$$\widehat{\mathrm{HFK}}(Y, K) = \bigoplus_{\mathfrak{s} \in \mathrm{Spin}^c(Y)} \widehat{\mathrm{HFK}}(Y, K, \mathfrak{s}).$$

The group has a $\mathbb{Q}$-graded Maslov grading (restricting to a relative $\mathbb{Z}$-grading in each summand) and a $\mathbb{Z}$-valued Alexander grading. Just as with knots in S^3, there is a spectral sequence from $\widehat{\mathrm{HFK}}(Y, K, \mathfrak{s})$ to $\widehat{\mathrm{HF}}(Y, \mathfrak{s})$, coming from the Alexander grading filtration. The invariant $\tau(Y, K, \mathfrak{s})$ is defined as the lowest filtration level whose image in $\widehat{\mathrm{HF}}(Y, \mathfrak{s})$ contains an element that maps under ι to the lowest-degree generator of $\mathbb{F}[U, U^{-1}]/U\mathbb{F}[U] \subset \mathrm{HF}^+(Y, \mathfrak{s})$. Much like with knots in S^3, these τ invariants provide genus bounds on smoothly embedded surfaces in manifolds bounded by Y, and they satisfy mirroring and additivity properties just like those of the correction terms.

For any knot $K \subset S^3$ and any prime power $m = p^e$, the branched cover $\Sigma_m(K)$ is a rational homology sphere with no p-torsion in $H_1(\Sigma_m(K); \mathbb{Z})$. If $\Delta \subset D^4$ is a smooth slice disk for K, then the m-fold branched cover of D^4 branched over Δ, $\Sigma_m(\Delta)$, is a smooth rational homology 4-ball whose boundary is $\Sigma_m(K)$. A simple argument using the long exact sequence for cohomology shows that the order of $H^2(\Sigma_m(K))$ is a perfect square, say k^2, and that the image of the restriction map $H^2(\Sigma_m(\Delta)) \to H^2(\Sigma_m(K))$ has order k. If we identify $H^2(\Sigma_m(K))$ with the set of spin^c structures on $\Sigma_m(K)$, this implies that the spin^c structures that extend over $\Sigma_m(\Delta)$ form a subset of square root order. The basic properties of the d and τ invariants imply:

Theorem 4.1. *If $K \subset S^3$ is smoothly slice and m is a prime power, then there exists an $H^2(\Sigma_m(K);\mathbb{Z})$-affine subspace $S \subset \mathrm{Spin}^c(\Sigma_m(K))$, with $|S|^2 = |\mathrm{Spin}^c(\Sigma_m(K))|$, such that for each $\mathfrak{s} \in S$, $d(\Sigma_m(K), \mathfrak{s}) = 0$ and $\tau(\Sigma_m(K), \tilde{K}_m, \mathfrak{s}) = 0$.*

The statement about d was proven by Jabuka and Naik [24]. The statement about τ was proven by Grigsby, Ruberman, and Strle [16], adapting Ozsváth and Szabó's original argument concerning τ for knots in S^3 [46]. This theorem is formally similar to the work of Casson and Gordon [4], whose sliceness obstructions also rely on square-root-order subgroups of $H^2(\Sigma_m(K);\mathbb{Z})$ obtained in the same manner. However, the Casson–Gordon invariants obstruct topological sliceness, while the Heegaard Floer ones obstruct only smooth sliceness.

While Theorem 4.1 applies to cyclic branched covers of any prime power multiplicity, it has primarily been used in the $m = 2$ case because the d invariants of double branched covers of low-crossing knots can often be computed using the skein exact triangle for HF^+, as will be described below.

4.1 Obstructing finite concordance order via d invariants

In this section, we restrict to the case where $m = 2$.

Jabuka and Naik [24] used the part of Theorem 4.1 concerning d invariants to obtain lower bounds on the concordance orders of certain small knots K. Specifically, they showed that some knots that represent torsion in the algebraic concordance group (the image of the map Ψ_1 described in the Introduction) have order > 4 in $\mathcal{C}_1$. By computing all the d invariants of $\Sigma_2(K)$, they found the d invariants of

$\Sigma_2(\#^4 K) = \#^4\Sigma_2(K)$ using additivity and explicitly checked Theorem 4.1 for every square-root order subgroup of $H^2(\Sigma_2(\#^4 K;\mathbb{Z}))$ to show that K has concordance order greater than 4. Of course, the same techniques could be used to obstruct a knot from having any particular finite order, but the number of subgroups to consider grows rapidly.

Grigsby, Ruberman, and Strle [16] then showed how to show that a knot has infinite concordance order. Specifically, they defined numerical invariants $\mathcal{D}_q(K)$ and $\mathcal{T}_q(K)$ ($q \in \mathbb{N}$), coming from the d and τ invariants of $\Sigma_2(K)$. Essentially, the $\mathcal{D}_q(K)$ control the behavior of $d(\#^n\Sigma_2(K), \mathfrak{s})$ on all square-root-order subgroups of $\mathrm{Spin}^c(\#^n\Sigma_2(K))$, and the $\mathcal{T}_q$ do the same for $\tau(\#^n\Sigma_2(K), \#^n\tilde{K}_2, \mathfrak{s})$. They proved:

Theorem 4.2. *Let K be a knot in S^3. Let p be prime, and suppose that p^m is the largest power of p that divides* $\det(K)$*. If K has finite concordance order, then for each integer $0 \le e \le \left\lfloor \frac{m+1}{2} \right\rfloor$, we have $\mathcal{D}_{p^e}(K) = \mathcal{T}_{p^e}(K) = 0$.*

Using this theorem and an algorithm specific to two-bridge knots, Grigsby, Ruberman, and Strle showed that all two-bridge knots through 12 crossings whose smooth concordance orders were previously unknown have infinite order.

Let $\mathfrak{s}_0 \in \mathrm{Spin}^c(\Sigma_2(K))$ denote the unique spin structure on $\Sigma_2(K)$, which is unique because $H^2(\Sigma_2(K);\mathbb{Z}_2) = 0$. If K bounds a slice disk Δ, then $\mathfrak{s}_0$ always extends over $\Sigma_2(\Delta)$, so the set $S \subset \mathrm{Spin}^c(\Sigma_2(K))$ provided by Theorem 4.1 must contain $\mathfrak{s}_0$. The Manolescu–Owens concordance invariant $\delta(K) \in \mathbb{Z}$ is defined as $2d(\Sigma_2(K), \mathfrak{s}_0)$ [40].

If $H^2(\Sigma_2(K);\mathbb{Z})$ is cyclic, it contains a unique subgroup G_q of order q for each q dividing $\det K$. In this case, the Grigsby–Ruberman–Strle invariants $\mathcal{D}_q(K)$ and $\mathcal{T}_q(K)$ are defined as

$$\mathcal{D}_q(K) = \sum_{\mathfrak{s} \in \mathfrak{s}_0 + G_q} d(\Sigma_2(K), \mathfrak{s})$$
$$\mathcal{T}_q(K) = \sum_{\mathfrak{s} \in \mathfrak{s}_0 + G_q} \tau(\Sigma_2(K), \tilde{K}_2, \mathfrak{s}),$$

and they are both 0 for any q not dividing $\det K$. For the general case, see [16, Definition 4.1].

9_{30}	9_{33}	9_{44}	10_{58}	10_{60}	10_{91}	10_{102}	10_{119}
10_{135}	10_{158}	10_{164}	$11a_{4}$	$11a_{5}$	$11a_{8}$	$11a_{11}$	$11a_{24}$
$11a_{26}$	$11a_{30}$	$11a_{38}$	$11a_{44}$	$11a_{47}$	$11a_{52}$	$11a_{56}$	$11a_{67}$
$11a_{72}$	$11a_{76}$	$11a_{80}$	$11a_{88}$	$11a_{98}$	$11a_{104}$	$11a_{109}$	$11a_{112}$
$11a_{126}$	$11a_{135}$	$11a_{160}$	$11a_{167}$	$11a_{168}$	$11a_{170}$	$11a_{187}$	$11a_{189}$
$11a_{233}$	$11a_{249}$	$11a_{257}$	$11a_{265}$	$11a_{270}$	$11a_{272}$	$11a_{287}$	$11a_{288}$
$11a_{289}$	$11a_{300}$	$11a_{303}$	$11a_{315}$	$11a_{350}$	$11n_{34}$	$11n_{45}$	$11n_{48}$
$11n_{53}$	$11n_{55}$	$11n_{85}$	$11n_{100}$	$11n_{110}$	$11n_{114}$	$11n_{130}$	$11n_{145}$
$11n_{157}$	$11n_{165}$						

Table 2: Knots through eleven crossings with previously unknown concordance order.

As of May 2008, the smooth concordance orders of sixty-six knots through eleven crossings, listed in Table 2, were unknown according to Cha and Livingston's database *KnotInfo* [6]. By computing the $\mathcal{D}_q$ invariants of all of these knots, we proved:

Theorem 4.3. *Each of the forty-five knots listed in Table 3 has at least one nonzero $\mathcal{D}_q$ invariant and therefore has infinite concordance order. For the remaining knots listed in Table 2, all of the $\mathcal{D}_q$ invariants vanish.*

We conclude this section by explaining the computations used in proving Theorem 4.3. We use techniques of Ozsváth and Szabó [47, 52, 51], which were also used by Jabuka and Naik [24].

Given a projection of K, let G be its Goeritz matrix (defined in [52, section 3]). Let $|G|$ denote the rank of G. The double cover Y_K bounds a 4-manifold X_G whose intersection form on H_2, $Q = Q_{X_G}$, is given by G (with respect to a basis of spheres). Let $\mathrm{Char}(G) \subset H^2(X_G;\mathbb{Z})$ denote the set of characteristic vectors for Q, i.e., vectors $\alpha \in H^2(X_G;\mathbb{Z})$ such that $\langle \alpha, v\rangle \equiv Q(v,v) \pmod 2$ for every $v \in H_2(X_G;\mathbb{Z})$. The restriction map $i^*\colon H^2(X_G) \to H^2(Y_K)$ partitions $\mathrm{Char}(G)$ into equivalence classes

Knot K	$\det(K)$	Nonzero $\mathcal{D}_q$	Knot K	$\det(K)$	Nonzero $\mathcal{D}_q$
9_{30}	53	$\mathcal{D}_{53} = 4$	$11a_{170}$	185	$\mathcal{D}_{37} = -4$
9_{33}	61	$\mathcal{D}_{61} = 4$	$11a_{189}$	149	$\mathcal{D}_{149} = -12$
9_{44}	17	$\mathcal{D}_{17} = 4$	$11a_{233}$	173	$\mathcal{D}_{101} = 16$
10_{58}	65	$\mathcal{D}_{13} = 4$	$11a_{249}$	117	$\mathcal{D}_{13} = -4$
10_{60}	85	$\mathcal{D}_{17} = 4$	$11a_{257}$	97	$\mathcal{D}_{97} = -8$
10_{102}	73	$\mathcal{D}_{73} = -12$	$11a_{265}$	109	$\mathcal{D}_{109} = 24$
10_{119}	101	$\mathcal{D}_{101} = -16$	$11a_{270}$	137	$\mathcal{D}_{137} = 12$
10_{135}	135	$\mathcal{D}_{37} = 4$	$11a_{272}$	149	$\mathcal{D}_{149} = 12$
$11a_{4}$	97	$\mathcal{D}_{97} = -24$	$11a_{287}$	181	$\mathcal{D}_{181} = -12$
$11a_{8}$	117	$\mathcal{D}_{13} = -4$	$11a_{288}$	205	$\mathcal{D}_{5} = 4, \mathcal{D}_{41} = 4$
$11a_{11}$	113	$\mathcal{D}_{113} = 12$	$11a_{289}$	145	$\mathcal{D}_{29} = 4$
$11a_{24}$	157	$\mathcal{D}_{157} = 12$	$11a_{300}$	153	$\mathcal{D}_{17} = -4$
$11a_{26}$	157	$\mathcal{D}_{157} = 12$	$11a_{303}$	149	$\mathcal{D}_{149} = 36$
$11a_{30}$	149	$\mathcal{D}_{149} = 12$	$11a_{315}$	157	$\mathcal{D}_{157} = 12$
$11a_{52}$	137	$\mathcal{D}_{137} = 16$	$11a_{350}$	185	$\mathcal{D}_{5} = 4, \mathcal{D}_{37} = 4$
$11a_{56}$	109	$\mathcal{D}_{109} = -8$	$11n_{48}$	29	$\mathcal{D}_{29} = -8$
$11a_{67}$	125	$\mathcal{D}_{25} = -4$	$11n_{53}$	37	$\mathcal{D}_{37} = -8$
$11a_{76}$	145	$\mathcal{D}_{29} = -4$	$11n_{55}$	61	$\mathcal{D}_{61} = 12$
$11a_{80}$	137	$\mathcal{D}_{137} = -12$	$11n_{110}$	41	$\mathcal{D}_{41} = -12$
$11a_{88}$	101	$\mathcal{D}_{101} = -8$	$11n_{114}$	53	$\mathcal{D}_{53} = -4$
$11a_{126}$	145	$\mathcal{D}_{5} = 4, \mathcal{D}_{29} = 4$	$11n_{130}$	53	$\mathcal{D}_{53} = 12$
$11a_{160}$	145	$\mathcal{D}_{29} = -4$	$11n_{165}$	85	$\mathcal{D}_{17} = -4$
$11a_{167}$	113	$\mathcal{D}_{113} = 12$			

Table 3: Knots in Table 2 with non-vanishing $\mathcal{D}_q$ invariants.

$\mathrm{Char}(G,\mathfrak{s})$ corresponding to the spin^c structures on Y_K. Given certain hypotheses on G, including that G is negative-definite, Ozsváth and Szabó [47, Corollary 1.5] proved that the correction terms for $\mathrm{HF}^+(Y_K)$ are given by the formula

$$d(Y_K,\mathfrak{s}) = \max_{\alpha\in\mathrm{Char}(G,\mathfrak{s})} \frac{\alpha^2+|G|}{4}. \tag{4.2}$$

The vectors in each equivalence class that realize this maximum may be determined algorithmically. Moreover, since $H^2(Y_K;\mathbb{Z}) \cong \mathrm{coker}(G)$, we may easily identify the affine structure on $\mathrm{Spin}^c(Y_K)$ (specifically, which spin^c structures are in the distinguished subgroup G_q) using the Smith normal form for G.

As shown in [52], the formula (4.2) holds whenever G is computed from an alternating projection. More generally, if K admits a projection that is alternating except in a region that consists of left-handed twists, Ozsváth and Szabó [51] show how to use Kirby calculus on X_G to obtain a matrix $\tilde{G}$ for Q that satisfies the correct hypotheses. (See also Jabuka–Naik [24] for a concise explanation.) All of the non-alternating knots in Table 2 satisfy this hypothesis, so we may compute the $\mathcal{D}_q$ invariants as described above.

4.2 Computing $\widehat{\mathrm{HFK}}(\Sigma_m(K),\tilde{K}_m)$

In this section, we describe an algorithm for computing the knot Floer homology group $\widehat{\mathrm{HFK}}(\Sigma_m(K),\tilde{K}_m)$ for any knot $K\subset S^3$. This material appeared in [31].

Any knot $K\subset S^3$ can be represented by means of a *grid diagram*, consisting of an $n\times n$ grid in which the centers of certain squares are marked X or O, such that each row and each column contains exactly one X and one O. To recover a knot projection, draw an arc from the X to the O in each column and from the O to the X in each row, making the vertical strand pass over the horizontal strand at each crossing. If we identify opposite edges of the square, we obtain a multi-pointed Heegaard diagram $\mathcal{H} = (T^2,\boldsymbol{\alpha},\boldsymbol{\beta},\mathbf{w},\mathbf{z})$ for (S^3,K), where the α circles are the horizontal grid lines, the β circles are the vertical grid lines, and the w (resp. z) basepoints are placed in the regions marked O (resp. X). Manolescu, Ozsváth, and Sarkar [41] showed that the knot Floer complex for such Heegaard diagrams is completely combinatorial, with the differential counting embedded rectangles. Subsequently, Manolescu, Ozsváth, Szabó, and Thurston [42] used grid diagrams to give a completely combinatorial definition and proof of invariance for knot (and link) Floer homology.

Let $m \geq 2$, and let $\tilde{T}$ be the surface obtained by gluing together m copies of T (denoted $T_0, \dots, T_{m-1}$) along branch cuts connecting the X and the O in each column. Specifically, in each column, if the X is above the O, then glue the left side of the branch cut in T_k to the right side of the same cut in T_{k+1} (indices modulo m); if the O is above the X, then glue the left side of the branch cut in T_k to the right side of the same cut in T_{k-1}. The obvious projection $\pi\colon \tilde{T} \to T$ is an m-fold cyclic branched cover, branched around the marked points. Each α or β circle in T intersects the branch cuts a total of zero times algebraically and therefore has m distinct lifts to $\tilde{T}$, and each lift of each α circle intersects exactly one lift of each β circle. (We will describe these intersections more explicitly in Subsection 4.2.2.)

Denote by $\mathfrak{R}$ the set of embedded rectangles in T whose lower and upper edges are arcs of α circles, whose left and right edges are arcs of β circles, and which do not contain any marked points in their interior. Each rectangle in $\mathfrak{R}$ has m distinct lifts to $\tilde{T}$ (possibly passing through the branch cuts as in Figure 39); denote the set of such lifts by $\tilde{\mathfrak{R}}$.

Let $\mathfrak{S}$ be the set of unordered mn-tuples $\mathbf{x}$ of intersection points between the lifts of α and β circles in T such that each lift contains exactly one point of $\mathbf{x}$. (We will give a more explicit characterization of the elements of $\mathfrak{S}$ later.) Let C be the $\mathbb{F}_2$-vector space generated by $\mathfrak{S}$. Define a differential d_0 on C by making the coefficient of $\mathbf{y}$ in $d_0(\mathbf{x})$ nonzero if and only if the following conditions hold:

- All but two of the points in $\mathbf{x}$ are also in $\mathbf{y}$.
- There is a rectangle $R \in \tilde{\mathfrak{R}}$ whose lower-left and upper-right corners are in $\mathbf{x}$, whose upper-left and lower-right corners are in $\mathbf{y}$, and which does not contain

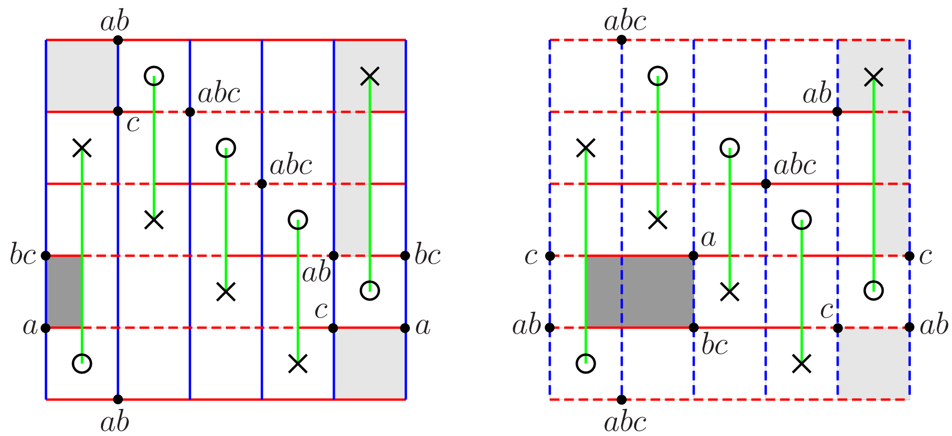

Figure 39: A lifted grid diagram $\tilde{\mathcal{H}} = (\tilde{T}, \tilde{\boldsymbol{\alpha}}, \tilde{\boldsymbol{\beta}}, \tilde{\mathbf{w}}, \tilde{\mathbf{z}})$ for $(\Sigma_2(K), \tilde{K}_m)$, where K is the right-handed trefoil. The solid and dashed lines represent different lifts of the α (horizontal/red) and β (vertical/blue) circles. The points marked a, b, and c belong to generators $\mathbf{a}$, $\mathbf{b}$, and $\mathbf{c}$, respectively. The dark shaded region is a rectangle from $\mathbf{a}$ to $\mathbf{b}$; the light shaded region is an octagon from $\mathbf{a}$ to $\mathbf{c}$.

any point of $\mathbf{x}$ in its interior.

In Section 4.2.2, we shall define two gradings (Alexander and Maslov) on C, as well as a decomposition of C as a direct sum of complexes corresponding to spin^c structures on $\Sigma_m(K)$. We shall prove the following theorem:

Theorem 4.4. *The complex (C, d_0) just described is equal to the knot Floer complex of a multi-pointed Heegaard diagram for $(\Sigma_m(K), \tilde{K}_m)$. Therefore, $H_*(C, d_0) \cong \widehat{\mathrm{HFK}}(\Sigma_m(K), \tilde{K}_m) \otimes V^{\otimes n-1}$, where $V \cong \mathbb{F}_2 \oplus \mathbb{F}_2$ with generators in bigradings $(0,0)$ and $(-1,-1)$.*[2]

We wrote a computer program (in C++ and *Mathematica*) that implements the computation of (C, d_0) in the case where $m = 2$. Using this program, we were able to compute $\widehat{\mathrm{HFK}}(\Sigma_2(K), \tilde{K}_2)$ for over fifty three-bridge knots. (Grigsby [14] found a

[2] Recall that if we have a genus-g Heegaard diagram for a pair (Y, K) with $g+k-1$ α circles, $g+k-1$ β circles, and basepoints $w_1, \dots, w_k$ and $z_1, \dots, z_k$, the homology of the Floer complex in which we count only disks that miss all the basepoints is isomorphic to $\widehat{\mathrm{HFK}}(Y, K) \otimes V^{\otimes k-1}$.

much more efficient algorithm for two-bridge knots.) The Poincaré polynomials for all of these groups are listed in [31]; we do not list them here.

Grigsby [15] proved that when K is a two-bridge knot, the groups $\widehat{\mathrm{HFK}}(S^3, K)$ and $\widehat{\mathrm{HFK}}(\Sigma_2(K), \tilde{K}_2, \mathfrak{s}_0)$ are isomorphic as bigraded groups up to an overall shift in the Maslov grading. We have found examples of three-bridge knots (e.g. the knots $11n_{49}$, $11n_{102}$, and $11n_{116}$) for which this isomorphism fails. However, our computations do support the following conjecture. Define the δ grading on $\widehat{\mathrm{HFK}}$ as the difference between the Alexander and Maslov gradings. We say that $\widehat{\mathrm{HFK}}(S^3, K)$ is *thin* if it is supported in a single δ grading.

Conjecture 4.5. *If $\widehat{\mathrm{HFK}}(S^3, K)$ is thin, then $\widehat{\mathrm{HFK}}(\Sigma_2(K), \tilde{K}_2, \mathfrak{s}_0)$ is thin and isomorphic to $\widehat{\mathrm{HFK}}(S^3, K)$. In general, for each Alexander grading i, the rank of $\widehat{\mathrm{HFK}}(\Sigma_2(K), \tilde{K}_2, \mathfrak{s}_0, i)$ is greater than or equal to the rank of $\widehat{\mathrm{HFK}}(S^3, K, i)$.*

A weaker conjecture would be that $\widehat{\mathrm{HFK}}(\Sigma_2(K), \tilde{K}_2, \mathfrak{s}_0) \cong \widehat{\mathrm{HFK}}(S^3, K)$ is thin whenever K is quasi-alternating (or perhaps merely alternating).

The behavior of the Maslov gradings, however, seems complicated. For example, for the knot 10_{145}, the ranks of $\widehat{\mathrm{HFK}}(S^3, K)$ and $\widehat{\mathrm{HFK}}(\Sigma_2(K), \tilde{K}, \mathfrak{s}_0)$ are the same in each Alexander grading, but $\widehat{\mathrm{HFK}}(S^3, K)$ is supported in two δ-gradings while $\widehat{\mathrm{HFK}}(\Sigma_2(K), \tilde{K}_2, \mathfrak{s}_0)$ is supported in three.

For the other spin^c structures on $\Sigma_2(K)$, it is not true that $\widehat{\mathrm{HFK}}(\Sigma_2(K), \tilde{K}_2, \mathfrak{s})$ must be thin for all $\mathfrak{s} \in \mathrm{Spin}^c(\Sigma_2(K))$ whenever $\widehat{\mathrm{HFK}}(S^3, K)$ is thin; counterexamples include the knots 10_{134} and $11n_{117}$, which are both quasi-alternating.

We may also obtain some further information towards computing the invariants $\tau(\Sigma_2(K), \tilde{K}_2, \mathfrak{s})$. Let $\mathfrak{E}_X$ denote the set of embedded, convex, octagonal domains in $\tilde{\mathcal{H}}$ that contain exactly one of the regions marked X and none of the regions marked O. (See Figure 39 for an example.) As drawn, such an octagon has two lower-left corners, two lower-right corners, two upper-left corners, and two upper-right corners. Define a map d_1 on C by making the coefficient of $\mathbf{y}$ in $d_1(\mathbf{x})$ is if and only if the following conditions hold:

- All but four of the points in $\mathbf{x}$ are also in $\mathbf{y}$.
- There is an octagon $E \in \mathfrak{E}_X$ whose lower-left and upper-right corners are in $\mathbf{x}$, whose upper-left and lower-right corners are in $\mathbf{y}$, and which does not contain any point of $\mathbf{x}$ in its interior.

Theorem 4.6. *The map d_1 induces a differential on $H_*(C, d_0)$, and the homology of $(H_*(C, d_0), d_{1*})$ is isomorphic to the E^2 page of the spectral sequence from $\widehat{\mathrm{HFK}}(\Sigma_2(K), \tilde{K}_2) \otimes V^{\otimes n-1}$ to $\widehat{\mathrm{HF}}(\Sigma_2(K)) \otimes V^{\otimes n-1}$.*

Determining the higher differentials in the spectral sequence combinatorially is a much more difficult problem. Moreover, even if this were possible, it would not guarantee that we could compute the invariants $\tau(\Sigma_2(K), \tilde{K}_2, \mathfrak{s})$, since *a priori* we need to know not only $\widehat{\mathrm{HF}}(\Sigma_2(K), \mathfrak{s})$ but the map $\iota : \widehat{\mathrm{HF}}(\Sigma_2(K), \mathfrak{s}) \to \mathrm{HF}^+(\Sigma_2(K), \mathfrak{s})$. However, in many sufficiently simple cases, knowing the maps d_0 and d_1 is sufficient to determine $\tau(\Sigma_2(K), \tilde{K}_2, \mathfrak{s})$ — if, for instance, $\widehat{\mathrm{HF}}(\Sigma_2(K), \mathfrak{s})$ has rank 1 in Maslov grading $d(\Sigma_2(K), \mathfrak{s})$ and $\widehat{\mathrm{HFK}}(\Sigma_2(K), \tilde{K}_2, \mathfrak{s})$ is supported in a single δ grading. Using Theorems 4.4 and 4.6, we were able to compute the $\mathcal{T}_q$ invariants for several of the non-alternating knots whose $\mathcal{D}_q$ invariants fail to obstruct them from having finite concordance order: 9_{44}, 10_{158}, 10_{164}, $11n_{100}$, and $11n_{145}$. However, the $\mathcal{T}_q$ invariants of these knots all vanish, so we do not obtain any new concordance information. The remaining knots in Table 2 are beyond the range of the computing resources presently available.

In the following sections, we first give some general facts about Heegaard diagrams for branched covers, and then use them to prove Theorems 4.4 and 4.6. We then show how this approach may be used to compute the invariants $\tau(\Sigma_2(K), \tilde{K}_2, \mathfrak{s})$ and $\mathcal{T}_q(K)$ for the examples just mentioned.

4.2.1 Heegaard diagrams for cyclic branched covers of knots

Given a knot $K \subset S^3$ and an integer $m \geq 2$, the cyclic branched cover $\Sigma_m(K)$ can be constructed explicitly from m copies of $S^3 - \operatorname{int} F$, where F is a Seifert surface for K, by connecting the negative side of a bicollar of F in the k^{th} copy to the positive side in the $(k+1)^{\text{th}}$ (indices modulo m). The inverse image of K in $\Sigma_m(K)$ is a knot $\tilde{K}_m$, which is nulhomologous because it bounds a Seifert surface (any of the lifts of the original Seifert surface F). For details, see Rolfsen's book [58, chapters 6, 10].

The group of covering transformations of $\Sigma_m(K) \to S^3$ is cyclic of order m, generated by a map $\tau_m \colon \Sigma_m(K) \to \Sigma_m(K)$ that takes the k^{th} copy of $S^3 - \operatorname{int} F$ to the $(k+1)^{\text{th}}$ (indices modulo m). If γ is a 1-cycle in S^3, then by using transfer homomorphisms, we see that for any lift $\tilde{\gamma}$ (which is not necessarily a cycle), the equation

$$\sum_{k=0}^{m-1} \tau_{m*}^k(\tilde{\gamma}) = 0 \tag{4.3}$$

holds in $H_1(\Sigma_m(K); \mathbb{Z})$. In particular, when $m = 2$, we have $\tau_{2*}(\tilde{\gamma}) = -\tilde{\gamma}$.

When m is a power of a prime p, the group $H_1(\Sigma_m(K); \mathbb{Z})$ is finite and contains no p-torsion [13, page 16]. This implies the action of the deck transformation group on $H_1(\Sigma_m(K); \mathbb{Z})$ has no nonzero fixed points: if $\tau_{m*}(\alpha) = \alpha$, then

$$0 = \alpha + \tau_{m*}(\alpha) + \cdots + \tau_{m*}^{m-1}(\alpha) = m\alpha$$

by (4.3), so $\alpha = 0$.

Let

$$\mathcal{H} = (S, \{\alpha_1, \dots, \alpha_{g+n-1}\}, \{\beta_1, \dots, \beta_{g+n-1}\}, \{w_1, \dots, w_n\}, \{z_1, \dots, z_n\})$$

be a multi-pointed Heegaard diagram for $K \subset S^3$ with genus g.[3] If $f \colon S^3 \to \mathbb{R}$ is a self-indexing Morse function compatible with $\mathcal{H}$, then $\tilde{f} = f \circ \pi \colon \Sigma_m(K) \to \mathbb{R}$ is a self-indexing Morse function for the pair $(\Sigma_m(K), \tilde{K}_m)$ whose critical points are simply the

[3] We denote the Heegaard surface by S rather than the usual Σ to avoid confusion with the notation $\Sigma_m(K)$.

inverse images of the critical points of f. This function induces a Heegaard splitting of $\Sigma_m(K)$ that projects onto the Heegaard splitting of S^3 given by $\mathcal{H}$. A simple Euler characteristic argument shows that the genus of the new Heegaard surface $\tilde{S} = \pi^{-1}(S)$ is $h = mg + (m-1)(n-1)$. Each α or β circle in S bounds a disk in $S^3 - K$ and hence has m distinct preimages in $\Sigma_m(K)$. Thus, we obtain a Heegaard diagram $\tilde{\mathcal{H}} = (\tilde{S}, \tilde{\boldsymbol{\alpha}}, \tilde{\boldsymbol{\beta}}, \tilde{\mathbf{w}}, \tilde{\mathbf{z}})$, where $\tilde{S}$ is a surface of genus h and $\tilde{\boldsymbol{\alpha}}$, $\tilde{\boldsymbol{\beta}}$, $\tilde{\mathbf{w}}$, and $\tilde{\mathbf{z}}$ are the inverse images of the corresponding objects under the covering map.

The generators of the complex $\widehat{\mathrm{CFK}}(\tilde{\mathcal{H}})$ may be described as follows:

Lemma 4.7. *Any generator* $\mathbf{x}$ *of* $\widehat{\mathrm{CFK}}(\tilde{\mathcal{H}})$ *can be decomposed (non-uniquely) as* $\mathbf{x} = \tilde{\mathbf{x}}_1 \cup \cdots \cup \tilde{\mathbf{x}}_m$*, where* $\mathbf{x}_1, \ldots, \mathbf{x}_m$ *are generators of* $\widehat{\mathrm{CFK}}(\mathcal{H})$*, and* $\tilde{\mathbf{x}}_i$ *is a lift of* $\mathbf{x}_i$ *to* $\tilde{\mathcal{H}}$*.*

Proof. Given a generator $\mathbf{x}$ of $\widehat{\mathrm{CFK}}(\tilde{\mathcal{H}})$, let $G_{\mathbf{x}}$ be a graph with vertices

$$\{a_1, \ldots, a_{g+n-1}, b_1, \ldots, b_{g+n-1}\}$$

and edges $\{e_x \mid x \in \mathbf{x}\}$, where e_x connects a_i to b_j if x is an intersection point between lifts of α_i and β_j. This is clearly a bipartite graph in which each vertex has incidence number m. By König's Theorem [9, Proposition 5.3.1], the edges of $G_{\mathbf{x}}$ can be partitioned (non-uniquely) into m perfect pairings, each of which corresponds to a lift of a generator of $\widehat{\mathrm{CFK}}(\mathcal{H})$. $\square$

For each generator $\mathbf{x}_0$ of $\widehat{\mathrm{CFK}}(\mathcal{H})$, let $L(\mathbf{x}_0)$ denote the generator of $\widehat{\mathrm{CFK}}(\tilde{\mathcal{H}})$ consisting of all m lifts of each point of $\mathbf{x}_0$. Using the action of the deck transformation τ_m on $\mathcal{H}$, we may write $L(\mathbf{x}_0) = \tilde{\mathbf{x}}_0 \cup \tau_m(\tilde{\mathbf{x}}_0) \cup \cdots \cup \tau_m^{m-1}(\tilde{\mathbf{x}}_0)$, where $\tilde{\mathbf{x}}_0$ is any lift of $\mathbf{x}_0$ to $\tilde{D}$.

Lemma 4.8. *All generators of* $\widehat{\mathrm{CFK}}(\tilde{\mathcal{H}})$ *of the form* $\mathbf{x} = L(\mathbf{x}_0)$ *are in the same spin*^{c} *structure, denoted* $\mathfrak{s}_0$*, which is fixed under the action of the deck transformation group. If* m *is a prime power, this property uniquely characterizes* $\mathfrak{s}_0$*. If* m *is a power of* 2*,* $\mathfrak{s}_0$ *is the unique spin structure on* $\Sigma_m(K)$*.*

Proof. (Adapted from Grigsby [15].) Let $\mathbf{x}_0$ and $\mathbf{y}_0$ be generators of $\widehat{\mathrm{CFK}}(\mathcal{H})$; we shall show that $L(\mathbf{x}_0)$ and $L(\mathbf{y}_0)$ are in the same spin^c structure. Let $\gamma_{\mathbf{x}_0,\mathbf{y}_0}$ be a 1-cycle in S consisting of arcs from $\mathbf{x}_0$ to $\mathbf{y}_0$ along the α circles and from $\mathbf{y}_0$ to $\mathbf{x}_0$ along the β circles. Let $\tilde{\gamma}_{\mathbf{x}_0,\mathbf{y}_0}$ be a lift of $\gamma_{\mathbf{x}_0,\mathbf{y}_0}$ to $\tilde{S}$. Then the difference $\mathfrak{s}_{\tilde{\mathbf{w}}}(L(\mathbf{x}_0)) - \mathfrak{s}_{\tilde{\mathbf{w}}}(L(\mathbf{y}_0))$ is Poincaré dual to the homology class in $H_1(\Sigma_m(K);\mathbb{Z})$ of the 1-cycle

$$\gamma_{L(\mathbf{x}_0),L(\mathbf{y}_0)} = \tilde{\gamma}_{\mathbf{x}_0,\mathbf{y}_0} + \tau_{m*}(\tilde{\gamma}_{\mathbf{x}_0,\mathbf{y}_0}) + \cdots + \tau_{m*}^{m-1}(\tilde{\gamma}_{\mathbf{x}_0,\mathbf{y}_0}),$$

which equals 0 by (4.3). Thus, $\mathfrak{s}_{\tilde{\mathbf{w}}}(L(\mathbf{x}_0)) = \mathfrak{s}_{\tilde{\mathbf{w}}}(L(\mathbf{y}_0))$.

If $f\colon S^3 \to \mathbb{R}$ is a self-indexing Morse function for (S^3, K) compatible with $\mathcal{H}$, its pullback $\tilde{f}\colon \Sigma_m(K) \to \mathbb{R}$ is τ_m-invariant. Using a Riemannian metric on $\Sigma_m(K)$ that is the pullback of a metric on S^3, the gradient $\vec{\nabla}\tilde{f}$ is τ_m-invariant and projects onto $\vec{\nabla}f$, and the flowlines for $\tilde{f}$ are precisely the lifts of flowlines for f. If N is the union of neighborhoods of flowlines through the points of $\mathbf{x}_0$ and $\mathbf{w}$, where $\mathbf{x}_0$ is a generator of $\widehat{\mathrm{CFK}}(\mathcal{H})$, then $\tilde{N} = \pi^{-1}(N)$ is the union of neighborhoods of flowlines through the points of $L(\mathbf{x}_0)$ and $\tilde{\mathbf{w}}$. By suitably modifying $\vec{\nabla}\tilde{f}$ on $\tilde{N}$, we may obtain a τ_m-invariant vector field that determines $\mathfrak{s}_{\tilde{\mathbf{w}}}(L(\mathbf{x}_0)) = \mathfrak{s}_0$.

If m is a prime power and $\mathfrak{s}_0'$ is another spin^c structure fixed under the action of τ_m, then the difference between $\mathfrak{s}_0$ and $\mathfrak{s}_0'$ is a class in $H_1(\Sigma_m(K);\mathbb{Z})$ that is fixed by τ_m and hence equals zero. Finally, if m is a power of 2, the unique spin structure must be τ_m-invariant, hence equal to $\mathfrak{s}$. ☐

Proposition 4.9. *If* $\mathbf{x} = \tilde{\mathbf{x}}_1 \cup \cdots \cup \tilde{\mathbf{x}}_m$ *as in Lemma 4.7, then the Alexander grading of* $\mathbf{x}$ *(computed with respect to a lift of a Seifert surface for* K*) is equal to the average of the Alexander gradings of* $\mathbf{x}_1, \dots, \mathbf{x}_m$*.*[4] *In particular, for any generator* $\mathbf{x}_0$ *of* $\widehat{\mathrm{CFK}}(\mathcal{H})$*, we have* $A(\mathbf{x}_0) = A(L(\mathbf{x}_0))$*.*

[4]Note that we have specified a Seifert surface in order to define the Alexander grading. When m is a prime power, however, $\Sigma_m(K)$ is a rational homology sphere, so the Alexander grading does not depend at all on the choice of Seifert surface.

Proof. We first consider the relative Alexander gradings. Let $F \subset S^3$ be a Seifert surface for K, and let $\tilde{F}$ be a lift of F to $\Sigma_m(K)$. The translates $\tilde{F}, \tau_m(\tilde{F}), \dots, \tau_m^{m-1}(\tilde{F})$ are all Seifert surfaces for $\tilde{K}_m$. Given two generators $\mathbf{x}$ and $\mathbf{y}$, the difference $A(\mathbf{x}) - A(\mathbf{y})$ equals the intersection number of the 1-cycle $\gamma_{\mathbf{x},\mathbf{y}}$ with any Seifert surface for $\tilde{K}_m$, where $\gamma_{\mathbf{x},\mathbf{y}}$ is a 1-cycle in $\tilde{\mathcal{H}}$ relating $\mathbf{x}$ and $\mathbf{y}$ as above. (If $\mathbf{x}$ and $\mathbf{y}$ are in the same spin^c structure, this intersection number equals $n_{\mathbf{z}}(D) - n_{\mathbf{w}}(D)$, where D is any domain from $\mathbf{x}$ to $\mathbf{y}$, and $n_{\mathbf{z}}(D)$ (resp. $n_{\mathbf{w}}(D)$) is the sum of the multiplicities of D at the z (resp. w) basepoints.) Therefore,

$$m(A(\mathbf{x}) - A(\mathbf{y})) = \gamma_{\mathbf{x},\mathbf{y}} \cdot \tilde{F} + \gamma_{\mathbf{x},\mathbf{y}} \cdot \tau_m(\tilde{F}) + \cdots + \gamma_{\mathbf{x},\mathbf{y}} \cdot \tau_m^{m-1}(\tilde{F}).$$

The projection $\pi_*(\gamma_{\mathbf{x},\mathbf{y}})$ is a 1-cycle in S that goes from points of $\pi(\mathbf{x})$ to points of $\pi(\mathbf{y})$ along α circles and from points of $\pi(\mathbf{y})$ to points of $\pi(\bar{\mathbf{x}})$ along β circles. Every intersection point of $\gamma_{\mathbf{x},\mathbf{y}}$ with one of the lifts of F projects to an intersection point of $\pi_*(\gamma_{\mathbf{x},\mathbf{y}})$ with F, so

$$\gamma_{\mathbf{x},\mathbf{y}} \cdot \tilde{F} + \gamma_{\mathbf{x},\mathbf{y}} \cdot \tau_m(\tilde{F}) + \cdots + \gamma_{\mathbf{x},\mathbf{y}} \cdot \tau_m^{m-1}(\tilde{F}) = \pi_*(\gamma_{\mathbf{x},\mathbf{y}}) \cdot F.$$

The restriction of $\pi_*(\gamma_{\mathbf{x},\mathbf{y}})$ to any α or β circle consists of m (possibly constant or overlapping) arcs. By perhaps adding multiples of the α or β circles, we can arrange that each of these arcs connects a point of $\mathbf{x}_1$ with a point of $\mathbf{y}_1$, a point of $\mathbf{x}_2$ with a point of $\mathbf{y}_2$, and so on. In other words,

$$\pi_*(\gamma_{\mathbf{x},\mathbf{y}}) \equiv \gamma_{\mathbf{x}_1,\mathbf{y}_1} + \cdots + \gamma_{\mathbf{x}_m,\mathbf{y}_m}$$

modulo the α and β circles in $\mathcal{H}$, whose intersection numbers with F are zero. We have:

$$\begin{aligned} A(\mathbf{x}) - A(\mathbf{y}) &= \frac{1}{m}(\gamma_{\mathbf{x}_1,\mathbf{y}_1} + \dots, + \gamma_{\mathbf{x}_m,\mathbf{y}_m}) \cdot F \\ &= \frac{1}{m}(A(\mathbf{x}_1) - A(\mathbf{y}_1) + \cdots + A(\mathbf{x}_m) - A(\mathbf{y}_m)) \end{aligned}$$

Thus, the Alexander grading of a generator of $\widehat{\mathrm{CFK}}(\tilde{\mathcal{H}})$ is given up to an additive constant by the average Alexander grading of its parts.

To pin down the additive constant, first note that the branched covering map $\pi\colon \Sigma_m(K) \to S^3$ extends to an *unbranched* covering map from the zero-surgery on $\tilde{K}_m$ to the zero-surgery on K, $\pi_0\colon Y_0 \to S^3_0(K)$, where $Y_0 = \Sigma_m(K)_0(\tilde{K}_m)$. Since this is a local diffeomorphism, it is possible to pull back spin^c structures. Let $\mathbf{x}_0$ be a generator of $\widehat{\mathrm{CFK}}(\mathcal{H})$ in Alexander grading 0, and let $\mathbf{x} = L(\mathbf{x}_0)$. (The symmetry $\widehat{\mathrm{HFK}}(S^3, K, i) \cong \widehat{\mathrm{HFK}}(S^3, K, -i)$ and the fact that $\operatorname{rank} \widehat{\mathrm{HFK}}(S^3, K) \equiv 1 \pmod 2$ [49] imply that such $\widehat{\mathrm{HFK}}(S^3, K, 0)$ has odd rank, so such a generator $\mathbf{x}_0$ always exists.) As in the discussion following Lemma 4.8, we may find a nonvanishing vector field that determines $\mathfrak{s}_{\tilde{\mathbf{w}}}(\mathbf{x}_0) = \mathfrak{s}_0$ and is τ_m-invariant. The unique nonvanishing extension (up to isotopy) of this vector field to Y_0 can also be made τ_m-invariant, so it is the pullback of an extension to $S^3_0(K)$ of a vector field determining $\mathfrak{s}_{\mathbf{w}}(\mathbf{x}_0)$. It follows that $\underline{\mathfrak{s}}_{\tilde{\mathbf{w}},\tilde{\mathbf{z}}}(\mathbf{x}) = \pi_0^*(\underline{\mathfrak{s}}_{\mathbf{w},\mathbf{z}}(\mathbf{x}_0))$. Now, if $\hat{\tilde{F}} \subset Y_0(\tilde{K}_m)$ is obtained by capping off $\tilde{F}$ in the zero-surgery, then $\pi_{0*}[\hat{\tilde{F}}] = [\hat{F}]$ in $H_2(S^0_3; \mathbb{Z})$. We therefore have:

$$\begin{aligned}
A(\mathbf{x}) &= \frac{1}{2}\left\langle c_1(\underline{\mathfrak{s}}_{\tilde{\mathbf{w}},\tilde{\mathbf{z}}}(\mathbf{x})), [\hat{\tilde{F}}]\right\rangle \\
&= \frac{1}{2}\left\langle c_1(\pi_0^*(\underline{\mathfrak{s}}_{\mathbf{w},\mathbf{z}}(\mathbf{x}_0))), [\hat{\tilde{F}}]\right\rangle \\
&= \frac{1}{2}\left\langle c_1(\underline{\mathfrak{s}}_{\mathbf{w},\mathbf{z}}(\mathbf{x}_0)), \pi_{0*}[\hat{\tilde{F}}]\right\rangle \\
&= \frac{1}{2}\left\langle c_1(\underline{\mathfrak{s}}_{\mathbf{w},\mathbf{z}}(\mathbf{x}_0)), [\hat{F}]\right\rangle \\
&= 0 = A(\mathbf{x}_0)
\end{aligned}$$

Thus, the additive constant must equal 0. ☐

Remark 4.10. When K is a two-bridge knot and $m = 2$, Grigsby [15] shows that for a specific diagram $\mathcal{H}$, the map L is surjective and preserves the relative Maslov grading. Therefore, for any two-bridge knot K, $\widehat{\mathrm{HFK}}(\Sigma_2(K), \tilde{K}_m, \mathfrak{s}_0) \cong \widehat{\mathrm{HFK}}(S^3, K)$, up to a possible shift in the absolute Maslov grading. It may be possible to extend this result to a wider class of knots, such as alternating knots. However, in general L is neither surjective nor Maslov-grading-preserving.

Finally, we consider the regions in $\tilde{\mathcal{H}}$. First, note that the preimage of any region R in $\mathcal{H}$ consists of either m distinct regions, each of which is projected diffeomorphically onto R, or a single region. When $\mathcal{H}$ is nice, each region of $\mathcal{H}$ that does not contain a basepoint is a simply connected polygon, so the former possibility holds. Thus, we obtain:

Proposition 4.11. *Let $\mathcal{H}$ be a nice Heegaard diagram for (S^3, K), and let $\tilde{\mathcal{H}}$ be its m-fold cyclic branched cover. Then $\tilde{\mathcal{H}}$ is nice.*

4.2.2 Grid diagrams and cyclic branched covers

Proof of Theorem 4.4. As described in the introduction to this section, any oriented knot $K \subset S^3$ can be represented by means of a grid diagram. By drawing the grid diagram on a standardly embedded torus in S^3, we may think of the grid diagram as a genus 1, multi-pointed Heegaard diagram $\mathcal{H} = (T^2, \boldsymbol{\alpha}, \boldsymbol{\beta}, \mathbf{w}, \mathbf{z})$ for the pair (S^3, K), where the α circles are the horizontal lines of the grid, the β circles are the vertical lines, the w basepoints are in the regions marked O, and the z basepoints are in the regions marked X.

A Seifert surface for K may be seen as follows. We may isotope K to lie entirely within H_α by letting the arcs of $K \cap H_\beta$ fall onto the boundary torus. In fact, it lies within a ball contained in H_α since the knot projection in the grid diagram never passes through the left edge of the grid. Take a Seifert surface F contained in this ball, and then isotope F and K so that K returns to its original position. F then intersects the Heegaard surface T^2 in n arcs, one connecting the two basepoints in each column of the grid diagram, and it intersects H_β in strips that lie above these arcs. The orientations of K and S^3 imply that the positive side of a bicollar for F lies on the *right* of one of these strips when the X is above the O and on the *left* when the O is above the X.

If we construct $\Sigma_m(K)$ by gluing together m copies of $S^3 - \operatorname{int} F$ as in Section 4.2.1, the Heegaard surfaces in each copy are connected exactly to each other as described in Section 1 to form a surface $\tilde{T}$. Hence, $\tilde{\mathcal{H}} = (\tilde{T}, \tilde{\boldsymbol{\alpha}}, \tilde{\boldsymbol{\beta}}, \tilde{\mathbf{w}}, \tilde{\mathbf{z}})$ is a Heegaard diagram for $(\Sigma_m(K), \tilde{K}_m)$ for which the results of Section 3 apply. In particular, it is a nice

Heegaard diagram since $\mathcal{H}$ is nice.

It remains to show that the domains that count for the differential in $\widehat{\mathrm{CFK}}(\tilde{\mathcal{H}})$ are precisely the lifts of those that count for the differential in $\widehat{\mathrm{CFK}}(\mathcal{H})$, as was asserted in Section 1. Since $\tilde{\mathcal{H}}$ is a nice diagram with no bigons, any domain that counts for the differential is an embedded rectangle R. The projection of R to $\mathcal{H}$, $\pi(R)$, is an immersed rectangle in $\tilde{\mathcal{H}}$ whose edges are contained in at most two α circles and two β circles. By lifting $\pi(R)$ to the universal cover of T^2, we see that $\pi(R)$ cannot intersect any α or β circle more than once, or else it would contain an entire column or row of the grid diagram and hence a basepoint. Therefore, $\pi(R)$ is an embedded rectangle that misses the basepoints, so it counts for the differential of $\widehat{\mathrm{CFK}}(\mathcal{H})$. $\square$

We shall now give a more explicit description of the generators of $\widehat{\mathrm{CFK}}(\tilde{D})$ and their gradings in order to facilitate computation.

In the grid diagram $\mathcal{H}$, we label the α circles $\alpha_0, \dots, \alpha_{n-1}$ from bottom to top and the β circles $\beta_0, \dots, \beta_{n-1}$ from left to right. Each α circle intersects each β circle exactly once: $\beta_i \cap \alpha_j = \{x_{ij}\}$. Generators of $\widehat{\mathrm{CFK}}(\mathcal{H})$ then correspond to permutations of the index set $\{0, \dots, n-1\}$ via the correspondence $\sigma \mapsto (x_{0,\sigma(0)}, \dots, x_{n-1,\sigma(n-1)})$.

For each grid point x, let $w(x)$ denote the winding number of the knot projection around x. Let $p_1, \dots, p_{8n}$ (repetitions allowed) denote the vertices of the $2n$ squares containing basepoints, and set

$$a = \frac{1-n}{2} + \frac{1}{8}\sum_{i=1}^{8n} w(p_i).$$

According to Manolescu, Ozsváth, and Sarkar [41], the Alexander grading of a generator $\mathbf{x}$ of $\widehat{\mathrm{CFK}}(\mathcal{H})$ is given by the formula

$$A(\mathbf{x}) = a - \sum_{x \in \mathbf{x}} w(x). \tag{4.4}$$

There is also a formula for the Maslov grading of a generator, but it is not relevant for our purposes.

The generators of $\widehat{\mathrm{CFK}}(\tilde{\mathcal{H}})$ can be described easily as follows. For any $i = 0, \ldots, n-1$ and $j = 0, \ldots, n-1$, each lift of β_i meets exactly one lift of α_j. Specifically, let $\tilde{\beta}_j^k$ denote the lift of β_j on the k^{th} copy of $\mathcal{H}$ (for $k = 0, \ldots, m-1$). Let $\tilde{\alpha}_j^k$ denote the lift of α_j that intersects the leftmost edge of the k^{th} grid diagram ($\tilde{\beta}_0^k$). Let $\tilde{x}_{i,j}^k$ denote the lift of $x_{i,j}$ on the k^{th} diagram. Define a map $g\colon \mathbb{Z}/n \times \mathbb{Z}/n \times \mathbb{Z}/m \to \mathbb{Z}/m$ by $g(i,j,k) = k - w(x_{i,j}) \bmod m$. The lift of α_j that meets a particular $\tilde{\beta}_i^k$ is given by the following lemma:

Lemma 4.12. *The point $\tilde{x}_{i,j}^k$ is the intersection between $\tilde{\beta}_i^k$ and $\tilde{\alpha}_j^{g(i,j,k)}$.*

Proof. We induct on i. For $i = 0$, we have $w(x_{0,j}) = 0$, and by construction $\tilde{\alpha}_j^k$ meets $\tilde{\beta}_0^k$. For the induction step, let S be the segment of α_j from $x_{i,j}$ to $x_{i+1,j}$. Note that $w(x_{i+1,j})$ is equal to $w(x_{i,j})+1$ if S passes below the X and above the O in its column, $w(x_{i,j}) - 1$ if it passes above X and below O, and $w(x_{i,j})$ otherwise. Similarly, if $\tilde{x}_{i,j}^k$ lies on $\tilde{\alpha}_j^l$, then by the previous discussion, $\tilde{x}_{i+1,j}^k$ lies on $\tilde{\alpha}_j^{l-1}$ in the first case, on $\tilde{\alpha}_j^{l+1}$ in the second, and on $\tilde{\alpha}_j^l$ in the third (upper indices modulo m). This proves the induction step. □

We may then identify the generators of $\widehat{\mathrm{CFK}}(\tilde{\mathcal{H}})$ with the set of m-to-one maps

$$\phi\colon \{0, \ldots, n-1\} \times \{0, \ldots, m-1\} \to \{0, \ldots, n-1\}$$

such that for each $j = 0, \ldots, n-1$, the function $g(\cdot, j, \cdot)$ assumes all m possible values on $\phi^{-1}(j)$. In other words, if we shade the m lifts of each α circle with different colors as in Figure 39 and arrange the copies of $\mathcal{H}$ horizontally, a generator is a selection of mn grid points so each column contains one point and each row contains m points, one of each color. It is not difficult to enumerate such maps algorithmically.

To split up the generators of $\widehat{\mathrm{CFK}}(\tilde{\mathcal{H}})$ according to spin^c structures, we simply need to express $\epsilon(\mathbf{x}, \mathbf{y}) = [\gamma_{\mathbf{x},\mathbf{y}}] \in H_1(\Sigma_m; \mathbb{Z})$ in terms of a $\mathbb{Z}$-module presentation for $H_1(\Sigma_m(K); \mathbb{Z})$. We obtain such a presentation from the Heegaard decomposition of $\Sigma_m(K)$: the generators a_j^k ($0 \leq j \leq n-1$, $0 \leq k \leq m-1$) corresponding to the

1-handles dual to the α circles and relations corresponding to the 2-handles spanned by the β circles. By Lemma 4.12, the relations are

$$0 = [\tilde{\beta}_i^k] = \sum_{j=1}^{n} a_j^{g(i,j,k)} \quad (0 \le i \le n-1, 0 \le k \le m-1).$$

To express $\epsilon(\mathbf{x}, \mathbf{y})$ in terms of this basis, one simply counts the number of times that a representative $\gamma_{\mathbf{x},\mathbf{y}}$ crosses the α circles.

To compute the Alexander grading of a generator $\mathbf{x}$, we decompose it as $\mathbf{x} = \tilde{\mathbf{x}}_1 \cup \cdots \cup \tilde{\mathbf{x}}_m$ using Lemma 4.7 and then use Proposition 4.9 and Equation (4.4) to write:

$$\begin{aligned} A(\mathbf{x}) &= \frac{1}{m}(A(\mathbf{x}_1) + \cdots + A(\mathbf{x}_m)) \\ &= \frac{1}{m}\sum_{k=1}^{m}\left(a - \sum_{x \in \mathbf{x}_k} w(x)\right) \\ &= a - \frac{1}{m}\sum_{k=1}^{m}\sum_{x \in \tilde{\mathbf{x}}_k} w(\pi(x)) \\ &= a - \frac{1}{m}\sum_{x \in \mathbf{x}} w(\pi(x)) \end{aligned}$$

Computing the relative Maslov grading between two generators in the same spin^c structure requires finding a domain D connecting them, which is simply a matter of linear algebra, and then using the formula $M(\mathbf{x}) - M(\mathbf{y}) = \mu(D) - 2n_{\mathbf{w}}(D)$. The relative Maslov grading between generators in different spin^c structures can be computed similarly using the formula of Lee and Lipshitz [28]. Specifically, since $\Sigma_m(K)$ is a rational homology sphere, there exists some q such that $q\gamma_{\mathbf{x},\mathbf{y}}$ plus a linear combination of α and β circles is the boundary of a domain D; the formula then says that $M(\mathbf{x}) - M(\mathbf{y}) = \frac{1}{q}(\mu(D) - 2n_{\mathbf{w}}(D))$. We do not know of a formula for the absolute $\mathbb{Q}$-grading, although it can sometimes be computed *post facto* in simple examples, as will be discussed below.

4.2.3 Higher differentials

Let $K \subset S^3$ be a knot presented by an $n \times n$ grid diagram $\mathcal{H} = (T^2, \boldsymbol{\alpha}, \boldsymbol{\beta}, \mathbf{w}, \mathbf{z})$, and let $\tilde{\mathcal{H}} = (\tilde{T}, \tilde{\boldsymbol{\alpha}}, \tilde{\boldsymbol{\beta}}, \tilde{w}, \tilde{z})$ be the nice Heegaard diagram for $(\Sigma_2(K), \tilde{K}_2)$ described in the previous section. The homology of the complex $\widehat{\mathrm{CF}}(\tilde{T}, \tilde{\boldsymbol{\alpha}}, \tilde{\boldsymbol{\beta}}, \mathbf{w})$ — where the differential counts disks that may go over the z basepoints — is isomorphic to $\widehat{\mathrm{HF}}(\Sigma_2(K)) \otimes V^{\otimes n-1}$. The Alexander grading makes this a filtered complex. The associated graded complex of this filtration is $\widehat{\mathrm{CFK}}(\tilde{T}, \tilde{\boldsymbol{\alpha}}, \tilde{\boldsymbol{\beta}}, \mathbf{w}, \mathbf{z})$, which we showed can be computed combinatorially as in Theorem 4.4. The E^1 page in the spectral sequence is the homology of the associated graded complex, $\widehat{\mathrm{HFK}}(\Sigma_2(K), \tilde{K}_2) \otimes V^{\otimes n-1}$. The goal of this section is to show that the E^2 page may also be computed combinatorially as in Theorem 4.6. Also, note that each page in this spectral sequence is isomorphic to the tensor product of $V^{\otimes n-1}$ with the corresponding page of the spectral sequence from $\widehat{\mathrm{HFK}}(\Sigma_2(K), \tilde{K}_2)$ to $\widehat{\mathrm{HF}}(\Sigma_2(K))$.

We write the differential ∂ on $\widehat{\mathrm{CF}}(\tilde{\mathcal{H}})$ as $\partial_0 + \partial_1 + \dots$, where $\partial_i(\mathbf{x})$ is the sum of the terms in $\partial(\mathbf{x})$ that are in Alexander grading $A(\mathbf{x}) - i$. That is, d_i counts holomorphic disks ϕ with $n_{\mathbf{w}}(\phi) = 0$ and $n_{\mathbf{z}}(\phi) = i$. Since $\partial^2 = 0$, we have $\partial_0^2 = 0$ and $\partial_0\partial_1 + \partial_1\partial_0 = 0$, which implies that ∂_1 induces a differential ∂_{1*} on $H_*(\widehat{\mathrm{CF}}, \partial_0)$, and the homology of this differential is the E^2 page of the spectral sequence. Thus, our goal is to identify all of the domains that count for ∂_1.

We now recall the work of Ozsváth, Stipsicz, and Szabó [45]. Although their discussion is in the context of 3-fold simple (non-cyclic) branched covers, the same argument works for double branched covers as well.

The diagram $\mathcal{H}$ has genus $n+1$, $2n$ α circles, $2n$ β circles, n w basepoints, and n z basepoints. We may add n α curves and n β curves to $\tilde{\mathcal{H}}$ and set $\tilde{\mathbf{w}}' = \tilde{\mathbf{w}} \cup \tilde{\mathbf{z}}$ to obtain a diagram $\tilde{\mathcal{H}}' = (\tilde{T}, \tilde{\boldsymbol{\alpha}}', \tilde{\boldsymbol{\beta}}', \tilde{\mathbf{w}}')$, with genus $n+1$, $3n$ α and $3n$ β circles, and $2n$ basepoints (Figure 40). Specifically, for $i = 0, \dots, n-1$, let $\alpha_{i+1/2} \subset T$ (resp. $\beta_{i+1/2} \subset T$) be a curve in the i^{th} row (resp. column) of the grid diagram that separates the O and X in that row (resp. column). Each such circle meets the

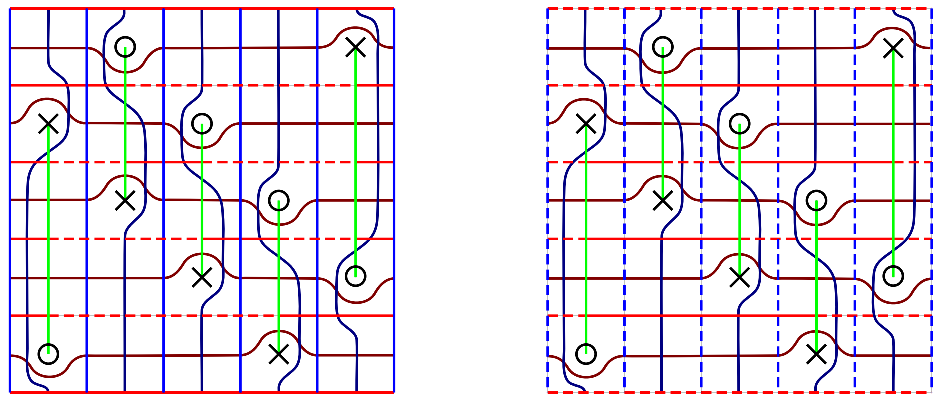

Figure 40: The extended Heegaard diagram $\mathcal{H}'$ defined by Ozsváth, Stipsicz, and Szabó [45]. All of the regions marked O or X contain w basepoints.

branch cuts an odd number of times, so it is doubly covered by a single circle $\tilde{\alpha}_{i+1/2}$ (resp. $\tilde{\beta}_{i+1/2}$). These preimages are the new curves in $\tilde{\boldsymbol{\alpha}}'$ and $\tilde{\boldsymbol{\beta}}'$. Notice that $\tilde{\alpha}_{i+1/2}$ and $\tilde{\beta}_{j+1/2}$ meet exactly twice for each i, j. The diagram $\tilde{\mathcal{H}}'$ presents $\Sigma_2(K)$ without reference to the knot $\tilde{K}_2$. A key property of both $\tilde{\mathcal{H}}$ and $\tilde{\mathcal{H}}'$ is that every basepointed region is an octagon and every non-basepointed region is a rectangle.

Since $\tilde{\mathcal{H}}'$ is nice, the non-negative homology classes ϕ with $n_{\tilde{\mathbf{w}}'}(\phi) = 0$ and $\mu(\phi) = 1$ are precisely the embedded rectangles in $\tilde{\mathcal{H}}'$ [62]. Regarding the classes that hit exactly one basepoint, Ozsváth, Stipsicz, and Szabó proved:

Theorem 4.13. *Let $\phi \in \pi_2(\mathbf{x}, \mathbf{y})$ be a non-negative homology class in $\mathcal{H}'$ with $\mu(\phi) = 1$ and $n_{\tilde{\mathbf{z}}'}(\phi) = 1$. Then the domain of ϕ is either:*

1. *an embedded octagon with local multiplicity $\frac{1}{4}$ at each corner, or*

2. *an embedded annulus with four marked points x_1, y_2, x_2, y_2 with local multiplicity $\frac{1}{4}$ on one boundary component and one marked point $x_3 = y_3$ with local multiplicity $\frac{1}{2}$ on the other boundary component.*

In the first case, ϕ always admits a holomorphic representative. In the second case, whether or not ϕ admits a holomorphic representative is independent of the choice of complex structure on $\tilde{T}$.

As the proof of this theorem is quite technical, we do not reproduce it here.

Proof of Theorem 4.6. Suppose $\mathbf{x}$ and $\mathbf{y}$ are generators of $\widehat{\mathrm{CFK}}(\tilde{\mathcal{H}})$ and $\phi \in \pi_2(\mathbf{x}, \mathbf{y})$ is a non-negative homology class with $\mu(\phi) = 1$, $n_{\tilde{\mathbf{w}}}(\phi) = 0$, and $n_{\tilde{\mathbf{z}}}(\phi) = 1$. We claim that the domain of ϕ must be an embedded octagon.

For $i = 0, \dots, n-1$, let p_i be the intersection point of $\alpha_{i+1/2}$ and $\beta_{j+1/2}$ that lies in the same region of $\mathcal{H}$ as the O in the i^{th} row. Let $\tilde{p}_i$ be one of the two lifts of p_i to $\tilde{\mathcal{H}}'$. Then $\mathbf{x}' = \mathbf{x} \cup \{\tilde{p}_i \mid i = 0, \dots, n-1\}$ and $\mathbf{y}' = \mathbf{y} \cup \{\tilde{p}_i \mid i = 0, \dots, n-1\}$ are generators of $\widehat{\mathrm{CF}}(\tilde{\mathcal{H}}')$. The domain of ϕ, viewed as a domain in $\tilde{\mathcal{H}}'$, represents a homology class $\phi' \in \pi_2(\mathbf{x}', \mathbf{y}')$. The local multiplicity of ϕ' at each point $\tilde{p}_i$ is zero, so $\mu(\phi') = \mu(\phi) = 1$ and $n_{\mathbf{w}'}(\phi') = 1$. Thus, the domain of ϕ is either an embedded octagon or an embedded annulus by Theorem 4.13.

In the second case, one boundary component of the domain of ϕ is either a complete α circle or a complete β circle in $\tilde{\mathcal{H}}$. However, each α and β circle abuts a region marked O on both sides, so the domain of ϕ must contain a point of $\tilde{\mathbf{w}}$. This contradicts the assumption that $n_{\tilde{\mathbf{w}}}(\phi) = 0$.

Thus, the only domains which count for ∂_1 are the embedded octagons, so ∂_1 agrees with the map d_1 appearing in the theorem. □

4.2.4 Computations of $\tau(\Sigma_2(K), \tilde{K}_2, \mathfrak{s})$

Finally, we explain the computations of $\tau(\Sigma_2(K), \widetilde{K}_2, \mathfrak{s})$ for the knots 9_{44}, 10_{158}, 10_{164}, $11n_{100}$, and $11n_{145}$. These are the five knots in Table 2 whose $\mathcal{D}_q$ invariants all vanish but for which we are able to compute $\widehat{\mathrm{HFK}}(\Sigma_2(K), \tilde{K}_2)$ using our implementation of Theorem 4.4. (Four of these knots have arc index 10; $11n_{100}$ has arc index 11, but the chain complex turns to be small enough for our computer program to process it.)

For any knot K, there are inequalities

$$\det(K) = \left|H^2(\Sigma_2(K); \mathbb{Z})\right| \leq \operatorname{rank} \widehat{\mathrm{HF}}(\Sigma_2(K)) \leq \operatorname{rank} \widetilde{Kh}(-K), \tag{4.5}$$

where $\widetilde{Kh}(-K)$ denotes the reduced Khovanov homology of the mirror of K with

$\mathbb{F}_2$ coefficients. (The last inequality follows from the spectral sequence found by Ozsváth and Szabó [52].) In particular, if $\det(K) = \operatorname{rank} \widetilde{Kh}(-K)$, then for each $\mathfrak{s} \in \operatorname{Spin}^c(\Sigma_2(K))$, we have $\widehat{\mathrm{HF}}(\Sigma_2(K), \mathfrak{s}) \cong \mathbb{F}$ in grading $d(\Sigma_2(K), \mathfrak{s})$. This equality holds for 9_{44} (with determinant 17) and 10_{158}, 10_{164}, and $11n_{100}$ (each with determinant 45). The knot $11n_{145}$ has determinant 9 but reduced Khovanov homology of rank 25.

For $K = 10_{158}$, we find that with a suitable identification of $\operatorname{Spin}^c(K)$ with $H^2(\Sigma_2(K); \mathbb{Z}) \cong \mathbb{Z}_{45}$, the d invariants and $\widehat{\mathrm{HFK}}$ groups are as listed in Table 4. (These d invariants are also computed in [24].) The discussion of Maslov gradings in Subsection 4.2.2 only provides relative $\mathbb{Q}$-gradings, but we may pin down the absolute gradings using the spin^c structures in which $\widehat{\mathrm{HFK}}(\Sigma_2(K), \tilde{K}_2, \mathfrak{s})$ has rank 1. Notice that in every spin^c structure, $\widehat{\mathrm{HFK}}(\Sigma_2(K), \tilde{K}_2, \mathfrak{s})$ is thin, so $\tau(\Sigma_2(K), \tilde{K}_2, \mathfrak{s})$ equals the Alexander grading of the unique nonzero group in Maslov grading $d(\Sigma_2(K), \mathfrak{s})$. According to Theorem 4.2, the relevant Grigsby–Ruberman–Strle invariants are $\mathcal{D}_3$, $\mathcal{D}_5$, $\mathcal{T}_3$, and $\mathcal{T}_5$, all of which are zero. The computations for 9_{44}, 10_{164}, and $11n_{100}$ proceed very similarly.

The computation for $11n_{145}$ is more complicated; see Table 5. Because the total rank of $\widetilde{Kh}(\bar{K})$ is greater than $\det K$, we do not know whether $\Sigma_2(K)$ is an L-space, and we cannot tell which elements $\widehat{\mathrm{HF}}(\Sigma_2(K), \mathfrak{s}_0)$ map to the bottom of the infinite tower in $\mathrm{HF}^+(\Sigma_2(K), \mathfrak{s}_0)$, as in the definition of $\tau(\Sigma_2(K), \tilde{K}_2, \mathfrak{s}_0)$. Since $\widehat{\mathrm{HFK}}(\Sigma_2(K), \tilde{K}_2, \mathfrak{s}_0)$ has elements with Maslov grading 0 in Alexander gradings 0 and 2, $\tau(\Sigma_2(K), \tilde{K}_2, \mathfrak{s}_0)$ could equal 0 or 2. However, we may use Theorem 4.6 to compute the E^2 page of the spectral sequence from $\widehat{\mathrm{HFK}}(\Sigma_2(K), \tilde{K}_2, \mathfrak{s}_0)$ to $\widehat{\mathrm{HF}}(\Sigma_2(K), \mathfrak{s}_0)$. While we cannot determine the entire page with available computer resources, we do find that the E^2 page does not contain any nonzero elements in positive Alexander grading. As a result, we see that $\tau(\Sigma_2(K), \tilde{K}_2, \mathfrak{s}_0) = 0$.

$\mathfrak{s}$	$d(\Sigma_2(K), \mathfrak{s})$	$\sum_{i,j} \operatorname{rank} \widehat{\mathrm{HFK}}_j(\Sigma_2(K), \tilde{K}, \mathfrak{s}, i)\, t^i q^j$	$\tau(\Sigma_2(K), \tilde{K}, \mathfrak{s})$
0	0	$q^{-3}t^{-3} + 4q^{-2}t^{-2} + 10q^{-1}t^{-1} + 15 + 10qt + 4q^2t^2 + q^3t^3$	0
± 1	$8/45$	$q^{8/45}(q^{-1}t^{-1} + 3 + qt)$	0
± 2	$32/45$	$q^{-13/45}(q^{-2}t^{-2} + 3q^{-1}t^{-1} + 3 + 3qt + q^2t^2)$	1
± 3	$-2/5$	$q^{-2/5}$	0
± 4	$38/45$	$q^{38/45}$	0
± 5	$4/9$	$q^{4/9}(q^{-1}t^{-1} + 3 + qt)$	0
± 6	$2/5$	$q^{2/5}$	0
± 7	$32/45$	$q^{-13/45}(q^{-2}t^{-2} + 3q^{-1}t^{-1} + 3 + 3qt + q^2t^2)$	1
± 8	$-28/45$	$q^{17/45}(q^{-2}t^{-2} + 3q^{-1}t^{-1} + 3 + 3qt + q^2t^2)$	-1
± 9	$2/5$	$q^{2/5}(2q^{-1}t^{-1} + 5 + 2qt)$	0
± 10	$-2/9$	$q^{-2/9}(2q^{-1}t^{-1} + 5 + 2qt)$	0
± 11	$-22/45$	$q^{-22/45}$	0
± 12	$-2/5$	$q^{-2/5}$	0
± 13	$2/45$	$q^{2/45}$	0
± 14	$38/45$	$q^{38/45}$	0
± 15	0	$q^{-1}t^{-1} + 3 + qt$	0
± 16	$-22/45$	$q^{-22/45}$	0
± 17	$-28/45$	$q^{17/45}(q^{-2}t^{-2} + 3q^{-1}t^{-1} + 3 + 3qt + q^2t^2)$	-1
± 18	$-2/5$	$q^{-2/5}$	0
± 19	$8/45$	$q^{8/45}(q^{-1}t^{-1} + 3 + qt)$	0
± 20	$-8/9$	$q^{1/9}(q^{-1}t^{-1} + 1 + qt)$	-1
± 21	$2/5$	$q^{2/5}$	0
± 22	$2/45$	$q^{2/45}$	0

Table 4: Values of $d(\Sigma_2(K), \mathfrak{s})$, $\widehat{\mathrm{HFK}}(\Sigma_2(K), \tilde{K}, \mathfrak{s})$, and $\tau(\Sigma_2(K), \tilde{K}, \mathfrak{s})$ for the knot $K = 10_{158}$.

$\mathfrak{s}$	$d(\Sigma_2(K),\mathfrak{s})$	$\sum_{i,j}\dim_{\mathbb{Z}/2}\widehat{\mathrm{HFK}}_j(\Sigma_2(K),\tilde{K},\mathfrak{s},i;\mathbb{Z}/2)t^iq^j$	$\tau(\Sigma_2(K),\tilde{K},\mathfrak{s})$
0	0	$q^{-5}t^{-3}+(2q^{-4}+q^{-2})t^{-2}+(q^{-3}+4q^{-1})t^{-1}$ $+7q+(q^{-1}+4q)t+(2+q^2)t^2+qt^3$	0
±1	$-8/9$	$q^{-8/9}(q^{-2}t^{-2}+3q^{-1}t^{-1}+5+3qt+q^2t^2)$	0
±2	$4/9$	$q^{4/9}$	0
±3	0	1	0
±4	$-2/9$	$q^{-2/9}(q^{-2}t^{-2}+3q^{-1}t^{-1}+5+3qt+q^2t^2)$	0

Table 5: Values of $d(\Sigma_2(K),\mathfrak{s})$, $\widehat{\mathrm{HFK}}(\Sigma_2(K),\tilde{K},\mathfrak{s})$, and $\tau(\Sigma_2(K),\tilde{K},\mathfrak{s})$ for the knot $K=11n_{145}$.

Chapter 5

Poetic conclusion

Our goal is one whose application's nice
For smooth four-manifold topology:
To tell if certain knots and links are slice
With bordered Heegaard Floer homology.

We seek concordance data that detect
Some links obtained by Whitehead doublings,
As well as knots we get when we infect
Along two of the three Borromean rings.

Some lengthy work with bordered Floer then proves
How τ for satellites like these is found.
We see, by this result and cov'ring moves,
That smooth slice disks our links can never bound.

The theorem's proved, the dissertation's done,
But all the work ahead has just begun.

Bibliography

[1] John Baldwin and W. Danny Gillam, *Computations of Heegaard-Floer knot homology*, preprint (2006), arXiv:math/0610167.

[2] Žarko Bižaca, *An explicit family of exotic Casson handles*, Proc. Amer. Math. Soc. **123** (1995), no. 4, 1297–1302.

[3] Jonathan Bloom, *A link surgery spectral sequence in monopole Floer homology*, preprint (2009), arXiv:0909.0816.

[4] Andrew J. Casson and Cameron McA. Gordon, *Cobordism of classical knots*, À la recherche de la topologie perdue, Progr. Math., vol. 62, Birkhäuser Boston, Boston, MA, 1986, With an appendix by P. M. Gilmer, pp. 181–199.

[5] Jae Choon Cha and Taehee Kim, *Covering link calculus and iterated Bing doubles*, Geom. Topol. **12** (2008), no. 4, 2173–2201.

[6] Jae Choon Cha and Charles Livingston, *Knotinfo: an online table of knot invariants*, `www.indiana.edu/~knotinfo`.

[7] Jae Choon Cha, Charles Livingston, and Daniel Ruberman, *Algebraic and Heegaard-Floer invariants of knots with slice Bing doubles*, Math. Proc. Cambridge Philos. Soc. **144** (2008), no. 2, 403–410.

[8] David Cimasoni, *Slicing Bing doubles*, Algebr. Geom. Topol. **6** (2006), 2395–2415.

[9] Reinhard Diestel, *Graph theory*, third ed., Graduate Texts in Mathematics, vol. 173, Springer-Verlag, Berlin, 2005.

[10] Ralph H. Fox and John W. Milnor, *Singularities of 2-spheres in 4-space and cobordism of knots*, Osaka J. Math. **3** (1966), 257–267.

[11] Michael H. Freedman and Frank Quinn, *Topology of 4-manifolds*, Princeton Mathematical Series, vol. 39, Princeton University Press, Princeton, NJ, 1990.

[12] Paolo Ghiggini, *Knot Floer homology detects genus-one fibred knots*, Amer. J. Math. **130** (2008), no. 5, 1151–1169.

[13] Cameron McA. Gordon, *Some aspects of classical knot theory*, Knot theory (Proc. Sem., Plans-sur-Bex, 1977), Lecture Notes in Math., vol. 685, Springer, Berlin, 1978, pp. 1–60.

[14] J. Elisenda Grigsby, *Combinatorial description of knot Floer homology of cyclic branched covers*, preprint (2006), arXiv:math/0610238.

[15] ———, *Knot Floer homology in cyclic branched covers*, Algebr. Geom. Topol. **6** (2006), 1355–1398 (electronic).

[16] J. Elisenda Grigsby, Daniel Ruberman, and Sašo Strle, *Knot concordance and Heegaard Floer homology invariants in branched covers*, Geom. Topol. **12** (2008), no. 4, 2249–2275.

[17] J. Elisenda Grigsby and Stephan Wehrli, *On the colored Jones polynomial, sutured Floer homology, and knot Floer homology*, preprint (2008), arXiv:0807.1432.

[18] ———, *On the naturality of the spectral sequence from Khovanov homology to Heegaard Floer homology*, preprint (2009), arXiv:0907.4378.

[19] Matthew Hedden, *Notions of positivity and the Ozsváth–Szabó concordance invariant*, to appear, arXiv:math/0509499.

[20] ———, *Knot Floer homology of Whitehead doubles*, Geom. Topol. **11** (2007), 2277–2338.

[21] Matthew Hedden and Philip Ording, *The Ozsváth-Szabó and Rasmussen concordance invariants are not equal*, Amer. J. Math. **130** (2008), no. 2, 441–453.

[22] Matthew Hedden and Liam Watson, *Does Khovanov homology detect the unknot?*, preprint (2008), arXiv:0805.4423.

[23] Jennifer Hom, *Bordered Heegaard Floer homology and the τ invariant of cable knots*, in preparation.

[24] Stanislav Jabuka and Swatee Naik, *Order in the concordance group and Heegaard Floer homology*, Geom. Topol. **11** (2007), 979–994.

[25] Louis H. Kauffman, *On knots*, Annals of Mathematics Studies, vol. 115, Princeton University Press, Princeton, NJ, 1987.

[26] Rob Kirby (ed.), *Problems in low-dimensional topology*, AMS/IP Stud. Adv. Math., vol. 2, Amer. Math. Soc., Providence, RI, 1997.

[27] Peter Kronheimer and Tomasz Mrowka, *Gauge theory for embedded surfaces. I*, Topology **32** (1993), no. 4, 773–826.

[28] Dan A. Lee and Robert Lipshitz, *Covering spaces and* $\mathbf{Q}$*-gradings on Heegaard Floer homology*, J. Symplectic Geom. **6** (2008), no. 1, 33–59.

[29] Adam S. Levine, *On knots with infinite smooth concordance order*, preprint (2008), arXiv:0805.2410.

[30] ———, *Slicing mixed Bing-Whitehead doubles*, preprint (2009), arXiv:0912.5222.

[31] ———, *Computing knot Floer homology in cyclic branched covers*, Algebr. Geom. Topol. **8** (2008), no. 2, 1163–1190.

[32] Jerome Levine, *Invariants of knot cobordism*, Invent. Math. 8 (1969), 98–110; addendum, ibid. **8** (1969), 355.

[33] ———, *Knot cobordism groups in codimension two*, Comment. Math. Helv. **44** (1969), 229–244.

[34] Robert Lipshitz, Peter Ozsváth, and Dylan Thurston, *Bimodules in bordered Heegaard Floer homology*, preprint (2010), arXiv:1003.0598.

[35] ———, *Bordered Heegaard Floer homology: invariance and pairing*, preprint (2009), arXiv:0810.0687.

[36] Charles Livingston, *Computations of the Ozsváth-Szabó knot concordance invariant*, Geom. Topol. **8** (2004), 735–742 (electronic).

[37] Charles Livingston and Swatee Naik, *Obstructing four-torsion in the classical knot concordance group*, J. Differential Geom. **51** (1999), no. 1, 1–12.

[38] ———, *Knot concordance and torsion*, Asian J. Math. **5** (2001), no. 1, 161–167.

[39] ———, *Ozsváth-Szabó and Rasmussen invariants of doubled knots*, Algebr. Geom. Topol. **6** (2006), 651–657 (electronic).

[40] Ciprian Manolescu and Brendan Owens, *A concordance invariant from the Floer homology of double branched covers*, Int. Math. Res. Not. IMRN (2007), no. 20, Art. ID rnm077, 21.

[41] Ciprian Manolescu, Peter Ozsváth, and Sucharit Sarkar, *A combinatorial description of knot Floer homology*, Ann. of Math. (2) **169** (2009), no. 2, 633–660.

[42] Ciprian Manolescu, Peter Ozsváth, Zoltán Szabó, and Dylan Thurston, *On combinatorial link Floer homology*, Geom. Topol. **11** (2007), 2339–2412.

[43] Ciprian Manolescu, Peter Ozsváth, and Dylan Thurston, *Grid diagrams and Heegaard Floer invariants*, preprint (2009), arXiv:math/0910.0078.

[44] Yi Ni, *Knot Floer homology detects fibered knots*, Invent. Math. **170** (2007), no. 3, 577–608.

[45] Peter Ozsváth, András Stipsicz, and Zoltán Szabó, *A combinatorial description of the $U^2 = 0$ version of Heegaard Floer homology*, preprint (2009), arXiv:math/0910.0078.

[46] Peter Ozsváth and Zoltán Szabó, *Knot Floer homology and the four-ball genus*, Geom. Topol. **7** (2003), 615–639 (electronic).

[47] ———, *On the Floer homology of plumbed three-manifolds*, Geom. Topol. **7** (2003), 185–224 (electronic).

[48] ———, *Holomorphic disks and genus bounds*, Geom. Topol. **8** (2004), 311–334 (electronic).

[49] ———, *Holomorphic disks and knot invariants*, Adv. Math. **186** (2004), no. 1, 58–116.

[50] ———, *Holomorphic disks and topological invariants for closed three-manifolds*, Ann. of Math. (2) **159** (2004), no. 3, 1027–1158.

[51] ———, *Knots with unknotting number one and Heegaard Floer homology*, Topology **44** (2005), no. 4, 705–745.

[52] ———, *On the Heegaard Floer homology of branched double-covers*, Adv. Math. **194** (2005), no. 1, 1–33.

[53] ———, *Holomorphic triangles and invariants for smooth four-manifolds*, Adv. Math. **202** (2006), no. 2, 326–400.

[54] Ina Petkova, *Cables of thin knots and bordered Heegaard Floer homology*, preprint (2010), arXiv:0911.2679.

[55] Jacob Rasmussen, *Khovanov homology and the slice genus*, preprint (2004), arXiv:math.GT/0402131.

[56] Jacob A. Rasmussen, *Floer homology and knot complements*, Ph.D. thesis, Harvard University, 2003, arXiv:math/0509499.

[57] Lawrence Roberts, *On knot Floer homology in double branched covers*, preprint (2006), arXiv:math/0706.0741.

[58] Dale Rolfsen, *Knots and links*, third ed., AMS Chelsea, Providence, 2003.

[59] Lee Rudolph, *Quasipositive annuli. (Constructions of quasipositive knots and links. IV)*, J. Knot Theory Ramifications **1** (1992), no. 4, 451–466.

[60] ———, *Quasipositivity as an obstruction to sliceness*, Bull. Amer. Math. Soc. (N.S.) **29** (1993), no. 1, 51–59.

[61] ———, *Quasipositive plumbing (constructions of quasipositive knots and links. V)*, Proc. Amer. Math. Soc. **126** (1998), no. 1, 257–267.

[62] Sucharit Sarkar and Jiajun Wang, *An algorithm for computing some Heegaard Floer homologies*, to appear, arXiv:math/0607777.

[63] Cornelia Van Cott, *An obstruction to slicing iterated Bing doubles*, preprint (2009), arXiv:math/0907.4948.